Effect of Asphalt Pavement Compaction on Interlayer Bonding and Tensile Strength of Asphalt Concrete under Low Temperatures and Temperature Cycling

By

Mohammad Ramezani Afjadi

A Thesis Submitted to the Faculty of Graduate and Postdoctoral Affairs in partial fulfillment of the requirements for the degree of

Doctor of Philosophy

in

Civil Engineering

Carleton University

Ottawa, Ontario

Abstract

The maintenance and rehabilitation of highway network systems are major road agency expenditures. The combined effects of environmental conditions, traffic loading, moisture, construction quality, and maintenance contribute significantly to rates of pavement deterioration and the length of asphalt pavement life. One of the important performance parameters for asphalt concrete pavements, particularly in cold regions, is the capability to withstand cyclic temperature changes. Such temperature cycles, especially those that alternate above and below freezing, lead to mechanical stresses that can cause failure.

This research presents the results and major findings of an experimental investigation performed on rectangular asphalt slab samples extracted from newly constructed pavements of actual highway projects, rather than gyratory-compacted samples that are created in the laboratory. The first phase (Test Series A) studied the effects of temperature cycles and compaction equipment on interlayer bonds by using a custom-made temperature cycling testing machine that allows the reproduction of several temperature cycles over a relatively short time (7-10 days). The second phase (Test Series B) focused on resistance to tensile stresses under cold temperatures. During Test Series B, a custom-made direct tensile strength test was employed to estimate the tensile strength of slab samples at different temperatures (i.e., 0°C, -10°C, or -20°C) for single- and double-layer samples. Test Series B included 171 asphalt samples 300mm long by 100mm wide, with thicknesses of 50mm for single layers and 100mm for double layers.

The results of Test Series A showed that samples compacted with an Asphalt Multi-Integrated Roller (AMIR) had superior interlayer bonding in comparison with the samples compacted with a Conventional Compacting Method (CCM). Those latter samples were shown to experience debonding during cyclic temperature changes, which would cause the different layers to act independently and have lower resistance to thermal stresses. The results of Test Series B showed that construction-induced cracking affects the tensile strength of asphalt pavements.

This research and its related laboratory tests explain how different types of equipment used for compacting asphalt can affect the tensile strength and interlayer bonding of asphalt pavement. Analysis of the results reveals that both resistance to temperature-cycling and the compaction method play important roles in the performance of Asphalt Concrete Pavement (ACP). The apparatus used for both of the proposed asphalt pavement performance test methods used in this study, the Carleton University Asphalt Temperature Cycling (CUATC) and Carleton University Asphalt Direct Tensile Strength (CUADTS) tests, were designed and assembled at the Civil and Environmental Engineering Laboratory of Carleton University. CUATC and CUADTS were designed with the aim of simulating actual field conditions and replicating field loading, temperatures, and boundary conditions as closely as practically possible, and have the potential to be used as routine quality control tests (with pass/fail criteria) for asphalt pavement end products extracted from road projects after compaction in order to test the quality of relevant asphalt placement and compaction processes.

Acknowledgements

I would like to express my great appreciation to Professor A. O. Abd El Halim for kindly accepting me as his PhD student. His guidance, support and valuable input were treasured throughout my studies at Carleton University. I am very sad that he passed away on September 19, 2019, and that I could not defend my thesis while he was still with us.

Special thanks to Professor Yasser Hassan, Chair of the Department of Civil and Environmental Engineering and my current thesis supervisor, for his support, advice, valued comments, and constructive criticisms.

I would like to acknowledge Carleton University for their financial support, and RW Tomlinson Limited for providing the asphalt specimens. I also thank Stanley Conley, Jason Arnott, and Stephen Vickers for their participation and assistance in operating the environmental chamber, design and construction of the testing tables and help during the test series; they greatly enabled and supported my work and helped me get results of better quality. The author is grateful to Dr. Bashar Dhahir for his assistance in the modelling and statistical analysis. I would like to acknowledge the experimental works completed jointly with Graziela Girardi, P.Eng at early stages of my studies at Carleton University. I would like to thank Dr. Mahmood Saffarzadeh and Engr. Mohammad Hossein Anjomshoaa for their consistent encouragement in pursuing and completing my doctoral degree. In addition, I would like to express my gratitude to the past and present staff of the Department of Civil and Environmental Engineering, including Sara Seiler, Thomas Morrice, Payal Chadha, Negin Alikhani, and Kay Casselman.

It is with genuine gratitude and warmth that I dedicate this work to:

- Professor A. O. Abd El Halim
- My wife, who never left my side and who was always there for me throughout my entire Ph.D. program
- My beloved daughter, Tara (Tara Joon)
- My father, who is the man I will always aspire to be
- My mother, who has been a constant source of support and encouragement
- My grandparents; although they are no longer of this world, their love for me knew no bounds, and my memories of them will live within me forever

Table of Contents

Abstract ..... **ii**

Acknowledgements ..... **iv**

List of Tables ..... **x**

List of Illustrations ..... **xii**

Abbreviations ..... **xviii**

Chapter 1. Introduction **1**

1.1 Background 1

1.2 Problem Statement and Research Questions 13

1.3 Research Objectives 14

1.4 Significance and Contribution to the Discipline 16

1.5 Research Scope and Organization 17

Chapter 2. Literature review **19**

2.1 Organization of Chapter 2 19

2.2 Asphalt Concrete Pavement Distresses 20

2.2.1 Cracking 22

2.2.2 Surface Deformation 24

2.2.3 Surface Defects 26

2.2.4 Pothole and Patch 28

2.2.5 Miscellaneous Distresses 28

2.2.6 Summary of Asphalt Pavement Distresses 29

2.3 Key Performance Parameters of Asphalt Mix 30

2.3.1 Rutting 33

2.3.2 Fatigue and Cracking Resistance 33

2.3.3 Resistance to Low Temperature Cracking 33

2.3.4 Stiffness 33

2.3.5 Moisture Susceptibility 34

2.3.6 Ability to Withstand Fluctuating Temperatures 34

2.4 Tensile Strength 34

2.5 Compaction and its Role in Performance Tests 35

2.6 Asphalt Multi-Integrated Roller (AMIR) Technology 39

2.7 Interlayer Bond 40

2.8 Temperature Cycle Testing (TCT) 43

2.9 Effect of Low Temperature and Thermal Cracking 45

2.10 Significance of Sampling Method 47

2.11 Current Laboratory Compaction Methods for Sample Preparation 50

2.12 Current Asphalt Mix Performance Test Methods 53

2.13 Simple Asphalt Performance Test Methods 53

2.14 Summary and Conclusion 56

Chapter 3. Experimental Investigation 58

3.1 Research Plan 58

3.2 Test Series A 64

3.2.1 Test Site - Test Series A 66

3.2.2 Field Sampling - Test Series A 67

3.2.3 Material (Asphalt Mix) - Test Series A 68

3.2.4 Preparation of Test Slabs in the Lab - Test Series A 69

3.2.5 Test Facility for Test Series A 70

3.2.6 Testing Procedure - Test Series A 74

3.3 Test Series B 79

3.3.1 Test Site – Test Series B 79

3.3.2 Field Sampling - Test Series B 79

3.3.3 Material (Asphalt Mix) - Test Series B 80

3.3.4 Preparation of Test Slabs in the Lab - Test Series B 81

3.3.5 Test Facility for Test Series B 85

3.3.6 Testing Procedure - Test Series B 88

Chapter 4. Results and Analysis 100

4.1 Results and Analysis - Test Series A (Temperature Cycling) 100

4.1.1 Paving day observations 100

4.1.2 Sampling day site observations 102

4.1.3 Observations during the test 103

4.1.4 Observations 2 years after construction 106

4.1.5 Test results and analysis – Test Series A 108

4.1.6 Relationship Between Variables – Test Series A 116

4.2 Results and Analysis - Test Series B 117

4.2.1 Statistical Significance and Hypothesis Test – Test Series B 125

4.2.2 Analysis of Variance – Test Series B 127

4.2.3 Test Series B – Bond Between Layers 129

Chapter 5. Conclusions 131

5.1 Summary of Conclusions for Test Series A 132

5.1.1 AMIR Roller 133

5.1.2 Conventional Compaction Method (CCM) Rollers 134

5.2 Summary of Conclusions for Test Series B 136

5.3 Recommendations for Future Research 137

References 138

Appendix A- Details of Addition Built for Testing Series B Apparatus 150

Appendix B- Summary of Trial for Test Series B 154

Appendix C- List of Asphalt Pavement Performance Test Methods 158

Appendix D- Relationship Between Variables for Test Series A 164

List of Tables

Table 2-1- Summary of asphalt distresses and their relationship to compaction, interlayer bonding, temperature cycles, and loading 30

Table 3-1. Main parameters of the mix designs used as binder course and surface course for Test Series A 69

Table 3-2. Summary of Test Series A 78

Table 3-3. Main Parameters of Mix Design used as binder course and surface course for Test Series B 80

Table 3-4. Test temperature for each of 16 groups in Test Series B 88

Table 3-5. Summary of Test Series B 90

Table 4-1. Percentage decrease in calculated tensile strength for each group of roller-compacted face down and roller-compacted face up samples..... 118

Table 4-2. The descriptive statistics, Test Series B Tensile Strength (N/mm2), Group 1 to 16 121

Table 4-3. Percentage decrease in maximum load (KN) for each group of roller-compacted face-down and face-up samples 122

Table 4-4. Descriptive statistics, Test Series B, Max Load (kN), Groups 1 to 16..... 123

Table 4-5. Results of the Independent T-Test for Single-layer Samples at -20^{o}C (Groups 12 & 16)..... 126

Table 4-6. Summary of the P-values, Results of the Independent T-Test 127

Table 4-7. Results of The Two-Way ANOVA Test for Double-layer Samples..... 128

Table 4-8. Results of The Two-Way ANOVA Test for Single-layer Samples..... 128

Table B-1. Examples of Trial Tests Performed before Test Series B……155

Table D-1. List of independent variables and their orders, Test Series A, Linear……..165

Table D-2. Models Summary, Test Series A, Linear Regression……166

Table D-3. Results of the ANOVA test for proposed models (Linear Regression), Test Series A……166

Table D-4. Coefficients for proposed three models (Linear Regression), Test Series A..167

Table D-5. Proposed three equations (Linear Regression), Test Series A……..168

List of Illustrations

Figure 1-1. Example of asphalt concrete pavement with severe cracks 2

Figure 1-2. City of Ottawa Temperature (°C), November 2019..... 4

Figure 1-3. Example of Cracks on Asphalt Pavement only 2 years after Construction 7

Figure 1-4. Examples of Traditional Steel Drum Rollers (SDR) 9

Figure 1-5. Example of Pneumatic-tire Compaction Rollers (rubber tire)..... 10

Figure 1-6. Example of Oscillating Rollers..... 10

Figure 1-7. Asphalt Multi-Integrated Roller (AMIR), August 2019 12

Figure 1-8. Asphalt Multi-Integrated Roller (AMIR), 2017 12

Figure 2-1 Example of asphalt pavement with multiple types of the distresses 20

Figure 2-2. Example of pavement with alligator cracks..... 22

Figure 2-3. Example of pavement with longitudinal Crack..... 22

Figure 2-4. Example of pavement with block cracks 23

Figure 2-5. Example of pavement with edge cracks..... 23

Figure 2-6. Example of pavement with slippage cracks 25

Figure 2-7. Raveling in Asphalt Pavement 27

Figure 2-8. Asphalt pavement with pothole..... 28

Figure 2-9. Asphalt pavement with pothole..... 28

Figure 2-10. Asphalt pavement with several patches 28

Figure 2-11. Test methods to determine interlayer bond properties in the lab and in the field (Raab and Partl 1999) 43

Figure 2-12. Field Core Sampling 49

Figure 2-13 Schematic of Superpave Gyratory Compaction by Dessouky, et al. 2004 (left) and Wany et al. 2019 (Right) 51

Figure 2-14. California Kneading Compactor (California Test 104, 2011) 51

Figure 2-15 Schematic of Segmented Steel Roller (left) and Pictures of the Segmented Steel Roller (Right) (Wistuba 2016) 52

Figure 3-1. Summary of Research Plan 62

Figure 3-2. Sampling Site Location Map (a) and Sampling Location for each Type of Compactor (b) 66

Figure 3-3. Photo of paving test road with AMIR rollers compacting the Southbound lane of Didsbury Road 67

Figure 3-4. Pictures from Sampling Day for Test Series B 68

Figure 3-5. Preparation of test slabs in the labs (glue applied) 70

Figure 3-6. 3D view of addition designed for Test Series A 71

Figure 3-7 – New Loading System for Test Series A 72

Figure 3-8. Photograph of the Testing Table for Test Series A 73

Figure 3-9. Test Table Schematic (Test Series A) 73

Figure 3-10. Elongation vs Time, Test A (Temperature Cycling Test) Performed on AMIR compacted samples 76

Figure 3-11. Examples of tested samples compacted with AMIR for Test Series A (TCT), 77

Figure 3-12. TCT, Examples of samples compacted with CCM 78

Figure 3-13. Sampling Lot (Ottawa, Canada, 2015), Marking & Saw-Cutting the Slabs ... 80

Figure 3-14. 600 mm x 300 mm asphalt slabs from the field for Test Series B 81
Figure 3-15. asphalt slabs after saw-cut to 300 mm x 100 mm for Test Series B 81
Figure 3-16. Preparation of Test Slabs in the Labs (glue applied) 82
Figure 3-17. Example of samples with roller-compacted face down. 83
Figure 3-18. A double-layer sample glued to the sampling sheets with its compacted face was facing down 83
Figure 3-19. Conditioning the samples inside the environmental chamber for 24 hours 84
Figure 3-20. Example of samples with roller-compacted face up. 84
Figure 3-21. Photograph of the testing table for CUADTS test designed by Abd El Halim 85
Figure 3-22. Photograph of the Hydraulic Actuator & Its Connection to Moving Plate... 86
Figure 3-23. Outline of the CUADTS testing table (Test Series B) 87
Figure 3-24. Specially designed testing table for CUADTS test on asphalt concrete 87
Figure 3-25. Example of double-layer sample tested for Test Series B (sample broken into 2 pieces)..... 91
Figure 3-26. Example of single-layer sample tested for Test Series B..... 91
Figure 3-27, Top view of a single-layer sample tested for Test Series B 92
Figure 3-28. Examples of samples tested for Test Series B (bottom layer broken but layers are separated) 92
Figure 3-29. Sample tested at 0°C for Test Series B (bottom layer broken but layers are separated)..... 93
Figure 3-30. Sample Test Result Stroke (Elongation) vs. Load at -10°C..... 93

Figure 3-31. Diagram of the Mounting Steel Plates 94

Figure 3-32. Schematic of Loads Applied to ACP Samples..... 95

Figure 3-33. Free-body Diagram of ACP Sample..... 96

Figure 3-34. Free-body Diagram of ACP Sample..... 97

Figure 3-35. Toughness: Area under the stress-strain curve..... 99

Figure 4-1. Photo from paving day. In the photo the right-hand lane (northbound) was compacted with CCM and left-hand lane (southbound) with AMIR 101

Figure 4-2. Photo from Paving day. Asphalt permeability tests in process for both areas 102

Figure 4-3. Photo from Sampling Day - Area 1 and Area 2. The right-hand lane (northbound) is compacted with TCR and the left-hand lane (southbound) with AMIR103

Figure 4-4. Example of CCM sample failing due to debonding during cyclic temperature testing 106

Figure 4-5. Example of AMIR sample failing due to tensile stress during cyclic temperature testing..... 106

Figure 4-6. Example of the asphalt mat for the area compacted by the AMIR, 2 years after construction 107

Figure 4-7. Two Examples of the asphalt mat cracked, for the area compacted by the Steel roller, 2 years after construction 108

Figure 4-8. Test Series A - Example elongation vs time for three cycles of an AMIR sample..... 109

Figure 4-9. Test Series A - Example elongation vs time for three cycles of a CCM sample 110

Figure 4-10. Elongation vs Time for 7 cycles of TCT for AMIR compacted sample 113

Figure 4-11. Crack Initiation & Crack Propagation 114

Figure 4-12.Test Series A - Elongation vs time for three cycles of 6 samples compacted with CCM..... 115

Figure 4-13. Test Series A - Elongation vs time for three cycles of 11 samples compacted with AMIR 116

Figure 4-14. The box plot of the results of Test Series B for single-layer sample at -20°C 117

Figure 4-15. The box plot of the results for double-layer samples, Group 3 to 8..... 120

Figure 4-16. The box plot of the results for single-layer samples, Group 11 to 16..... 120

Figure 4-17. The box plot of the results for Max Load (KN) applied to double-layer samples, Group 3 to 8..... 124

Figure 4-18. The box plot of the results for Max Load (KN) applied to single-layer samples, Group 3 to 8..... 124

Figure 4-19. Asphalt slabs disconnect at the bond line prior to test..... 130

Figure A-1. Test Series B Apparatus Parts Before Assembly.....150

Figure A-2. 3D View of Designed Weight System 151

Figure A-3. View of the Load plates.....151

Figure A-4. View of the Vertical Threaded Bar.....152

Figure A-5. View of the Linear Variable Differential Transducers (LVDT) During Installation……152

Figure A-6. Test Series B Apparatus After Assembly and Installation……153

Figure B-1. Example of Trial Series 1, Connection of sample to plate is by tack coat…..154

Figure B-2. Examples of Trial Series 2 (Testing slabs side by side)…… 155

Figure D-1. Graph associated with proposed linear regression model for Test Series A ……170

Abbreviations

AASHTO - American Association of State Highway and Transportation Officials

AC - Asphalt-binder/Asphalt Cement

ACP – Asphalt Concrete Pavement

AMIR - Asphalt Multi-Integrated Roller

ASTM - American Society for Testing and Materials

CCM - Conventional Compaction Method

CUADTS - Carleton University Asphalt Direct Tensile Strength

CUATC - Carleton University Asphalt Temperature Cycling

DOT - Department of Transportation

FHWA - Federal Highway Administration

HMA - Hot Mix Asphalt

IDT - Indirect Tension Test (monotonic loading)

MTO - The Ministry of Transportation of Ontario

NCHRP - National Cooperative Highway Research Program

OPS - Ontario Provincial Standards for roads & public works

OPSS - Ontario Provincial Standard Specifications

OT – Overlay Tester

PG - Performance grade

RAP – Recycled Asphalt Pavement / Reclaimed Asphalt Pavement

SDR - Steel-Drum Roller

Superpave - Superior Performing Asphalt Pavements

TC - Temperature Cycling

TCR - Traditional Compaction Rollers

TCT - Temperature Cycle Testing

TxDOT - Texas Department of Transportation

U.S.DOT - United States Department of Transportation

Chapter 1. Introduction

1.1 Background

Road infrastructure and highways provide essential links for moving goods, services, and people, which is essential to the nation's continued growth, competitiveness, and prosperity. Road agencies are responsible for the design and construction of highway network systems and for their considerable ongoing maintenance. Maintenance and repair of highway network systems are major road agency expenditures. The limited budgets of road agencies and periods of underinvestment in infrastructure in the past have resulted in a need for both new infrastructure and obligations to rehabilitate and maintain the current infrastructure. Considering the high costs for road rehabilitation and construction, various levels of government have struggled to satisfy the increasing demands with their limited resources.

For example, the Province of Ontario as of 2016 had more than 40,000 km of highway lanes covering an overall distance of about 17,000 km, as well as approximately 5,000 bridges and culverts with a total value of $82 billion. The Ministry of Transportation Ontario (MTO) in 2016 estimated and planned to spend $14 billion over the following ten years for road and bridge maintenance, and about $4 billion for road and bridge expansion. Between 2013 and 2018, the MTO awarded about $7.6 billion worth of construction contracts for projects like re-paving, repair of existing bridges, and for

expanding current highways and building new bridges (Ministry of Transportation Ontario 2018). In the USA, the Federal Highway Administration and Federal Transit Administration in their biennial report to the Congress reported an $836 billion backlog of unmet capital investment needs for highways and bridges (United States Department of Transportation, Federal Highway Administration (FHWA) 2016). The report also showed that in 2012, highway capital spending totaled $105.2 billion, while spending on maintenance totaled $35.1 billion. As a result, various levels of government have struggled to satisfy increasing demands with limited resources.

Figure 1-1. Example of asphalt concrete pavement with severe cracks

The combined effects of environmental conditions, traffic loading, moisture, construction quality, and maintenance contribute significantly to rate of pavement deterioration and length of asphalt pavement life. All these parameters influence pavement performance, but the root cause of early pavement cracking is still unknown. Fatigue and cracking resistance, moisture susceptibility, resistance to low temperature cracking, deformation resistance (rutting) and stiffness have been named by researchers as key performance parameters of asphalt pavement (Witczak et al. 2002; Zaumanis et al. 2018; Hofko and Blab 2016). Resistance to cyclic temperature changes is also another performance parameter which is used for multi-layer materials in different industries (i.e.,

ceramics, coating, electronic systems). Knowing that asphalt concrete pavement (ACP) in Canada and the northern regions of US are subjected to temperature cycles for several weeks at the beginning and end of winter cycles from above to below freezing, and vice versa, resistance to cyclic temperature changes was also proposed to be added to the list of the key performance parameters for ACP. The focus of this study is on two of the above-mentioned performance parameters, namely resistance to cyclic temperature changes, and resistance to low temperature cracking in addition to tensile strength.

ACP is typically laid in different lifts, or layers, depending on the desired final thickness, even though at the time of pavement design and evaluation all the layers are considered as one thick layer that is totally bonded together. Adequate bonding between construction lifts is critical if the completed pavement structure is to behave as a single unit and provide the required strength. If adjoining layers do not bond, they are essentially multiple independent layers and are not equipped to accommodate the anticipated stresses, including traffic-imposed bending stresses. Kruntcheva et al. (2006) studied the properties of asphalt concrete layer interfaces and showed that the bond strength of interfaces between different contacting materials is influenced greatly by the pressure applied during compaction. In this research, the interlayer pavement bonding will be studied as pavement goes through temperature cycling.

In addition to interlayer bonding, another important performance requirement for ACP, particularly in cold regions, is the ability to withstand substantial temperature cycles, i.e., resistance to cyclic temperature changes. ACP in Canada and the northern regions of the US is subjected to temperature cycles, where the temperature for several weeks at

the beginning and end of winter cycles from above to below freezing, and vice versa. For example, most cities in the southern areas of Canada experienced more than 60 days during 2019 with such temperature cycles, where the temperature rose from below to above freezing and then went back to below freezing within 24 hours (i.e., Ottawa 86 days, Montreal 82 days, and Toronto 87 days) (Environment and Climate Change Canada, 2019).

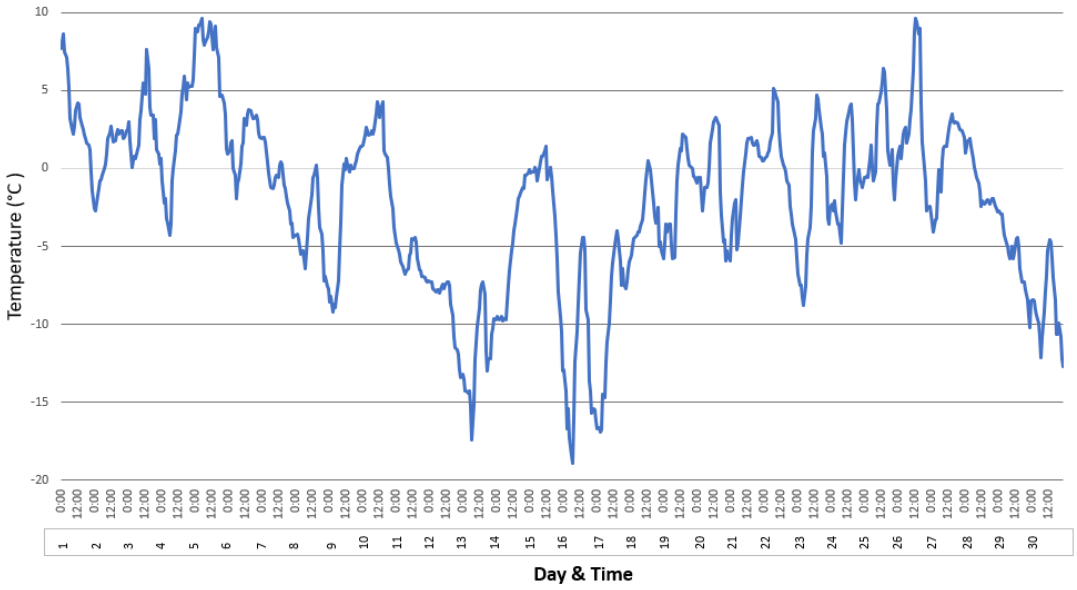

Figure 1-2. City of Ottawa Temperature (°C), November 2019

These repeating temperature cycles and temperature variations, which cause expansion and contraction in ACP, can lead to mechanical stresses and cause asphalt failure. Therefore, the ability to withstand substantial temperature cycles is listed among asphalt pavement's performance parameters, and the study of potential negative impacts of temperature cycling on pavement performance has become of special interest to the author, and is also one of this thesis's objectives. Furthermore, current tests for Superior Performing Asphalt Pavements (Superpave) do not offer any test method to measure the

capability of asphalt pavement to withstand temperature cycles, and such a test could have the potential to be considered for the quality control of asphalt pavement in the future.

After pavement has gone through the above-mentioned temperature cycling, it is inevitable that pavement in these areas must face the cold and relatively long winters and resist against low-temperature cracking. The status of ACP after completing those harsh temperature cycles will be crucial to its ability to withstand the thermally induced tensile stress due to pavement's tendency to contract with decreasing temperature. Therefore, resistance to low temperature cracking is another ACP performance aspect. Superpave asphalt binder tests pay fair attention to the asphalt cement properties that can influence low temperature cracking. Research has shown that low temperature cracking is a major distress in cold regions (Tabatabaee et al. 2012). ACP can also crack very early on, i.e., at the construction stage, thereby reducing the strength and fatigue resistance of the ACP layer and facilitating further crack development. Therefore, there is a growing need to evaluate the cracking resistance of ACP. Numerous studies have shown that cracking is the predominant failure mode in the northern US and Canada (Marasteanu et al. 2007; Hesp et al. 2009). Cracking is expensive not only in terms of the costs related to repairing the cracks, but also because it can significantly shorten pavement life and/or cause a very uncomfortable ride (Gavin et al. 2003). An internal audit by the MTO in 2000 identified significant pavement cracking throughout Ontario years before it was expected, resulting in increased cost to taxpayers for highway repairs or repaving (Auditor General of Ontario, 2018). The 2016 audit by the Office of the Auditor General of Ontario identified several

highway projects where pavements had to be fixed for cracks much earlier than their expected life of 15 years, and some as early as only one year after the highway was open to the public, and the cost of premature cracking that the Ministry paid to repair these highways was found to be in the millions of dollars (Auditor General of Ontario, 2018). A stiffer mix was used by designers to mitigate rutting issues in the early life of HMA, but this in practice caused more reflective cracking and has not helped reduce cracking resistance (Roberts et al. 2002). Researchers have since developed Superpave, an alternative system to the Marshall method for specifying material components and asphalt mix design using the Superpave Gyratory Compactor (SGC), and other mix designs intended to increase pavement lifecycle (Roberts et al. 2002). Although studies have showed that these efforts did improve the product marginally, they did not delay early deterioration (Figure 1-3). ACP can crack very early in the process (i.e., at the construction stage), thereby reducing the strength and fatigue resistance of the asphalt layer, which can facilitate further crack development. Hairline cracks will expand, and subsequently, areas with minor cracking might then have extensive cracks, and areas of slight depression or minor damage could become potholes. Studies show that cracks forming in the pavement surface allow infiltration of damaging substances, including water, impurities (chlorides, de-icing chemicals, fuels), debris, and oxygen, all of which can accelerate the failure of pavement surfaces and reduce serviceability. Thus, the later asphalt pavement cracks, the later further deterioration takes place and the longer its service life. Therefore, there is a growing need to evaluate the cracking resistance of asphalt mixtures. This was one of the reasons that studying the tensile strength and

cracking resistance of ACP at 0°C, -10°C, and – 20°C temperatures became another objective of this thesis.

Figure 1-3. Example of Cracks on Asphalt Pavement only 2 years after Construction

Furthermore, the sampling and testing required to evaluate pavement characteristics are significant challenges that asphalt researchers and the industry are faced with. Many road authorities are switching to the Superpave volumetric mix design system in an effort to extend the service life of asphalt pavement; however, this mix design and the QA/QC tests associated with Superpave are mostly based on gyratory-compacted laboratory samples. In the author's view, the mechanism by which SGC compacts HMA has very little in common with the steel roller compaction used in road construction, and therefore the HMA is not treated equally by these two machines in reaching the required density. As a consequence, the differences involved could result in different HMA performance. The performance of steel rollers may not be simulated closely in asphalt laboratories by the SGC, and therefore gyratory-prepared samples could

have different characteristics and crack resistance than those extracted from actual roads (Arraigada et al. 2018). To evaluate the performance of asphalt pavement, instead of using gyratory-compacted laboratory samples, a new special direct tensile strength test for rectangular samples extracted from road projects was proposed. This test utilized a machine assembled in an environmental chamber. This special direct tensile strength test method and proposed equipment have shown promise as tensile and bond strength evaluation tools (Abd El Halim et al. 1990a, 1990b; Raab et al. 2009). The use of gyratory-compacted samples will not allow researchers to study the quality of the compaction received on the job site by actual construction rollers, however to avoid this weakness and to study the effect of different compaction methods on the key performance parameters of asphalt pavement, gyratory-compacted samples were avoided throughout this research and rectangular samples extracted from road projects were used for testing programs of this research.

Compaction also affects the performance of ACP, and this has long been recognized as an important factor in long-term ACP performance. The technique, magnitude, duration, and direction of compaction all have effects on the resulting pavement structure (Nevitt 1957). Today, compaction is the only aspect of the ACP process that has not been changed or improved since the start of its utilization in ACP construction in the late 19th century; steel rollers have been used since the first hot-laid surfaces were placed. Historically, a heavy cylinder rotating around a central axis to pack the materials and flatten the surface was utilized for flattening and compacting the different pavement layers, including asphalt concrete. Light rollers are pushed or pulled

manually by workers. The first rollers that were used in road construction were animal-drawn, and later became self-powered vehicles. Currently, compaction rollers in ACP construction refer to using a combination of the three rollers used in the same construction job, which are:

Steel-drum rollers (Figure 1-4)

Pneumatic-tire compaction rollers, rubber tire (Figure 1-5)

Vibratory or oscillating rollers (Figure 1-6)

Figure 1-4. Examples of Traditional Steel Drum Rollers (SDR)

The Steel-Drum Roller (SDR) is considered as the main roller for current ACP conventional compaction method (CCM), as it quickly increases the density of fresh asphalt by compressing the underlying HMA, and is usually the preferred machine for the initial breakdown pass in most applications.

Figure 1-5. Example of Pneumatic-tire Compaction Rollers (rubber tire).

Figure 1-6. Example of Oscillating Rollers.

Although problems with compacting asphalt mixes have generally been ascribed to the mix alone, Abd El Halim et al. (1990a) showed that surface cracks initiated by a steel wheel roller could explain the frequent reports of early deterioration and performance decline of ACP. They also found that construction cracks can significantly reduce the resistance of pavement to thermal stresses and accelerate deterioration. The

forces applied by a heavy, slow-moving conventional steel roller on a small curved contact area create intense pressure, typically 1.3 MPa, on the asphalt surface. Furthermore, due to the pushing and pulling of the asphalt mat in front of and behind the drum, the steel roller creates horizontal forces which result in the creation of microcracks at the time of construction.

Abd El Halim et al. (1990a, 1990b) introduced a new compaction method for asphalt pavement that uses an Asphalt Multi-Integrated Roller (AMIR), where the cylindrical shape is replaced with a moving flat surface (Figure 1-7 & Figure 1-8). Results of different field experiments have shown that AMIR produces pavements with less water permeability (Igboke et al. 2020; Awadalla 2015; Abd El Halim 2016) and more uniform compaction along and across the mat while achieving the required density with fewer passes compared to conventional compaction using steel rollers (Raab 2019; Omar Abd El Halim 2015; Awadalla et al. 2017; Chelliah 2019).

In this research, these two compaction methods (CCM and AMIR) were compared while evaluating the ability of ACP to withstand temperature cycles.

Figure 1-7. Asphalt Multi-Integrated Roller (AMIR), August 2019

Figure 1-8. Asphalt Multi-Integrated Roller (AMIR), 2017

1.2 Problem Statement and Research Questions

This research focuses on asphalt's ability to withstand temperature cycles, and will address the following questions:

1. How is the interlayer bonding of ACP affected by thermal cycling and temperature changes?
2. Do compaction methods affect the capability to withstand temperature cycles and maintain interlayer bonding? Which of the compaction methods (CCM or AMIR) provides better interlayer bonding and superior temperature cycling resistance?

After evaluating the bonding for ACP that has experienced temperature cycles above and below zero, the next question is how these samples' tensile strength changes when the ACP is subjected to low temperatures for longer times. The focus of the second phase of this research is on the cracking resistance and tensile strength of asphalt pavement at low temperatures (0°C, -10°C, or -20°C), and will address the following questions:

3. How does ACP's tensile strength change at low temperatures?
4. Does the compaction method affect the tensile strength and bonding between pavement layers? For this research, the hypothesis is that the difference between the average strength for samples *"with construction-induced cracks"*, and that for samples *"without construction-induced cracks"* is significant.

1.3 Research Objectives

This study focuses on resistance to cyclic temperature changes, resistance to low-temperature cracking, and also tensile strength. Specifically, the study examines the interlayer bond between ACP layers under the effect of temperature cycles fluctuating above and below freezing. An experiment was designed to study potential debonding early in the ACP life. The loss of interlayer bond could weaken the tensile strength of the pavement structure and eventually shorten pavement life. Thus, the first objective of the testing program in this study was to assess the effect of temperature cycles on ACP interlayer bonds constructed using different compaction equipment. Specifically, the experiment used samples compacted in the field with the conventional compaction method (CCM), which involves using a train of vibratory rollers, pneumatic rollers, and static steel rollers, and other samples also compacted in the field using AMIR, which does not require the use of other rollers in the compaction process. Each sample tested in this phase of the program comprised two layers of hot-mix asphalt (HMA) constructed according to the practices of the Ministry of Transportation of Ontario (MTO). These samples will be referred to as double-layer samples, and this first phase of testing is referred to as Testing Series A. The aim is to improve the understanding of the role that temperature cycling and compactors play in the interlayer bonding and tensile strength of ACP, and their impact on the long-term performance of asphalt pavement.

The experiment was designed to also investigate the pavement strength under low-temperature conditions in the cold winter season if the bond survives the temperature cycles in the beginning of the winter season, since if the pavement layers

are debonded, the individual layers would contract independently from each other during the cold winter season. Therefore, the second objective of this research is to study the tensile strength of asphalt pavement that has already undergone periods of temperature cycling, and study how the samples behave when subjected to different low temperatures for sustained periods of time in the winter season. The tests in this second phase, referred to as Test Series B, involve tensile stress testing of slab ACP samples under constant temperatures. Both the single- and double-layer samples are tested in this phase. In this part of the research, the asphalt's conventional compaction method (CCM) will be examined to study the effect of construction-induced cracks created by CCM on the tensile strength and interlayer bonding of asphalt pavement.

The other objective of this study is to propose simple and practical performance-related test methods for:

- Resistance to low-temperature cracking (measuring the effect of cracking on the tensile strength of HMA)
- Ability to withstand fluctuating temperatures
- Evaluating interlayer bonding

The intent is to propose a simple performance test that can be routinely performed during the construction or laboratory mix design process and production. The aim is to introduce new sampling and testing methods in order to use samples from actual roads and test them by simulating the field conditions and replicating the field loading, temperatures, and boundary conditions as closely as possible. In the laboratory mix design, the results obtained from this proposed test method can be used to determine if

the HMA is susceptible to premature cracking, and also to determine the capabilities of the proposed mix in withstanding temperature cycling. In field quality control, this proposed test method can assess of the quality of the placement and compaction processes.

1.4 Significance and Contribution to the Discipline

- A key finding of this study will shed light on the important role that ACP's ability to withstand fluctuating temperatures plays in shortening or extending the life of the pavement.
- The other key finding of this study is to propose two new test methods and design and build the required apparatus, and also to test ACP samples with these test methods and present the results. These two new relatively simple test methods are used to evaluate key HMA performance parameters, including cracking resistance, tensile strength, resistance to low-temperature cracking, and ability to withstand fluctuating temperatures.
- Another important finding of this research is that it illustrates the effects of construction cracks on the tensile and bond strength of asphalt pavement, and how the research shows the significance of the effects of different compaction roller types on tensile and bond strength. The tests and results provide a better understanding of the failure mechanisms and highlight the significance of construction methods on the service life of asphalt pavement.

- Lastly, the sampling method presented and used for this research, i.e., by using samples from actual road projects, could be a practical alternative to sampling methods currently in use in the asphalt industry. The proposed sampling method allows the quality of the compaction asphalt receives during construction to be examined, instead of trying to simulate the compaction in the laboratory.

1.5 Research Scope and Organization

The scope of the research is limited to HMA prepared as per Ontario Provincial Standards (OPS) and placed in accordance with the guidelines of the Ministry of Transportation (MTO) in eastern Ontario (Ontario Provincial Standard Specifications OPSS 310 ,2016). Only two types of asphalt compaction methods are reviewed: the Conventional Compaction Method (CCM) with steel drum rollers, and Asphalt Multi-Integrated Roller (AMIR).

This proposal consists of four chapters. Chapter 1 contains the introduction to this research, listing research questions, research objectives, and contributions of the results of this study to the discipline. Chapter 2 presents the literature review related to this research, wherein asphalt distresses are briefly reviewed and a summary of asphalt distresses and their relationship to compaction, interlayer bonding, temperature cycles, and loads is presented. Key performance parameters of asphalt mixes are presented, and then the effects of compaction on the results of the performance tests are reviewed. Subsequently, the effects of temperature, compaction, and interlayer bonding are reviewed before presenting the previous and current test methods and sampling

methods. The current asphalt mix performance test methods are also discussed. Chapter 3 presents the research plan and describes in detail the experimental investigations completed during this study. The proposed test methods are described in detail in this chapter. It also has details of the apparatus used for Test Series A (TCT) and Test Series B (direct tensile strength test) as well as how the apparatus for the temperature cycling tests, Carleton University Asphalt Temperature Cycling (CUATC), was designed, built, and used for Test Series A. Chapter 4 presents the results obtained from the field and laboratory investigations as well as the analysis conducted, along with discussion of the obtained results. Chapter 5 summarizes the findings, conclusions, remaining research tasks, and recommendations for future research.

Chapter 2. Literature review

Asphalt concrete pavement is a composite material made up of different gradations of aggregates bound together by the use of bitumen (also called asphalt cement (AC)/ asphalt binder). The properties and performance of ACP are affected by the combination of these components, their separate properties, and their preparation and placement methods. This research aims to study the effect of temperature cycling on pavement interlayer bonding as well as the impact of different compaction methods (CCM vs AMIR) on such bonding. Furthermore, this work seeks to study the tensile strength and bonding of asphalt pavement in temperatures from +20°C to -20°C, using samples from actual highway projects rather than those produced in a laboratory. In addition, a relatively simple performance-related test method is also proposed to evaluate the asphalt end-product after placement and compaction.

2.1 Organization of Chapter 2

To start, the asphalt pavement distresses are reviewed (Section 2.2), and the different distresses and their relationship to compaction, interlayer bonding, temperature cycles and external loads are summarized and presented (Section 2.2.6). Then, the key performance parameters of the asphalt mix are listed (Section 2.3). The effects of compaction on the performance of the pavement, as well as previous studies regarding the relationship of different asphalt distresses to compaction (Section2.5), are reviewed before studying the interlayer bonding (Section 2.7), temperature cycle testing (TCT) (Section2.8), and thermal cracking (Section 2.9). Furthermore, important factors related to this research, including the role of compaction (Section 2.5) as well as the

significance of the sampling method (Section 2.10) and current laboratory compaction methods for sample preparation (Section 2.11) are reviewed. After that, current asphalt mix performance test methods used by various testing agencies (Section 2.12 and Appendix C) are studied. After that, simple asphalt performance test methods are reviewed (Section 2.13). The current performance tests for each key Hot Mix Asphalt (HMA) performance parameter (i.e., rutting, cracking and fatigue resistance potential, low temperatures, stiffness, and moisture sensitivity) could be found in Appendix C.

2.2 Asphalt Concrete Pavement Distresses

Pavement engineers analyse and diagnose possible causes of asphalt pavement distress and recommend the most effective corrective approaches.

Figure 2-1 Example of asphalt pavement with multiple types of the distresses

In this section, different asphalt pavement distress types are reviewed. Awareness of the interaction of distress types with compaction and bonding will help researchers diagnose the causes of distress and recommend appropriate remedies. The Distress Identification Manual for a Long-Term Pavement Performance Project (LTPP) by Miller and Bellinger (2014) groups distress types into the following categories:

- Cracking
    - Fatigue Cracking

    - Longitudinal Cracking
    - Block Cracking
    - Edge Cracking
    - Transverse Cracking
    - Reflection Cracking
- Surface Deformation
    - Settlement (Grade Depression)
    - Rutting
    - Shoving/ Slippage Cracks/ Corrugation
    - Upheaval (Swell)
- Surface Defects
    - Polished Aggregate
    - Raveling
    - Stripping
    - Bleeding
- Potholes and Patching
    - Potholes
    - Patch/Patch Deterioration/ Patch Failure
- Miscellaneous Distresses
    - Lane-to-Shoulder Dropoff
    - Water Bleeding and Pumping

2.2.1 Cracking

Fatigue Cracking (e.g. Alligator)

Fatigue cracking involves a chain of interconnected cracks caused by the failure of an asphalt surface or base under cyclic traffic loading (Huang 1993), and typically occurs in areas subjected to repetitive traffic loading. This major pavement structural issue, which involves load-associated distress mechanisms, can be initiated by weaknesses in the surface, binder, or sub-grade, a surface or binder that is too thin, poor drainage, ineffective compaction, or a combination of these.

Figure 2-2. Example of pavement with alligator cracks

Longitudinal Cracking

Longitudinal cracks are parallel to the pavement centerline or laydown direction. According to Zhang et al. (2015), air voids, effective binder content, and PG grade are significant influences. Poorly constructed paving joints, longitudinal segregation caused by improper operation of the paver, reflective cracking, and daily temperature cycling are other causes for longitudinal cracking. These cracks, particularly when they are under the

Figure 2-3. Example of pavement with longitudinal Crack

wheel path, can be the early phase of fatigue cracking (i.e., before the cracks become interconnected) (Park and Kim, 2015).

Block Cracking

Block cracks look like large, roughly interconnected rectangles. Block cracking is not load-related distress. Instead, they are caused by shrinkage of the pavement while expanding and contracting with temperature cycles (Freeman and Ragsdale, 2013). This could be due to old or dried-out mix or a poor choice of asphalt binder in the mix design.

Figure 2-4. Example of pavement with block cracks

Edge Cracking

Edge cracks are crescent-shaped, continuous cracks located within 600 mm of the edge of the pavement, just adjacent to an unpaved shoulder. Longitudinal cracks outside the wheel path are also considered as edge cracks. Edge cracks are typically compaction-related and caused by a lack of lateral support because of the weak material, excess moisture, and/ or inadequate compaction (Adlinge and Gupta 2013).

Figure 2-5. Example of pavement with edge cracks

Transverse Cracking

Transverse cracks are generally perpendicular to the pavement centerline or laydown direction and can be caused by reflective cracking and daily temperature cycling. Transverse cracks with uniform crack spacing can be due to low-temperature cracking or the asphalt grade being too hard for the climate conditions (Adlinge and Gupta 2013). Thermal cracking of HMA pavement is a non-load related distress, and could appear regardless of traffic loading. Most of the time, the cracks form perpendicularly to the centerline of the pavement. Because pavements contract as the temperature drops below freezing, stresses develop in the ACP, and when the developed stresses exceed the pavement's tensile strength, the pavement cracks. Also, as pavements age and become more brittle (due to asphalt binder hardening), ACP will be less flexible and eventually more vulnerable to thermal cracking.

Reflection Cracking

Reflection cracking occurs directly over a crack in the underlying pavement layer or in rigid pavement joints.

2.2.2 Surface Deformation

Settlement/Grade Depression (bird baths)

Depressions are localized pavement surface areas with slightly lower elevations than the surrounding pavement. "Bird baths" form naturally as the result of settlement due to insufficient compaction of the material under the asphalt layers during construction, and/or a localized low bearing capacity of granular layers beneath the asphalt. These shallow indentations in the asphalt can be dangerous when the

temperature drops and the water freezes. As well, areas with grade depression could be subject to other forms of asphalt distresses, such as small or large potholes or other types of cracks.

Rutting

A rut is a longitudinal surface depression (channelized depression) in the wheel path, and it could also have associated transverse displacement. Poor compaction of the asphalt, binder course, or subgrade during construction, insufficient pavement thickness, weak asphalt mix, or plastic fines in the mix that do not provide enough stability to support traffic are among the reasons for rutting.

Shoving/ Slippage Cracks/ Corrugation

Shoving is indicated by crescent-shaped cracks or tears in the surface asphalt layer(s). It is longitudinal displacement of a localized area of the pavement surface that forms ripples across the pavement. It is generally caused by braking or accelerating vehicles, and is typically located on hills or curves or at intersections; it can also have an associated vertical displacement. Shoving cracks are the result of new material that has

Figure 2-6. Example of pavement with slippage cracks

moved over the underlying course due to insufficient bonding between layers (Adlinge and Gupta, 2013).

Upheaval (Swell)

Upheaval is a localized upward movement in pavement caused by swelling of the subgrade. It can be caused by expansive soils that swell due to moisture or frost heave (i.e., ice under the pavement).

2.2.3 Surface Defects

Polished Aggregate

Polishing is usually caused by repeated abrasion of the asphalt surface due to traffic, which smooths the sharp edges of the coarse aggregate and wears away the surface binder to expose the aggregate. The tendency of the aggregate to polish or resist is related to its geological source. When aggregates are polished, their skid resistance is decreased, which is a severe deficiency particularly for roads with high-speed traffic (Lavin, 2003).

Raveling

Raveling (i.e., dislodging aggregates caused by stripping) is a depletion of surface material and ongoing separation of aggregate particles in pavement that wears away the asphalt pavement surface. It is also a sign of pavement aging (Huang 1993).

Figure 2-7. Raveling in Asphalt Pavement

Stripping

Stripping is the displacement of asphalt cement film from aggregate surfaces by water. It typically starts at the bottom of the compacted bituminous layer, where the tensile stresses are greatest due to cyclic loading, and it moves upward to the surface (Tunnicliff and Root, 1984). Stripping is difficult to detect since it usually begins at the bottom of the bituminous layer and can resemble other distress mechanisms (e.g., fatigue cracking).

Bleeding

Bleeding is excess bituminous binder on the pavement surface, usually found in the wheel paths.

2.2.4 Pothole and Patch

Pothole

Potholes are probably the most well-known form of pavement distress. These bowl-shaped depressions of various sizes in pavement surfaces are the end of the development cycle of most types of pavement distress. As potholes are typically the result of other distresses, it is difficult to diagnose the cause precisely. The functional failure of potholing can require costly repair work (de OS and Carlos 1991).

Figure 2-8. Asphalt pavement with pothole

Figure 2-9. Asphalt pavement with pothole

Patch/Patch Deterioration/ Patch Failure

A patch is normally an area of pavement surface that has been removed and replaced, or where additional material has been applied after the original construction.

Figure 2-10. Asphalt pavement with several patches

2.2.5 Miscellaneous Distresses

Lane-to-Shoulder Dropoff

This distress is a lip caused by an elevation difference between the edge of a paved lane and the surface of the shoulder. The lip is about equal to the

thickness of the top course of asphalt on a finished lane. This condition can be hazardous to motorists and is a safety concern.

Water Bleeding and Pumping

Water bleeding is when water seeps or flows beneath the pavement through cracks and joints at the surface, and pumping is when water is driven out of the asphalt due to moving loads. These types of distress can have different causes, including poor drainage, high water tables, permeable pavement due to inadequate compaction during construction, or poor mix design.

2.2.6 Summary of Asphalt Pavement Distresses

Table 2-1 is a summary of asphalt distresses and their relationship to compaction, interlayer bonding, temperature cycles, and load. As illustrated in this table, several important and common asphalt stresses like fatigue cracking, settlement, and raveling are related to compaction.

Table 2-1- Summary of asphalt distresses and their relationship to compaction, interlayer bonding, temperature cycles, and loading

Asphalt Distress Category	Asphalt Distress	Is the distress related to **compaction**?	Is the distress related to asphalt **interlayer bonding**?	Is the distress directly related to **temperature cycles**?	Is the distress **load** related?
Cracking	Fatigue Cracking	Yes	Yes	Yes	Yes
	Longitudinal Cracking	Yes	-	-	
	Block Cracking	-	-	Yes	No
	Edge Cracking	Yes	-	-	-
	Transverse Cracking	Yes	-	Yes	No
	Reflection Cracking	-	-	Yes	Yes
Surface Deformation	Settlement	Yes	-	-	
	Rutting	Yes	-	-	Yes
	Shoving/Slippage	-	Yes	-	Yes
	Upheaval (Swell)	-	-	-	-
Surface Defects	Polished Aggregate	-	-	-	Yes
	Raveling	Yes	-	Yes	Yes
	Stripping	-	-	-	-
	Bleeding	-	-	-	-
Potholes & Patching	Potholes	Yes	Yes	Yes	Yes
	Patches	Yes	Yes	Yes	Yes

2.3 Key Performance Parameters of Asphalt Mix

The Superpave mix design system (AASHTO MP2 and PP28), introduced by the United States' Strategic Highway Research Program (SHRP) and which ran between 1987 and 1991, is based on mix volumetric properties. Asphalt performance tests are used to relate laboratory mix designs to actual field performance. The HMA design method used in the Superpave method has 3 phases: (1) asphalt binder and aggregate material

selection; (2) aggregate blending and volumetric mixture design; and (3) compacting samples in the laboratory using a Superpave Gyratory Compactor (SGC) and performing volumetric analyses on HMA samples. Unlike the Marshal and Hveem mix design methods, tests of Superpave to evaluate the performance of designed asphalt mixture methods have not yet been implemented (Witczak et al. 2002). For traffic volumes exceeding 10^6 equivalent single-axle loads (ESALs), the Superpave mix design procedure requires the relatively complex AASHTO TP7 and TP9 tests to be performed. AASHTO TP7 is performed to check for creep behaviour (with the repeated shear at constant stress ratio test), and AASHTO TP9 is performed to check on the potential of the mix design for permanent deformation, fatigue cracking, and low-temperature cracking. The U.S. Federal Highway Administration (FHWA) has made several attempts to identify and recommend a simple test method (for HMA mixes, and not asphalt binder) that should provide reliable information on the probable performance of an HMA design during the volumetric mixture design process by using the SGC to compact the asphalt materials in the laboratory. The focus of all the proposed and evaluated tests was to determine and quantify the main properties of HMA that can be used in a distress-prediction model to relate those properties to material (aggregate and binder) characterization. Essentially, the aim was to find a simplified test method to assist designers during the design stage when using the Superpave method, and it was always anticipated that those simple performance test methods would be used for the quality control of the end products.

Currently, the Superpave design method has performance tests for asphalt binders but it does not have any official performance tests to complement a designed

asphalt mixture. The need for the incorporation of asphalt mixture performance testing for design and construction QA to improve the performance of all asphalt mixtures has been recognized by the FHWA and the asphalt paving industry. One of the objectives of this research is to develop a simple testing method to evaluate the performance of asphalt pavement after it has been compacted in the field. The intent of HMA performance testing is to develop a simple and inexpensive test that can be routinely used to assess the key HMA performance parameters and play a role in the quality control and acceptance of HMA mixtures. However, researchers have different views of what the key HMA performance parameters actually are. Rutting, fatigue cracking, and thermal cracking have been named by the asphalt industry experts as among the important distress types to be measured by any future simple performance test (SPT).

Below are some of the parameters that are considered as key HMA performance parameters (Witczak 2002; Zhang et al. 2016; Blab 2013; Birgisson et al. 2003; Sánchez-Leal 2007; Izzo and Tahmoressi 1999; Kandhal 1992; Chen and Huang 2008):

- Deformation resistance (rutting)
- Fatigue and cracking resistance
- Resistance to low temperature cracking
- Stiffness
- Moisture susceptibility

The above parameters are not listed in order of importance, and sometimes researchers combine two or more parameters and report them as one. For example, some report stiffness and fatigue cracking resistance under one category. The author

believes that another important performance parameters, especially for cold regions, to be added to the above list is:

- Ability to withstand fluctuating temperatures

2.3.1 Rutting

Deformation resistance (rutting) is an important performance parameter of asphalt pavement. Though it largely depends on mix design, it could also be influenced by construction methods, such as compaction (Gibb 1998).

2.3.2 Fatigue and Cracking Resistance

Resistance to fatigue cracking is another important performance parameter, and it depends not only on the structural design of the mix, but subgrade support, quality of construction, and compaction method as well (Ziari et al. 2019; Pell 1967; Monismith and Deacon 1969). Therefore, properties that can influence fatigue cracking are important for evaluation to extend the life of asphalt pavement.

2.3.3 Resistance to Low Temperature Cracking

Good fracture properties are an essential requirement for ACP, especially in cold regions in which cracking due to high thermal stresses that develop at low temperatures is a major failure mode. This is focus of this study and the subject of Test Series A of this research.

2.3.4 Stiffness

The HMA stress-strain relationship, characterized by elastic or resilient modulus, is also an important ACP performance parameter. Stiffness of the HMA is so important

that some research has suggested that it be used as a simple performance test (SPT) parameter to complement the Superpave volumetric mix design (Pellinen and Witczak 2002). Dynamic modulus was recommended by Pellinen and Witczak (2002) as the SPT parameter for rutting as well as for fatigue cracking.

2.3.5 Moisture Susceptibility

Moisture can damage asphalt mixtures in several ways, including adhesive bond failure between the aggregate surface and asphalt binder and cohesive failure within the asphalt mix. Currently, several deformation resistances, such as Hamburg Wheel Tracking, and tensile strength tests (i.e., AASHTO T283/ ASTM D4867) are used to evaluate the moisture susceptibility of HMA mixtures.

2.3.6 Ability to Withstand Fluctuating Temperatures

Pavement placed in cold regions is subjected to temperature cycles where the temperature for several weeks of each year cycles from above to below freezing, and vice versa. These temperature cycles can lead to mechanical stresses. This performance parameter is also a subject of this study.

2.4 Tensile Strength

Tensile strength is a material property of HMA mixtures, and it has a great impact on most ACP performance parameters (since it is related to pavement cracking). The tensile behaviour of compacted ACP plays an important role in asphalt performance, as compacted ACP layers can suffer from cracking due to tensile failure. For example, “bottom-up” cracking begins at the bottom of the asphalt surface where the tensile stress or strain is highest under the wheel load, and the cracking then propagates upwards

toward the surface, where visible cracks appear. The tensile strength of asphalt is even more important for areas with low temperatures, and this is one of the topics focused on in this study.

2.5 Compaction and its Role in Performance Tests

Asphalt compaction also affects ACP performance, and has long been recognized as an important factor in the long-term performance of ACP. The compaction technique, magnitude, duration, and direction have consequential effects on the resulting pavement structure (Nevitt 1957). Several studies (Lees et al. 1969, Paterson 1974, Harvey et al. 1997) have confirmed that the final orientation of aggregate particles can differ with the method of compaction, which in turn influences the ACP performance. Geller (1984), who studied the development of different types of compaction equipment, indicated in his research that “compaction has always been emphasized as perhaps the single most important factor for achieving satisfactory pavement service life." Geller’s research also highlights the importance of the field compaction details (i.e., roller pattern) and the inability to predict pavement performance and behaviour before knowing the details of compaction that asphalt mix is going to receive. Finn and Epps (1980), via their laboratory and field studies, highlighted the importance of reaching high densities in HMA at the time of construction. Results of another study by Finn (1967) demonstrated that all desirable mix properties could be improved by a high degree of compaction. The results of the test program by Bell et al. (1984) showed that the most significant factor affecting mix performance is the percent compaction. The results of their study indicated that an increase in void content is correlated with a decrease in resistance to permanent

deformation and fatigue life of asphalt pavement. Hughes (1989) showed that better compaction can enhance strength, resistance to deformation, impermeability, and durability of asphalt. Hughes underlined the significance of asphalt cement properties, aggregate properties, and mix properties on the ability to reach the desired level of compaction. The findings of Aschenbrener et al. (2019) illustrate that test sections where contractors achieved the higher density, resulted in better quality HMA per the standard specifications of their road authority. Aschenbrener and Tran (2020) concluded that the most important factors affecting the long-term performance of asphalt pavements is in-place density of HMA, which is obtained through field compaction. If mechanical testing of asphalt mixture pavement is to be effective, it is very important that the samples being tested are representative of the asphalt pavement in its compacted state at the construction site.

Linden et al. (1989) suggested that both fatigue cracking and age-hardening of dense asphalt concrete mixtures is intensified by inferior compaction (with a high level of air voids). Increases in permeability and water infiltration due to pavement distress or improper compaction can also cause de-bonding of pavement layers, according to the findings of Muench et al. (2008), who gathered evidence on de-bonding in Washington State. It is important to note that problems with compacting asphalt mixes have generally been attributed to the mix alone by many asphalt pavement researchers.

Awadalla et al. (2017) conducted a study to evaluate pavement field permeability and core extraction at eight sites in eastern Ontario, in Canada. They performed indirect tensile strength, lab permeability, and relative density tests on field-recovered cores, and

their findings highlight the relationships between the relative density, permeability, and indirect tensile strength of ACP. The test results confirm that when relative density and indirect tensile strength decreases, the permeability increases exponentially.

Several studies have confirmed the importance of effective ACP compaction and its relationship to ACP performance. Current compaction equipment, such as steel roller compactors, have caused concerns regarding their side effects and negative impact on ACP performance. Abd El Halim et al. (2008) showed that surface cracks caused by a steel wheel roller could explain the frequently reported early deterioration of asphalt pavements. Applying a mechanistic approach, the authors explained how the applied forces of a heavy, slow-moving roller and the small curved contact area apply extreme pressure (typically 1.38 MPa) on the asphalt surface. The steel drum rollers both push the mat in front of the drum and pull the mat behind the drum. This process also creates horizontal forces that can generate hairline surface cracking on fresh asphalt layers. Even though pneumatic rollers (or rubber tire rollers) help seal the asphalt surface and reduce voids, they do not eliminate the hairline cracks created by a steel wheel roller, so the cracks remain on the surface. If the ACP cracks very early in the process (i.e., at the construction stage), strength and fatigue resistance are reduced, which can facilitate the development of other pavement distresses and reduce the pavement's life. The authors also found that construction cracks significantly reduce the resistance of pavement to thermal stresses and accelerate deterioration.

Steel-drum rollers (Figure 1-4 and Figure 1-6) are self-propelled compaction devices that generally have two drums. The drums can be either static or vibratory. Roller

weight is typically between 1 to 18 tonnes. Due to the important role of Steel-Drum Rollers (SDRs) in current asphalt compaction procedures, compaction done with traditional compaction rollers is sometimes called a Conventional Compaction Method (CCM). Traditional Steel-Drum Compaction Rollers (TSDCR) and Traditional Compaction Rollers (TCR) are also other names used for SDR by the asphalt industry and researchers. In this document, any reference to asphalt compacted with a Steel Drum Roller (SDR) or CCM means that the asphalt is compacted with the above-listed three types of roller (static smooth, vibratory, or oscillating and pneumatic tire) in accordance with MTO standards and specifications.

Rajendran Chelliah (2019) studied compaction methods and reported that both the AMIR and CCM compaction methods can meet the required minimum percent of compaction required by the OPSS 313; however, AMIR-compacted pavement has at least 6% higher strength in Falling Weight Deflector testing. Also, asphalts compacted with AMIR have less permeability in comparison with CCM. Furthermore, AMIR-compacted pavement showed a 19.5% higher indirect tensile strength when compared with CCM for the same mix.

2.6 Asphalt Multi-Integrated Roller (AMIR) Technology

In the 1980s, Professor Abd El Halim used a multi-layered rubber belt to create a single flat contact area for compaction, and brought his compaction concept into reality by inventing the Asphalt Multi-Integrated Roller (AMIR). The AMIR was tested in Egypt (1986), Australia (from 1997-2006), and Canada (from 1989 to 2020), and many studies had been completed reviewing its performance (including but not limited to Abd El-Halim and Svec (1990a, 1990b), Said et al. (2008), Raab et al. (2009), Abd El Halim et al. (2015, 2016), Awadalla (2015), Omar Abd El Halim (2015), Girardi et al. (2017), Awadalla et al. 2017, Raab 2019, Chelliah 2019, and Igboke et al. (2020). Unlike CCM rollers, which transfer stress in the form of intense pressure pulse for a very short duration of time through their circular shape steel tire, AMIR employs a multi-layered rubber belt to apply vertical pressure for a much longer duration. Abd El-Halim noted that an asphalt mat will receive the shape of the steel roller in CCM and deforms (a Sag span curve), and that compression of the soft hot layer of asphalt between dense base bottom layer and the top rigid steel roller will cause the formation of hairline construction cracks due to the relative rigidity concept. Since the base bottom layer and soft hot layer of asphalt could not be changed, the traditional steel rolling method was replaced by AMIR to overcome the problem, with promising results. The surface of ACP compacted with AMIR has a tighter texture compared with the surface of pavement compacted with CCM. The AMIR achieved better density distribution uniformity, less permeability, and was less costly, as it was replacing three rollers. AMIR-compacted ACP has shown superior performance

with a smaller number of passes (8-10 passes) in comparison with the CCM method, which uses three rollers with a combined total of 17-22 passes (Chelliah 2019).

2.7 Interlayer Bond

Research interest in interlayer bonding has existed for several decades. Debonding between adjoining layers results in a substantial reduction in the shear strength of the overall pavement structure, consequently making the asphalt pavement more vulnerable to cracking and other distresses (rutting, potholes, etc.).

Asphalt is normally placed in layers 50 mm to 70 mm thick (after compaction) and up to 200 mm (8”) in total, depending on the type of compaction equipment. Depending on the road pavement design and desired final thickness, ACP is typically placed in several lifts or layers. At the time of the pavement design and evaluation, it is always assumed that all of the layers are 100% bonded together, and they are considered as one thick layer. If the final compacted pavement structure is to behave as a single unit and provide the required strength, it is crucial that the adjoining asphalt layers maintain their bonds and do not separate throughout the life of the pavement. If adjoining layers become debonded, they are then basically just multiple independent layers just lying on top of each other, and are not prepared to carry the anticipated stresses.

Interface bonding is a combination of adhesion, friction, and mechanical interlocking between the layers, with the tack coat providing the adhesion. The tack coat is a thin bituminous liquid asphalt, emulsion, or cutback film applied between layers of HMA pavement lifts to promote bonding. Though interface bonds are affected by many

factors, the temperature of the interface and applied stress are the most significant. Many factors affect interlayer bond strength, including but not limited to (Romanoschi 1999):

- Temperature
- Normal pressure
- Tack coat type/ dilution/ application rate, application details (Das et al. 2017)
- Surface roughness (Tashman et al. 2008)/surface cleanliness
- Mix type

As is understood from the outcome of these various studies, a wide range of variables affect this ACP performance parameter. Each study focused on one or two of these variables, and therefore the results of the study are not general and are mostly specific to those study variables. To add to the complexity of the matter, studies are also done using different testing devices, shear rates, and specifications, and therefore comparing the results of different studies becomes challenging and sometimes not possible.

Loss of bonding results in reduced fatigue life (Shahin et al. 1986; Wills and Timm 2006; Harvey et al. 1997). Muench and Moonaw (2008) performed a relatively comprehensive study on bonding by analyzing 3,042 core logs. Out of the 3,042 cores, a minimum of 328 (10.8%) were documented as de-bonded. They concluded that de-bonding happened due to:

- An inadequately compacted surface layer or infiltration of water through surface distress (i.e., cracks, etc.)

- Poor tack coat application

The outcome of Muench and Moonaw's study is in line with several other studies showing the effect of construction method on the level of permeability of an asphalt surface layer (Abe El Halim and Mostafa 2006; Igboke et al. 2020; Rickards et al. 1999). These studies showed that pavements compacted with AMIR produce less permeable surfaces than ACP compacted with CCM. Therefore, it is expected to see better interlayer bonds for ACP compacted with AMIR.

Kruntcheva et al. (2006) studied the properties of asphalt concrete layer interfaces, and their research showed that the bond strength of interfaces between different materials is influenced greatly by the pressure received during compaction of the layers. Splitting of layers happened because, in order to achieve the desired fully bonded condition, a higher degree of compaction of the interfacing materials was required.

Xu et al. (2021) studied the interlayer bonding of ACP in different seasons, including the effect of temperature changes, and they concluded that interlayer bonds become weaker under the higher temperatures of summer when compared to winter temperatures. As a consequence of this, the upper layer has to carry a greater share of the horizontal tensile stresses induced by ambient temperature and external loading, and will become vulnerable to cracking and failure. The high temperatures in summer lower the interlayer bond strength between the upper and lower layers, and also raise the shear stress at the interlayer points.

Christiane Raab (2010), as part of her studies on the interlayer bonding of asphalt pavement, has reviewed and presented a great variety of existing interlayer bond-related test methods and procedures. Figure 2-11 presents an overview of the methods commonly used to assess interlayer bonds and other interfaces.

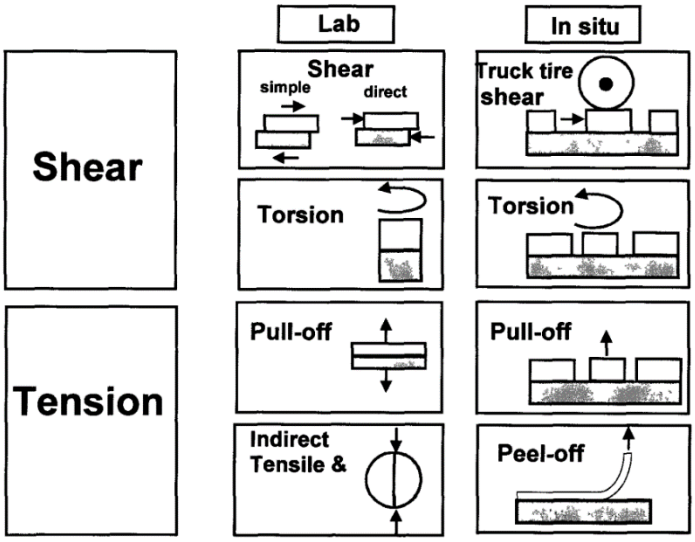

Figure 2-11. Test methods to determine interlayer bond properties in the lab and in the field (Raab and Partl 1999)

2.8 Temperature Cycle Testing (TCT)

On a typical early winter day in North America, the temperature begins to decrease in the afternoon and can drop from above zero to below zero Celsius. In many Canadian cities, temperatures could reach -5°C or lower at midnight between November and March, and become warmer in the morning when the sun rises. This temperature cycle occurs several times each year: at the end of autumn and the beginning of spring. Asphalt pavement in Canada and the northern US is subjected to daily temperature cycling from above zero to below zero every year. In addition to the temperature cycles

with normal drops and increases in temperature, there is also the potential for 'flash freezing', which is a rapid drop in temperature that typically occurs a few times a year. Below are a few examples of recent flash freeze events in the Ottawa area (Environment and Climate Change Canada, 2019):

- In Ottawa: from +6°C to -16°C, December 01, 2014.
- In Ottawa: from 1°C to -23°C, January 06, 2014.
- In Ottawa: from 5°C to -14°C, January 05, 2015.
- In Ottawa: from +1°C to -28°C, December 13 to 16, 2016.

The thermal cycling test is used to assess reliability of products in different industries (i.e., ceramics, coating, dental restorations, electronic systems) as one of the many environmental accelerated testing methodologies (Gale and Darvell 1999; Vassen et al. 2000; Andersson and Rowcliffe 1996). TCT helps researchers to study the thermal stability and thermal shock behaviour of materials and their ability to withstand thermal and mechanical stresses and eventually, failure (fatigue, etc.). For example, research done by Chow and Atluri (1997) on the effect of temperature cycling on aircraft structural panels found that specimens that undergo a thermal-mechanical cycle are more sensitive to de-bonding in the adhesive layer than similar specimens that undergo mechanical fatigue loading at a constant temperature. Also, the fatigue life of a specimen undergoing thermal cycles could be reduced by more than 60% in comparison with a specimen loaded at room temperature only. Temperature Cycle Testing (TCT) is usually performed to determine the capability of specimens to resist and withstand extremely low and/or high temperatures and cyclical exposure to these extremes. TCT can exacerbate fatigue

failures, which are mechanical breakdowns due to cyclical thermomechanical loadings (Delak et al. 1999; Szucs et al. 2007; Nemeth 2001. In general, thermal stressing created by these temperature cycling tests is of value to researchers in materials engineering fields, as it helps researchers to know if the bond between adjoining layers is reliable. Thermal cycling methods can accelerate the fatigue failures of samples consisting of multiple layers; this will assist those studying the service life of those materials.

2.9 Effect of Low Temperature and Thermal Cracking

Pavement design is based on historic (and will also soon be based on predicted future) climate patterns that reflect local weather, ranges of temperature, and precipitation levels. ACP, like most substances, expands when temperatures rise and contracts when temperatures decrease.

The surface of the pavement and the top segment of the top layer (i.e., 0-20mm) are the main areas that absorb or lose heat at faster rate than the rest of the pavement layer and are affected by the ambient and surface temperatures. The next area below this region will react to the heat gain or loss from the surface region and transfer it to the underlying areas. Consequently, the thermal tensile stresses induced throughout the thickness of the ACP are not uniform. These stresses are greater at the pavement's surface, as this part of the pavement is affected by the ambient temperature. The thermally induced stresses in the ACP gradually decrease from the top to the bottom. When contraction due to a temperature drop is prevented, tensile stresses generated in the asphalt material can cause it to fracture if the maximum tensile strength is reached.

Researchers have studied thermal cracking for years, and have applied numerous diverse methods to evaluate the low temperature behaviour of asphalt mixes. Understanding the relevant failure mechanisms and accurately predicting thermal cracking still remains a challenge. Several studies have attempted to describe the primary mechanism of various types of thermal cracking to predict the formation of cracks (Haas et al. 1987). Research by Tabatabaee et al. (2012) showed that low-temperature cracking is a major distress in cold regions. They proposed that excessive brittleness due to increased stiffness and diminished capability to adapt to stress generates a buildup of thermally induced stress that ultimately causes cracks in the pavement. Empirical models (Fromm et al. 1972; Chang et al. 1976; Haas et al. 1987) are based on field investigations and laboratory tests, and associate the spacing of cracks with major environmental factors and material properties. Most analytical models (Carpenter and Lytton 1975; Lytton et al. 1983; Hiltunen and Roque 1994) employ fracture mechanics to predict the propagation of thermal cracks. Timm et al. (2002) investigated several empirical and mechanistic models and found that they do not fully explain the factors leading to the consistently spaced cracks observed in the field. Bolzan and Huber (1993) conducted research to determine if running the Direct Tensile Test (DTT) regularly would provide suitable data for highway agencies; however, they selected temperatures from 4°C to 25°C, thereby limiting the testing to above-zero conditions.

Obviously, it is unavoidable that low-temperature cracking will occur for pavements constructed in the cold regions of the world and that all these pavements will suffer from thermal contraction cracking. Thus, it is understandable that pavement

engineers are eager to increase ACP's resistance against the mentioned thermal contraction cracking by different means. One of the most popular methods used to increase the cracking resistance of ACP has historically been improving asphalt concrete mixes. In this research, improving interlayer bonding and improving ACP compaction are studied to enhance ACP's thermal cracking resistance

2.10 Significance of Sampling Method

Sampling is just as important as testing, and precautions should be taken to obtain samples that represent the true nature and condition of the materials. Currently, most asphalt materials are sampled either at the point of manufacture (asphalt plant), when in storage (asphalt truck), or immediately upon delivery (from loose asphalt offloaded from a truck before being processed by the asphalt finisher). However, there should be additional sampling to control asphalt pavement end-products (in-service), and performance should be evaluated using samples from compacted asphalt pavement. As mentioned earlier, asphalt sampled from loose HMA taken at the hot mix plant, a loaded truck, or after delivery of HMA to a construction site behind the paver (before compaction) will not be able to show the quality of compaction received at the construction site. Generally, samples are taken for one of the following purposes:

- To represent, as closely as possible, the average bulk of the materials sampled; and

- To ascertain the maximum variation in the materials' characteristics.

In the view of the author, HMA sampled before being compacted at a construction site by construction rollers does not truly represent the asphalt end product, and if used

for performance tests, it may reflect results that are very different from the actual performance of the asphalt over its real lifetime. This highlights the importance of "asphalt sampling" in the process of proposing simple performance testing for ACP. Below are some current standards for asphalt sampling methods according to the American Society for Testing and Materials (ASTM):

1. D140 Standard Practice for Sampling Asphalt Materials. This applies to the sampling of asphalt materials at the point of manufacture (only loose HMA).
2. D979 Standard Practice for Sampling Bituminous Paving Mixtures at points of manufacture, storage, delivery, or in place. As noted in the standard, this practice should not be used to sample compacted bituminous paving mixtures (only loose HMA); for compacted bituminous paving mixtures D5361 to be used.
3. D5361 Standard Practice for Sampling Compacted Asphalt Mixtures for Laboratory Testing

ASTM D5361 is the main method for sampling compacted asphalt mixtures. It is a procedure to obtain a sample (core) of compacted asphalt mixture from a pavement for laboratory testing. To apply this standard, a core drill or power saw is recommended. As per this standard, for the quality control of asphalt construction projects, the extracted samples will be used later to measure the different properties of compacted asphalt pavement, including:

- Tensile strength (ASTM D6931, Indirect Tensile (IDT) Strength of Asphalt Mixtures)
- Stability:

    - Marshall Stability and Flow of Asphalt Mixtures, ASTM D6927
    - Hveem
- Resilient or dynamic modulus:
    - ASTM D7369, Determining the Resilient Modulus of Bituminous Mixtures by Indirect Tension Testing
- Pavement thickness and density
- Extraction testing to determine the mix gradation and asphalt properties

Figure 2-12. Field Core Sampling

The unique attribute of the D5361 standard is that it is designed to measure the properties of samples from compacted asphalt pavement on the construction site, not only laboratory-made samples. However, for field core samples (Figure 2-12), researchers are concerned with how the torque applied to the asphalt layer while drilling affects the interlayer bonds. This occurs when the core drill bit penetrates the upper asphalt layer and torques the mat on top; here, the bottom layer is still connected to the upper layer, and drilling could compromise the bonding between the layers. Therefore, the interlayer bonds of the field core samples might not accurately represent the average bonding of the materials sampled. Thus, the bonding between layers of actual in-service (field) asphalt pavement might be superior to the bonding in field core test samples.

2.11 Current Laboratory Compaction Methods for Sample Preparation

All current test practices that use samples prepared in the lab require the asphalt mixture to be compacted when attempting to simulate the compaction the mixture would undergo in the field. The goal of all current lab compaction methods is to prepare samples in the lab that have similar performance to those compacted in the field; that is, replicating samples that were compacted by actual compactors on site and establishing, as closely as possible, an average of the end product asphalt pavement in service. The main current test methods for compacting asphalt mix in the laboratory are listed below:

1. Compacting by Gyratory Machine (See Figure 2-13)
    a. ASTM D6925: Standard Test Method for Preparation and Determination of the Relative Density of Asphalt Mix Specimens using the Superpave Gyratory Compactor

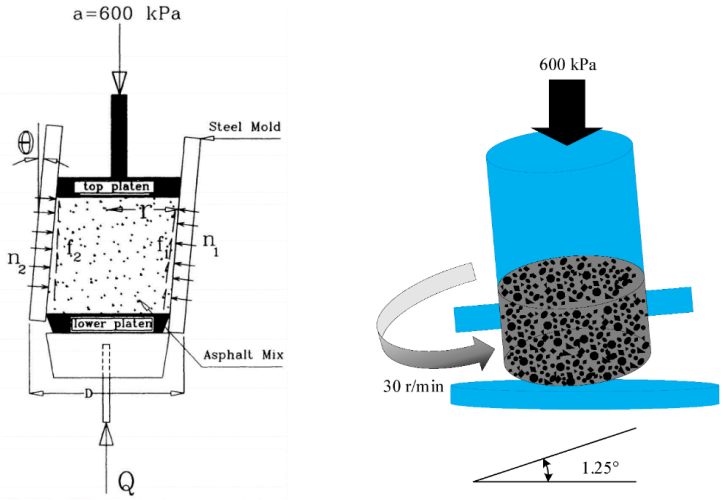

Figure 2-13 Schematic of Superpave Gyratory Compaction by Dessouky, et al. 2004 (left) and Wany et al. 2019 (Right)

2. Compacting by California Kneading Compactor
    a. ASTM D1561/D1561M: Practice for the Preparation of Bituminous Mixture Test Specimens using a California Kneading Compactor. (California Test 104, 2011).
    b. California Test 104: Method of Operation and Calibration for Electronically Controlled Kneading

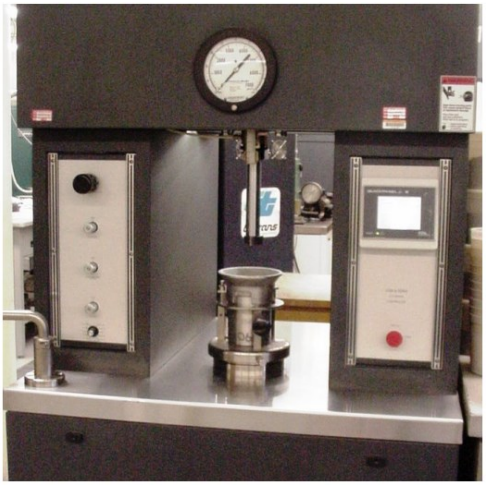

Figure 2-14. California Kneading Compactor (California Test 104, 2011)

3. Compacting by Segmented Rolling Compactor
    a. D8079-16: Standard Practice for Preparation of Compacted Slab Asphalt Mix Samples Using a Segmented Rolling Compactor. This test method replicates the fabrication of asphalt mix slabs using an automatic apparatus that combines the vertical displacements of a segmented rolling compactor foot and the horizontal movements of a rolling compactor foot relative to the compactor tray, thereby producing compacted asphalt slabs with the target theoretical density that are suitable for volumetric and physical property testing.
    b. EN 12697-33 Segmented Steel Roller: Entails a rectangular mould and a segmented smooth steel roller (see Figure 2-15)

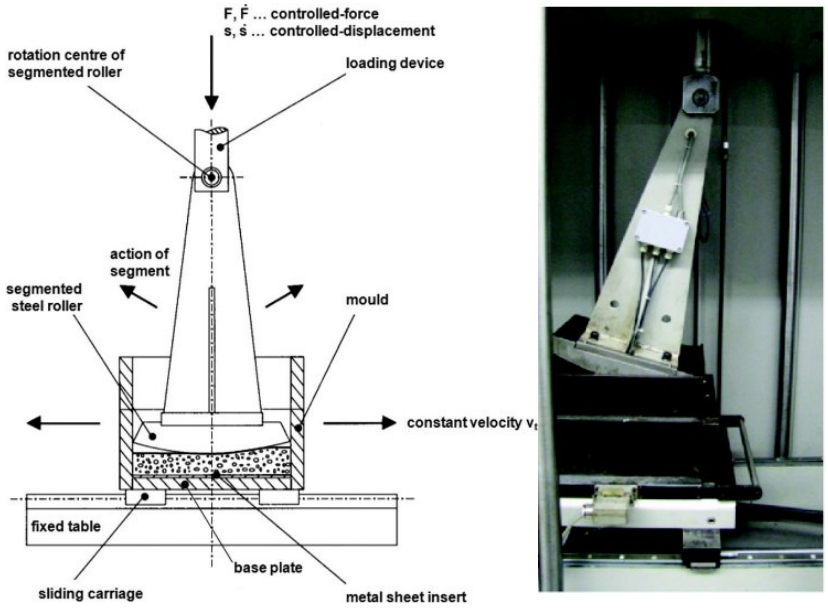

Figure 2-15 Schematic of Segmented Steel Roller (left) and Pictures of the Segmented Steel Roller (Right) (Wistuba 2016)

The steel roller compactor is the lab specimen compaction method that delivers asphalt paving slabs with properties that most closely simulate those in the field. The slabs can be compacted to target mixture densities using loads equivalent to those of full-scale compaction equipment. Current ACP tests conducted on specimens prepared from gyratory-compacted samples or field cores show that asphalt laboratory experiments based solely on lab-prepared samples sometimes give totally different results in comparison with what the performance of the asphalt placed on the field is. For example, Arraigada et al. (2018) reviewed the findings of research based solely on laboratory experiments, while a Swiss laboratory research project by Seeberger et al. (2014), concluded that mixtures with a high percentage of local RAP can perform comparably to standard hot mix asphalt. However, Arraigada et al. (2018) examined the findings of this research in the field. Sample cores were obtained to evaluate the volumetric and

mechanical properties of the materials, and the results showed that the reference subject (standard MHA) outperformed the pavement with high Recycled Asphalt Pavement (RAP) content. In other words, Arraigada et al.'s (2018) findings, based on samples received from the field that were compacted with steel rollers, are opposite to what was reported by Seeberger et al. (2014) based on laboratory-prepared samples.

2.12 Current Asphalt Mix Performance Test Methods

Examination of the performance of road asphalt pavement is a major objective of many pavement studies, and government agencies (i.e., Texas Department of Transportation) and standards-setting bodies (i.e., AASHTO, ASTM, and CEN) have introduced different performance-based test methods. Appendix C has a summary of some of the performance test methods currently in use by different agencies. In Appendix C, the author also briefly reviews a few of these tests.

2.13 Simple Asphalt Performance Test Methods

The U.S. National Cooperative Highway Research Program (NCHRP) VIA PROJECT 9-19 attempted to introduce a Simple Performance Tests (SPT), and recommended three test-parameter combinations to proceed to the field validation stage (Witczak et al. 2002):

- The dynamic modulus term (determined from the triaxial dynamic modulus test) to study HMA rutting and HMA fatigue cracking;
- The flow time, F_t, determined from the triaxial static creep test; and
- The flow number, F_n, determined from the triaxial repeated load test.

Therefore, based on Witczak et al.'s (2002) research, the Triaxial Dynamic Modulus Test (ASTM D3497), Triaxial Static Creep Test, and Triaxial Repeated Load Test (by AASHTO T 378) are 3 simple recommended performance tests, and here we will briefly review them.

The Triaxial Dynamic Modulus Test is performed by applying a uniaxial sinusoidal (i.e., haversine) compressive stress to an unconfined or confined HMA cylindrical test specimen. The dynamic modulus is calculated by recording the applied stress, and the respective recoverable axial strain response of the sample is measured. It should be noted that the dynamic modulus values obtained by a triaxial dynamic modulus test are measured at one effective temperature which ranges between approximately 25 to 60°C and therefore does not cover temperatures below 25°C and below-zero temperatures, and more importantly, are for specimens cored from gyratory compacted mixtures and not extracted from actual paved roads. Since gyratory-compacted samples will not allow a quality control team to review the effects of compaction received on a job site by actual construction rollers, therefore in the view of the author, it cannot be a good candidate for performance tests of newly paved roads.

The Triaxial Static Creep Test, also known as Confined Static Creep Test, consists of a static axial load being applied to a cylindrical sample which is under confining pressure to better simulate in situ stress conditions. Creep compliance parameters and flow time will be calculated and reported by the help of the recorded load, confining pressure, and measured axial and radial deflection during the test (Roberts et al. 1991; Witczak et al. 2002). Testing is performed on laboratory-prepared specimens, with test

temperatures ranging between 25 to 60°C. The same vulnerabilities mentioned above for the triaxial dynamic modulus test are applicable for this test.

The Triaxial Repeated Load Test applies a repeated fixed load and cycle duration to a cylindrical test sample. By measuring the horizontal deformation and an assumed Poisson's ratio, the sample's resilient modulus will be calculated. Cumulative permanent deformation as a function of the number of load cycles is determined and can be correlated to rutting potential. Brown et al. (2001) and Rushing and Little (2014) showed that repeated load tests correlate better with actual in-service pavement rutting than static creep tests. The same as for the last two tests, the triaxial repeated load test's specimens are cored from gyratory compacted mixtures.

Many of the test protocols being considered for routine use are very complex, so a simple performance test is still required. The following principal evaluation criteria for test methods should be considered for future asphalt performance testing processes:

- Accuracy: Good correlation of the HMA-response characteristics to actual field performance
- Reliability: A minimal number of false positives and negatives
- Ease of use
- Reasonable equipment costs

As mentioned, current performance tests can be too expensive and complex to run routinely.

2.14 Summary and Conclusion

In this chapter, first, the summary of ACP distresses was presented to highlight the importance of the quality of compaction, interlayer bonding, and temperature cycles on different ACP distresses and eventually length of pavement life. Then, previous studies regarding the effect of compaction, interlayer bonding, and low-temperature cracking were reviewed. In addition to reviewing existing compaction methods for road paving projects, previous studies regarding the benefits of AMIR compaction were also reviewed. In regard to sampling and sample preparation for ACP performance tests, concerns associated with the use of gyratory-compacted and laboratory-created samples were discussed and highlighted as to why these samples cannot be ideal representatives of actual asphalt placed on highway projects. It was discussed that samples should be extracted from end-product ACP after being placed and compacted on a highway. The tests performed on such samples will be able to evaluate the quality of compaction that ACP receives on a job site. After a brief review of current test methods, the lack of a test method that can simulate the temperature cycling ACP will experience was pointed out, and the need for a new simple performance test to enable evaluation of the ACP end-product quality was discussed. It was discussed that not only do temperature cycles (above and below zero Celsius) exist, but also that the ACP in most Canadian cities will experience it for relatively long periods (more than 60 days every year). Knowing that pavements constructed in these cold regions have to resist against thermal contracting cracking during the harsh winter conditions, it is important to study the effect of the mentioned temperature cycles on key ACP performance parameters (including but not

limited to interlayer bonding). Knowing the state of the key ACP performance parameters after going through several temperature cycles will help pavement engineers to better estimate the ability of ACP to resist the loading and thermal stresses that ACP will face over cold and long winters. Knowing the above concerns and situations, in this research, experimental investigations and the test methods proposed in Chapter 3 were designed to study the capability of ACP to withstand cyclic temperature changes and the effect of compaction equipment on interlayer bonds by using a custom-made temperature cycling testing machine. The mentioned TCT method and apparatus will enable researchers to reproduce several temperature cycles in a relatively short time and closely simulate the environments of relevant cities. Also, all samples were extracted from highway projects, and gyratory samples were avoided to enable studying of the compaction received by ACP at the time of construction. This allowed us to study different compactors (steel rollers vs AMIR) and their effects on interlayer bonding and the temperature cycling resistance of the mentioned ACPs. Knowing the status of ACP after going through TCT, we studied the tensile strength of ACP slab samples at different temperatures (i.e., 0°C, -10°C, or 20°C) using rectangular samples from actual highway projects. This enabled studying the impact of construction methods.

Chapter 3. Experimental Investigation

3.1 Research Plan

As discussed in Chapters 1 and 2, Superpave does not have a performance test for QA/QC to be used for evaluating the quality of compaction at construction sites (Hajj et al. 2019) while assessing the key performance parameters of the asphalt mix (listed in Section 2). Most of the current asphalt performance test methods (listed in Appendix C) use laboratory-made (compacted in the lab) samples from loose HMA taken at a hot mix plant, a loaded truck, or after delivery of HMA to a construction site behind the paver before compaction (e.g., by shovel to acquire the HMA materials). In the view of the author, parts of the current QC/QA program are in need of several modifications to ensure the successful implementation of roadway sampling and to encourage high-quality HMA construction. Since collected samples should be representative of the installed mixture in order to assess the actual variability of a construction process, the author believes that asphalt samples to be evaluated for performance should be acquired after the placement of the HMA when the compaction process is completed. In this way we can account for variability introduced by the paving equipment and evaluate the quality of the compaction applied to HMA. Paving contractors typically want to avoid any sampling taking place behind the paver for several reasons, including that this sampling interrupts the paving process and affects the final surface of the installed pavement. In order to obtain samples from asphalt end-products compacted on a job site, and also to address concerns regarding the coring of the asphalt pavement (as described in Section 2.10), for this research a new sampling method is proposed. It is suggested that

rectangular compacted MHA specimens be extracted from the pavement by saw-cutting the asphalt concrete and lifted very carefully, as described in detail in Sections 3.3.1 and 3.2.1 of this chapter, and sent to an asphalt lab for further performance testing.

Abd El Halim et al. (1990a, b) proposed a direct tensile test for asphalt concrete and built a special test table to perform the mentioned direct tensile testing on asphalt slabs. The author has found potential in this proposed sampling test method and testing apparatus, and decided to further develop and improve, where possible, the testing apparatus, and suggests two simple asphalt performance test methods (Test Series A and B) for the design and QA/QC of asphalt pavement. After performing several trial tests in order to develop new test methods, these two test methods are employed to test key asphalt pavement performance parameters, including cracking resistance, tensile strength, resistance to low-temperature cracking, and ability to withstand fluctuating temperatures. Also, the proposed testing methods are employed to evaluate the quality of compaction that an asphalt mix receives at the construction site.

In developing these test methods, it was always the goal to propose test methods that could simulate the field conditions of pavement subjected to thermal stresses and introduce an accelerated test methodology. The ultimate goal was to propose a test method that can be successfully used to simulate cracking and interlayer bond conditions that result from mix preparation, delivery to construction site, placing, and compaction quality.

As a first step, the testing apparatus (test table) was used to test several trial test methods (examples of 2 trial series are presented in Appendix B). After reviewing the

results, the test table was modified and redesigned to enable conducting of the proposed performance test methods and to find answers to the research questions. Test Series A, which focuses on the ability of asphalt to withstand temperature cycles, was designed and performed for samples compacted by CCM as well as samples compacted by AMIR, and Test Series B, which focuses on resistance to tensile stresses under cold temperatures, was designed and performed for samples compacted with a conventional compaction method (steel roller).

Based on the earlier discussion, the work was broken down into stages, as described below, in order to manage several tasks that must be accomplished to achieve the objectives of the research.

Stage 1: Developing the testing methods. To start, the test apparatus that was employed by Abd El Halim (Abd El Halim et al. 1990a, b) was modified and upgraded to be used for Test Series A (Carleton University Asphalt Direct Tensile Strength (CUADTS)). Several pre-test trial tests were performed before Test Series A was proposed. A few examples of these trial test series are presented in Appendix B. Test Series B was developed to cover those research objectives (Section 0) that were not addressed by Test Series A, and to find answers to the research questions (Section 1.2) that Test Series A did not answer.

Stage 2: Field sampling for each of the above-mentioned Test Series. After coordinating with the road construction contractor (R.W. Tomlinson Limited) and the MTO, the road projects to be used for sampling for Test Series A and B were selected and samples were obtained from those sites, as explained in Section 3.3.1 and Section 3.2.1.

Stage 3: Laboratory investigations. The received specimens were tested at the Civil and Environmental Engineering Laboratory of Carleton University, as described in detail in Sections 3.3.4, 3.3.6, 3.2.3, and 3.2.6.

Stage 4: Data processing and analysis. Eventually, the results of Test Series A and B were carefully reviewed, studied, compared, and analysed (see Chapter 4. for details). Figure 3-1 provides a summary of the research plan followed for this study.

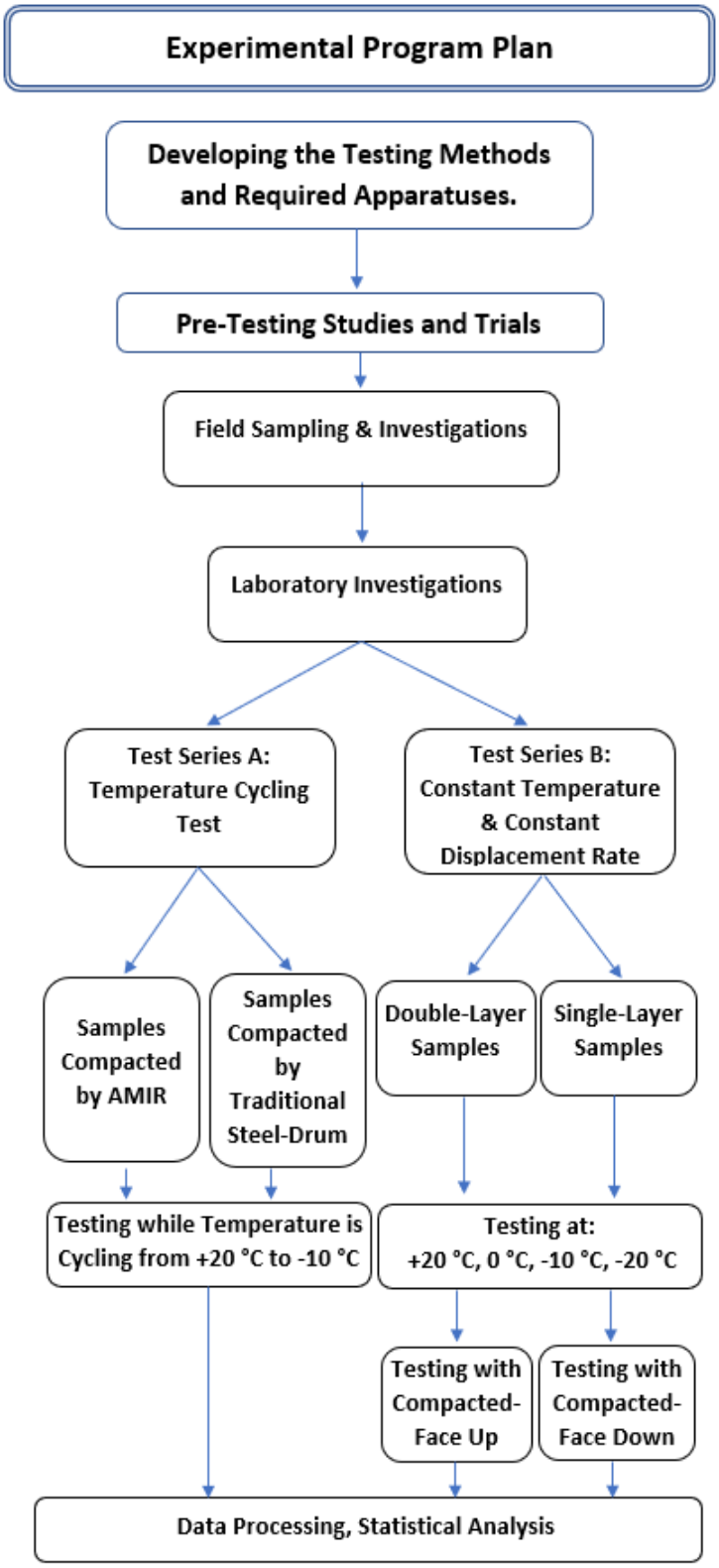

Figure 3-1. Summary of Research Plan

Test Series A, Section 3.2, focuses on asphalt's ability to withstand temperature cycles. It was designed and performed on ACP samples compacted by the two compaction methods (CCM and AMIR) using the proposed CUATC test method in order to find answers to the below questions:

- How is the interlayer bonding of ACP affected by thermal cycling and extreme temperature changes?
- Do compaction methods affect interlayer bonding and the capability to withstand temperature cycles and interlayer bond? Which of the compaction methods (CCM or AMIR) provides better interlayer bonding and superior temperature cycling resistance?

Test Series B (Constant Displacement Rate and Constant Temperature), Section 3.3, was designed and performed using the proposed Carleton University Asphalt Direct Tensile Strength (CUADTS) test method in order to find answers to the below questions:

- How does ACP's tensile strength change at low temperatures (0°C, -10°C, or -20°C)?

The results of Test Series B will determine whether the average tensile strength for samples "with construction-induced cracks" is significantly different from the average tensile strength for samples "without construction-induced cracks". The hypothesis of the research is that the difference between the average calculated stresses for the mentioned two groups of samples is significant.

The aim of these two test series was not only to study asphalt pavement's capability to withstand temperature cycling when compacted with different methods

(CCM vs AMIR), but also to improve the understanding of the role that compactors play in ACP tensile strength and interlayer bonding, and to consider the impact of construction methods on the long-term performance of ACP.

Furthermore, the research plan was organized to address the other objective of the research, which was to propose simple and practical performance-related test methods that can be routinely used during the construction or laboratory mix design and production processes. In the view of the author, the CUATC and CUADTS test methods are adequate in simulating the field conditions and replicating field loadings, temperatures, and boundary conditions as closely as possible. For the purposes of asphalt pavement construction field quality control (QA/QC), the CUATC and CUADTS test methods can also cover the determination of the quality of the placement and compaction processes.

3.2 Test Series A

Test Series A was developed to evaluate pavement's interlayer bonding and resistance to cyclic temperature changes by modifying a testing table previously designed and built to evaluate the tensile strength of ACP slab layers (Abd El Halim et al. 1990a, 1990b).

The results of Test Series A were studied to find out how asphalt pavements perform when they are compacted with different methods (CCM vs. AMIR). The aim was to develop a simple and practical performance test to evaluate the tensile strength, interlayer bonding, and cracking resistance of asphalt pavement as it undergoes temperature cycling. In order to develop this test, several other tests with different

loadings, temperature cycling timings, and temperatures were considered, tried, and studied before the final version of the test was selected for Test Series A. The goal was to simulate, as closely as possible, the temperature situation that asphalt pavements experience after being placed on roads.

From a mechanical point of view, ACP is multi-phase composite material that has its own complexities due to its special characteristics, which include but are not limited to heterogeneity (i.e., being made of several materials with dramatically different mechanical and physical properties), anisotropy (having different properties in different directions), and nonlinear inelasticity (i.e., does not return to its original shape and size after deformation). A good understanding of the key mechanical characteristics of ACP, such as the fracture properties of asphaltic materials, linear viscoelastic, and non-linear viscoelasticity, is required by asphalt researchers in order to fully understand the mechanism of thermal cracking. As discussed in Chapter 2, there have been many efforts by researchers to understand the complicated phenomenon of thermal cracking, and if possible, formulate, model, and/or simulate it in the laboratory. The temperature-dependency of the fracture behaviour of AC is still under study by researchers in order to better understand it. As part of these efforts, creep and recovery testing is one of the ways to explore the non-linear viscoelastic property of AC materials.

In Test Series A, the tensile strength and bonding shear strength of asphalt pavement layers were assessed by placing rectangular specimens under constant loading (a load-controlled test) and temperature cycling and measuring the degree of permanent deformation. Each 300mm x 100mm sample was subjected to a specific number of cycles,

starting at a low temperature (-10°C), then ambient (room) temperature (+ 20°C), and then again to the low temperature (-10°C) before going back to ambient temperature. The range -10°C to +20°C that was selected based on the trend of the temperature cycles observed in early winter days. Having said that, the range -10°C to +20°C for this study was only one of many temperature ranges that could have been selected that ranged between above and below 0°C. For example, -10°C to +10°C or -15°C to +10°C could have been other possible temperature ranges used for this study.

3.2.1 Test Site - Test Series A

The samples for Test Series A were taken from an actual highway project location. A 200-m section of Didsbury Road in Ottawa, Ontario, Canada (near Terry Fox Drive and HWY 417; see Figure 3-2 (a), site location map) was paved as a test road using different asphalt compaction rollers.

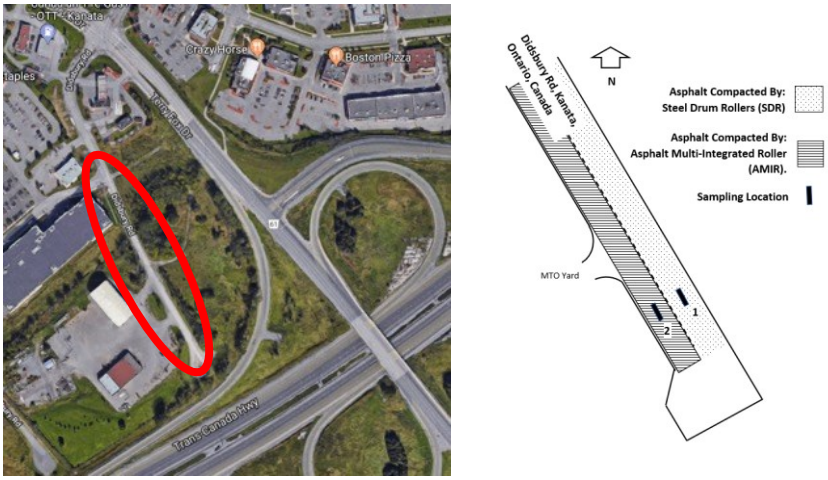

(a) (b)

Figure 3-2. Sampling Site Location Map (a) and Sampling Location for each Type of Compactor (b)

The northbound lane was compacted using CCM, and the southbound lane was compacted using AMIR. For construction of this test road, the Ontario Provincial Standard Specifications OPSS 310 (2016) for the construction of HMA were followed.

Figure 3-3. Photo of paving test road with AMIR rollers compacting the Southbound lane of Didsbury Road

Figure 3-2 (b) shows the sampling location for each type of compactor, Area 1, and Area 2:

- Area 1: Compaction with CCM (steel, pneumatic tire, and oscillating), double-layer asphalt on a granular base
- Area 2: Compaction with AMIR (Asphalt Multi-Integrated Roller), double-layer asphalt on a granular base

3.2.2 Field Sampling - Test Series A

The road was paved on November 15, 2017, with samples being taken on December 19, 2018, and the sample locations were randomly chosen at the construction

site. Figure 3-4 shows the paved road being cut into 300mm × 100mm sections using circular saw to get the rectangular slab samples.

The sample size of 300mm × 100mm was selected after several trials. Originally, 300 x 600mm was the size selected for this test series, but it was noticed that many of the 300 x 600mm samples got damaged during the transport, storing, and testing. Therefore, after several trials, 300mm × 100mm was found to be a good size for this test series.

The samples were labeled with the date, time, and location, and the roller used for compaction. The samples were delivered to the Civil and Environmental Engineering Laboratory of Carleton University within two hours of cutting.

(a) Saw-cutting the pavement, (b) Saw-cutting the pavement, (c) rectangular samples before being sent to asphalt lab

Figure 3-4. Pictures from Sampling Day for Test Series B

3.2.3 Material (Asphalt Mix) - Test Series A

The material used for Test Series A was all identical for the southbound and northbound lanes. All the samples were extracted from one construction site. The asphalt mix used for the binder course of all samples was Superpave 12.5mm FC2 PGAC 70-34, and the asphalt mix used for the surface course of all samples was Superpave 19 PGAC 64-34, both of which are designed to meet the aggregate gradations specified by the

Ministry of Transportation of Ontario (MTO). Table 3-1 presents the design properties of the binder and surface course asphalt used for Test Series A as per the job mix received from the road contractor.

Table 3-1. Main parameters of the mix designs used as binder course and surface course for Test Series A

Property	**Binder Course Mix**	**Surface Course Mix**
SUPERPAVE ASPHALT CEMENT MIX	SP 12.5mm FC2 RAP	SP 12.5FC2 PG70-34
ANTI-STRIPPING	1.0% Hydrated Lime	---
BINDER CONTENT (MASS %)	4.7	4.8
AIR VOIDS %	4.0	4.0
VOIDS IN MINERAL AGGREGATES	14.36	15.1

3.2.4 Preparation of Test Slabs in the Lab - Test Series A

The 300mm × 100mm samples were cleaned and then placed on a table with the roller-compacted face up, as shown in Figure 3-5. Epoxy adhesive (Hilti HIT-RE 500 V3) was applied to both ends of the sample, while the middle 100mm was kept free of glue. This 100mm section with no glue would experience the elongation. The samples were then turned upside down and the surface with glue was placed on the testing plates, with the sample placed at the center of the transfer plate (steel mounting plates) and the unglued center of the sample aligned with the joint between the plates (Figure 3-5).

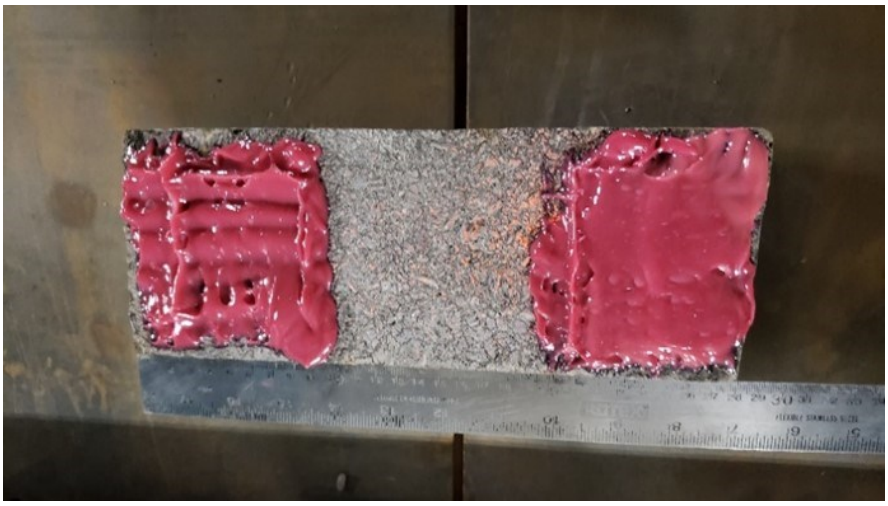

Figure 3-5. Preparation of test slabs in the labs (glue applied)

The samples were then put under low pressure by placing a weight of approximately 5kg on top to prevent sliding. The adhesive was allowed to cure for 24 hours (minimum recommended curing time by manufacturer is 6.5 hours at 20°C). To condition the samples, they were placed in the environmental chamber and allowed to reach the specified testing temperature (for Test Series A, -10°C) for 24 hours before the start of the test.

3.2.5 Test Facility for Test Series A

Initially, the test table built by Abd El Halim et al. (1990a, b) for direct tensile ACP testing was also used for Test Series A. However, after several attempts it was clear that the table required several modifications, and particularly the hydraulic actuator, as its l00KN capacity was too high to apply the low load required for Test Series A (i.e., less than 1KN). Considering the fact that Test Series A was aimed at evaluating the performance of asphalt pavement in withstanding temperature cycles, several tests were preformed to find the adequate loading for the tests. It was noted that loads above 1KN would make

most of the samples break when the sample reached 20°C during the temperature cycling. With loads above 1KN, samples break during the first temperature cycle, and this did not allow evaluation of the samples' temperature cycling resistance. Therefore, loadings of below 1 KN were selected for Test Series A. To address this, a dead load mechanism was designed and built at the Civil and Environmental Engineering Laboratory of Carleton University, and was added to the test table (Figure 3-6 (a)). Figure 3-6 (a) shows the 3D design of the new loading mechanism. This loading system (Figure 3-7) for the existing table setup could apply a steady, relatively low load to a sample under tension, while varying the temperature over an extended period of time. Figure 3-6 (b) illustrates the 3D design of the new loading system together with the vertical threaded bar system, detachable pull bar, and moving plate. As mentioned before, Test Series A is a load-controlled test.

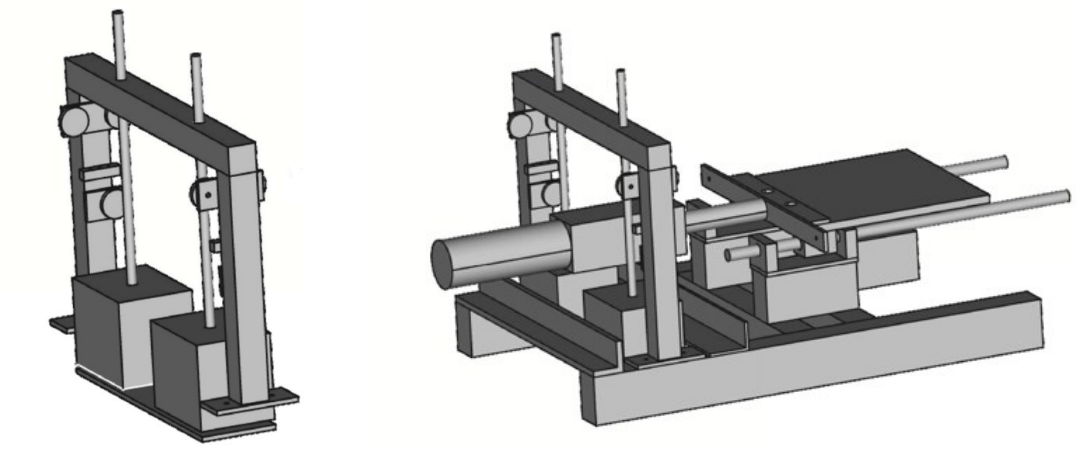

(a) (b)

Figure 3-6. 3D view of addition designed for Test Series A

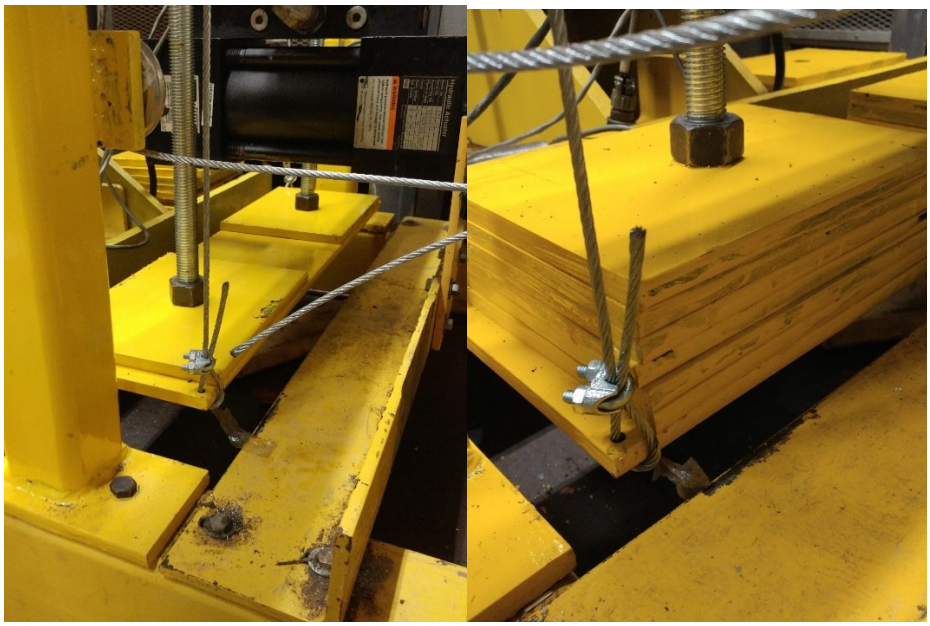

Figure 3-7 – New Loading System for Test Series A

The idea was to add an adjustable vertical gravity force to the front table in the setup, thereby allowing a load to be applied through a cable and pulley system. The principal components were (for more details see Appendix A):

- A weight system including a lower span plate, force cables, and load plates of approximately 55.4N each
- A vertical threaded bar system
- A detachable pull bar
- A Linear Variable Differential Transducer (LVDT) mechanism to monitor table motion

The custom-made test table designed and modified for this series, termed the Carleton University Asphalt Temperature Cycling (CUATC) testing machine, was designed and assembled at the Civil and Environmental Engineering Laboratory of Carleton

University, and is shown in Figure 3-8. The CUATC was placed in an environmental chamber to apply cyclic temperature changes over an extended period of time.

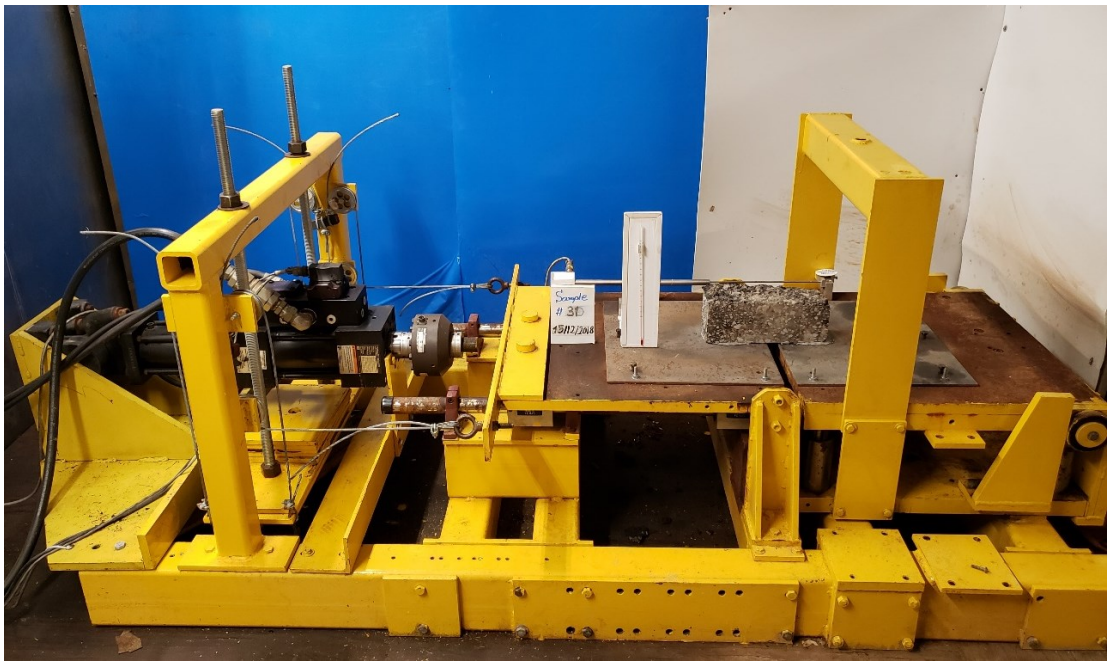

Figure 3-8. Photograph of the Testing Table for Test Series A

A constant load was applied by hanging masses (gravity force), as shown in Figure 3-8. Figure 3-9 shows the schematic of the test table used for Test Series A.

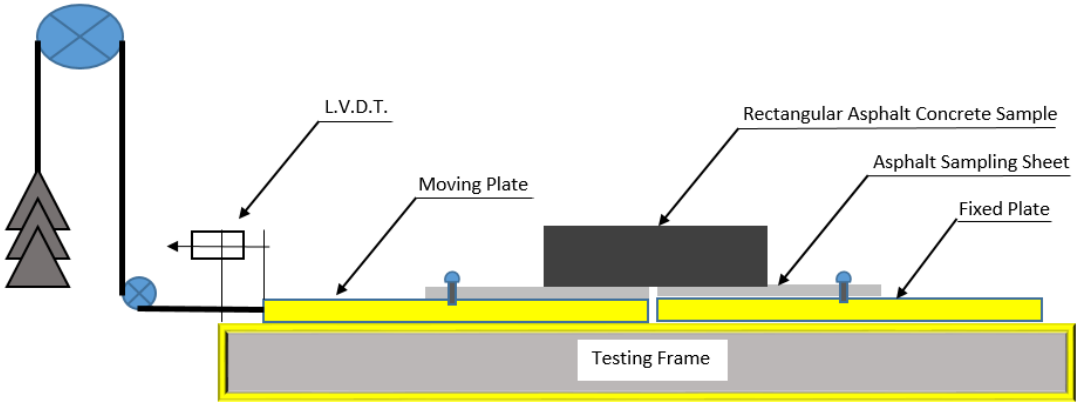

Figure 3-9. Test Table Schematic (Test Series A)

3.2.6 Testing Procedure - Test Series A

Several trial test series were performed before selecting the final test method for Test Series A. Appendix B has the details of those trial tests. Here are a few examples of those trial tests:

- Trial tests to find the minimum loading the apparatus could apply to the sample
- Trial tests to stablish the cycle times, high temperature, low temperature, number of cycles, and appropriate load
    - Several tests were performed with loads ranging from 0.416 KN to 0.9147KN to find the adequate loading for the test. In the beginning, multiple tests were performed for 7-day cycles with different loadings.
- Trial tests to find a way to accelerate the testing and minimize the duration. Several tests were performed, with the load being increased every 3 days to accelerate the test. During the trial, there were tests as short as one day and as long as 14 days.

After careful review of all the trial tests, study of the failures, and considering the objectives of the test, the final test setup was selected for Test Series A.

The minimum number of 24-hour cycles was chosen to be seven (7), and the load was constant (0.5268 kN; equivalent to 0.05268 MPa normal tensile stress) for the first 72-hour cycle. If a sample did not fail after 72 hours of cyclic temperature under a 0.5268kN load, the load was increased by 0.1108 kN for a total of 0.6376 kN (equivalent to 0.0638 MPa normal tensile stress). If no failure were observed after the sample went through three more cycles (72 hours), the load was again increased by 0.1108 kN and the

test continued until the sample broke, and then the sample's elongation was measured. It should be noted that the above-mentioned loads were applied to enable the study of the temperature cycles and also to simulate ACP field conditions in the laboratory. While no actual calculation was performed to estimate the range of load or stress developed in an asphalt layer due to continuity, the applied load of 0.5268 kN was assumed to be representative of the load applied to the specimen from its surrounding ACP's layer when located in an asphalt mat as part of road pavement. This load may be different from the actual load on a similar size of ACP as part of actual road asphalt mat, but it was found in the initial trials to be appropriate for this study for a reasonable test duration. The subsequent increase in loading, after 3 cycles, from 0.5268kN to 0.6376 kN was done to expedite the process and reduce the testing time.

Figure 3-10 presents a typical diagram for the change in length (elongation) versus time in a cyclic temperature test. The test started at -10°C temperature and with a 0.5268 kN load on the sample at point (a), then the temperature was set to gradually rise to +20°C. After 12 hours at +20°C temperature (point b), the temperature was then set to gradually return to -10°C. At the end of the first cycle, after 24 hours of testing (point c), the sample had undergone a temperature change of -10°C to +20°C then back to -10°C. Figure 3-10 illustrates that the samples would undergo an elongation during high temperature (between (a) and (b)), referred to as the primary phase of the cycle, due to the combined effect of creep under the applied tension and thermal expansion. On the other hand, the low temperature (between (b) and (c)), referred to as the cycle's secondary phase, resulted in thermal contraction. The net effect of this cycle was a net

elongation. The same pattern of elongation and contraction is repeated in the second and third temperature cycles (points d to g). Upon completion of the third cycle (point g), 72 hours from the start of the test, the temperature was -10°C. The pattern of the first three cycles was repeated again but the magnitude of elongation in each cycle was expectedly higher. If the sample did not break after the first six cycles (144 hours), the load was increased by another 0.1108 kN, for a total of 0.7484 kN, and the pattern was again repeated but with even higher elongation in each cycle.

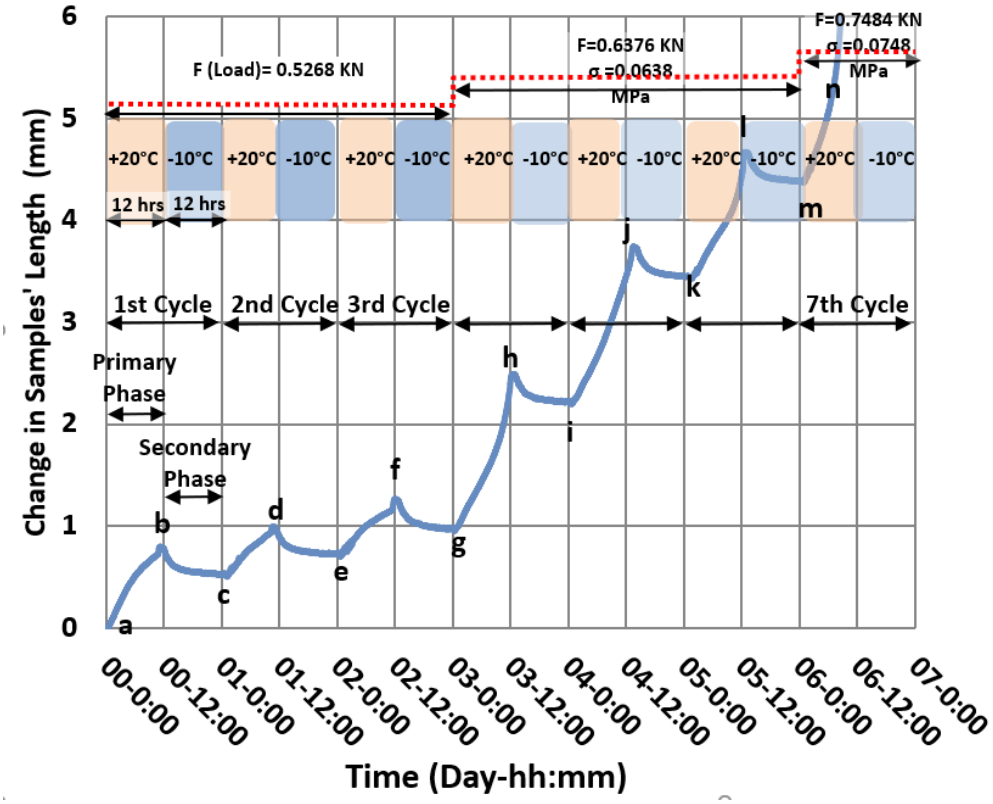

Figure 3-10. Elongation vs Time, Test A (Temperature Cycling Test) Performed on AMIR compacted samples

The field samples compacted by both CCM and AMIR were tested according to the Test Series A method, and the results were examined thoroughly. The elongation

(permanent strain) was measured after the sample failed or the planned number of temperature cycles was completed (7-day). Figure 3-11 shows an AMIR-compacted sample which was tested as part of Test Series A according to the CUATC test, and Figure 3-12 shows two samples compacted with CCM and tested according to CUATC. As shown in Figure 3-12, most of the samples compacted by CCM debonded during the CUATC test.

In the view of the researcher, Test Series A is simulating field daily temperature cycles closely, it is relatively simple and low-cost that could be employed as one of the future asphalt performance tests.

Table 3-2 presents the summary of Test Series A.

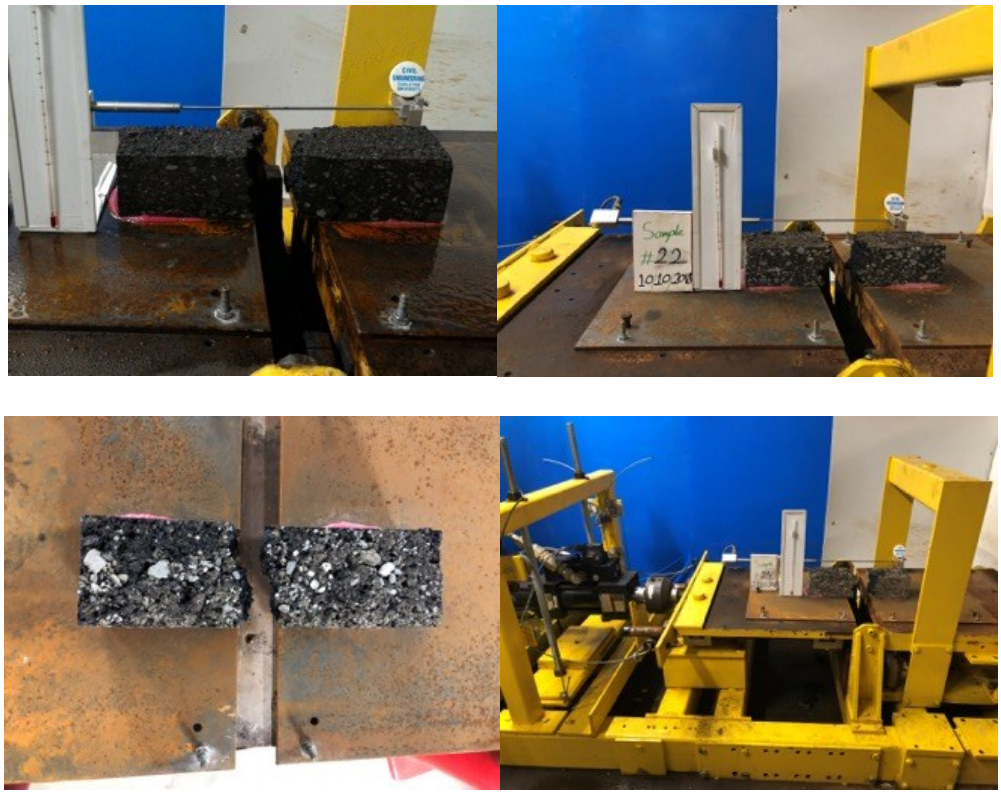

Figure 3-11. Examples of tested samples compacted with AMIR for Test Series A (TCT),

Figure 3-12. TCT, Examples of samples compacted with CCM

Table 3-2. Summary of Test Series A

Asphalt Mix	SP 12.5mm FC2 RAP PGAC 70-34 for binder course & top course
Test	Temperature cycling test while samples are under constant load using CUADTS test table (Load-controlled test)
Type of Loading	Constant Load
Asphalt Samples Size (When Received in the Lab)	300 mm (L) x 100 mm (W)x 100mm (T)
Sample Thickness	Only double-layer samples
Asphalt Samples Size (When tested)	300 mm (L) x 100 mm (W)x 100mm (T)
Compaction Method	Group 1 - Asphalt Multi-Integrated Roller (AMIR) Group 2 – CCM, Traditional steel drum, pneumatic-tired (rubber) & vibratory rollers in accordance with OPSS 310
Testing Temperature	Temperature cycling from -10°C to +20°C and again +20°C to -10°C
Temperature Cycling During Each Test	Yes, each cycle 24 hours
Total Samples Tested	30
Test Durations for Each Sample	0.5 Hour, applying adhesive and preparing samples on sampling sheet 12 Hours, curing of glued sample to sampling sheet 24 Hours, conditioning in environmental chamber (minimum is 6 hours) 168 to 264 Hours (7 to 11 days), for testing on the table

3.3 Test Series B

3.3.1 Test Site – Test Series B

The samples used in this study were from an actual road construction project location. The sampling lot was constructed on an access road near the junction of Highway 417 and Lees Avenue in Ottawa, Ontario. The HMA material was from a highway paving project under construction the same day, and the compaction was done with the same crew and equipment using a Conventional Compaction Method (CCM). Ontario Provincial Standard Specifications (OPSS) for the placement and compaction of hot mix asphalt designed for the Superpave method were followed.

3.3.2 Field Sampling - Test Series B

The mixes were laid in a 10m x 30m area at the paving site. This area was divided into two parts. One part was paved only with only one layer of HMA and compacted to a thickness of 50mm for our single layer samples and the second part was paved with two layers of HMA, a binder course together with surface course with a total thickness of the 100mm. After 30 days, the slabs were marked and saw-cut to 300 x 600mm (Figure 3-13), then the specimens were extracted from the pavement. They were lifted very carefully to avoid deformation damage or crack propagation, then transported to the laboratory. More than 100 samples, each 300 x 600mm, were received in the laboratory. This number was much more than required numbers in anticipation of damages to samples while transporting, storing and testing.

Figure 3-13. Sampling Lot (Ottawa, Canada, 2015), Marking & Saw-Cutting the Slabs

3.3.3 Material (Asphalt Mix) - Test Series B

The asphalt mixes used in this study were Superpave 12.5mm FC2 PGAC 70-34 and Superpave 19 PGAC 64-34, both of which are designed to meet the aggregate gradations specified by the Ministry of Transportation of Ontario (MTO).

Table 3-3 presents the design properties of the binder and surface course asphalt used for Test Series B as per the job mix received from the road contractor.

Table 3-3. Main Parameters of Mix Design used as binder course and surface course for Test Series B

Property	**Binder Course Mix**	**Surface Course Mix**
Superpave Asphalt Cement Mix	SP 19 PG64-34	SP 12.5FC2 PG70-
Binder Content (mass %)	4.6	4.8
Air Voids %	4.0	4.0
Voids in mineral aggregates (VMA %)	14.36	15.1
Bulk relative density (BRD)	2.447	2.378
Air temperature at construction site	+20°C	+20°C
Date of construction	Sep, 2015	Sep, 2015

3.3.4 Preparation of Test Slabs in the Lab - Test Series B

The 600 mm x 300 mm asphalt slabs from the field (Figure 3-14) were saw-cut in the lab to the test size of 300 mm x 100 mm (Figure 3-15). This was because it was noticed that larger samples like 600 mm x 300 mm were hard to move around inside the laboratory and vulnerable to cracking. A marking scheme kept track of the sample locations during compaction, and the rolling direction was identified on each sample.

Figure 3-14. 600 mm x 300 mm asphalt slabs from the field for Test Series B

Figure 3-15. asphalt slabs after saw-cut to 300 mm x 100 mm for Test Series B

The transportation, storage, handling and preparation procedures for each sample are critical, as they can affect test results. The proposed test is relatively simple and quick.

The following section discusses the slab preparation. The 300 mm x 100 mm samples were cleaned, then placed on a table with the surface to be glued face up, as shown in Figure 3-16 Epoxy adhesive (Hilti HIT-RE 500V3) was applied to both ends of the sample, while the middle 100 mm was kept free of glue. This 100 mm section with no glue was going to experience the elongation.

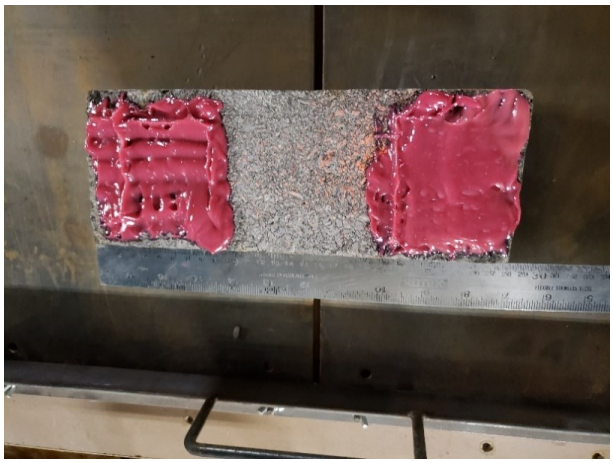

Figure 3-16. Preparation of Test Slabs in the Labs (glue applied)

At this point, the samples were placed on the centre of the transfer plate (steel mounting plates) as shown in Figure 3-18, with the unglued centre of the sample aligned with the joint between the plates. The samples were then put under low pressure by placing a weight (approximately 5kg) on top to prevent sliding. The adhesive was allowed to cure for 24 hours (minimum recommended curing time by manufacturer is 6.5 hours at 20°C). All samples were from same sampling lot, with the exact same HMA mix, and received similar compaction, so all the specimens were identical. These samples where divided into two groups (as the samples were alike, no specific criteria were used to select the samples for each group). Samples of one group were used for testing with their

compacted faces upward, and the specimens in the other group were tested with their compacted faces was downward.

Figure 3-17 shows examples of the samples with roller-compacted face down. Glue was applied on compacted surface (Figure 3-17 Left). Then the surface with glue was placed on sampling sheet (Figure 3-17 Right).

Figure 3-17. Example of samples with roller-compacted face down.

Figure 3-18 shows a double-layer sample glued to the sampling sheets with its compacted face, facing down.

Figure 3-18. A double-layer sample glued to the sampling sheets with its compacted face was facing down

To condition the samples, the plates and the attached samples were put in an environmental chamber capable of achieving the planned test temperatures (i.e., +20°C, 0°C, -10°C, and -20°C) (Figure 3-19).

Figure 3-19. Conditioning the samples inside the environmental chamber for 24 hours

The samples remained in the chamber for 24 hours, and then sampling sheets were bolted to the plates on the pulling table and the side plates removed. Side plates were only used to ease the handling of the sampling sheets (with the slabs glued on). The weight of each sample, together with the two sampling sheets, sometimes required two persons to carry them and place them carefully on the test table.

Figure 3-20. Example of samples with roller-compacted face up.

3.3.5 Test Facility for Test Series B

Performing the CUADTS test on rectangular asphalt concrete samples requires a test facility (Figure 3-21) equipped with fixed and movable plates inside an environmental chamber with a temperature range of +20°C to - 20°C (the environmental chamber of the Civil and Environmental Engineering Laboratory of Carleton University has a temperature range of +60° to - 40°C). The testing table was designed and assembled in the environmental chamber.

Figure 3-21. Photograph of the testing table for CUADTS test designed by Abd El Halim

The facility consisted of (Raab et al. 2009):

- A hydraulic actuator with l00 KN capacity and 250mm stroke;(Figure 3-22).

- A direct tensile strength testing table for asphalt concrete samples, equipped with fixed and moving mounting plates.
- A moving plate connected to a load cell and a positioning system consisting of a linear variable displacement transducer (LVDT) that feeds a data acquisition computer; this moving plate, on a Teflon sheet to reduce friction, forces the load cell to adjust accordingly to eliminate the loads required to move the plate.

Figure 3-22. Photograph of the Hydraulic Actuator & Its Connection to Moving Plate

- A data acquisition system to monitor and control the test equipment.

It should be noted that the Teflon sheet, i.e., Polytetrafluoroethylene (PTFE), is known for its slipperiness and very low friction, which can offer a massive improvement in the sliding component. The PTFE sheet can also withstand temperatures as low as -260°C and still retain its properties.

The schematic of the test table used for the CUADTS test is shown in Figure 3-23

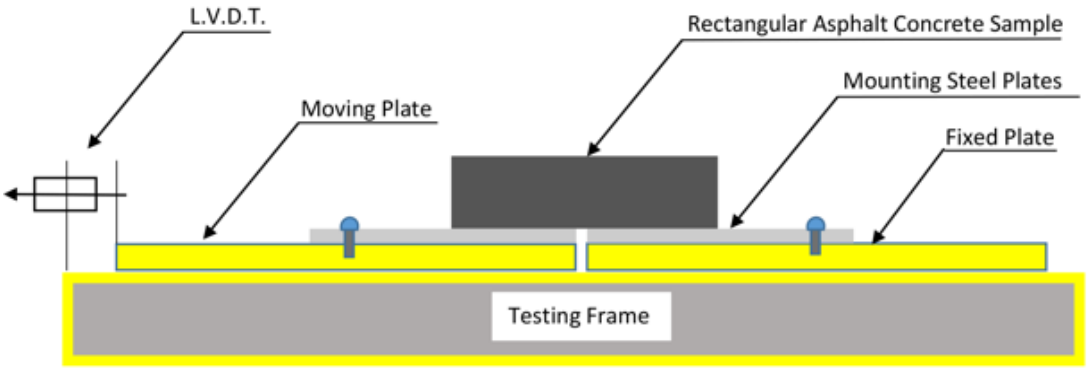

Figure 3-23. Outline of the CUADTS testing table (Test Series B)

Each asphalt concrete slab was glued to a two-piece transfer plate (steel mounting plates) as shown in Figure 3-24 and Figure 3-16. The steel mounting plates were placed on the fixed and movable plates of the table. These transfer plates were fixed by bolts to the fixed and movable plates underneath.

Figure 3-24. Specially designed testing table for CUADTS test on asphalt concrete

3.3.6 Testing Procedure - Test Series B

When a sample was ready for testing and fixed to the testing table, the pulling table was activated, and the sample was pulled apart at a constant strain rate of 0.06mm per second until it failed; the constant force was only applied in the horizontal direction. Each test continued until the sample failed. Failure was observed in two modes:

- Sample broke into 2 pieces or
- The asphalt layers of a double-layer samples were separated.

If neither failure mode took place, a total displacement of 15mm was defined as the failure point. The test was performed on samples glued to plates on their roller-compacted face (face-down samples) and repeated for samples glued on the face that was connected to the base layer in the field (face-up samples). The samples were tested in 16 groups of single and double-layer samples, at the indicated temperatures of +20°C, 0°C, -10°C, and -20°C (Table 3-4).

Table 3-4. Test temperature for each of 16 groups in Test Series B

Temperature	**Roller-Compacted Face**	**+20°C**	**0°C**	**-10°C**	**-20°C**
Double-layer samples	**Up**	Group 1	Group 2	Group 3	Group 4
	Down	Group 5	Group 6	Group 7	Group 8
Single-layer samples	**Up**	Group 9	Group 10	Group 11	Group 12
	Down	Group 13	Group 14	Group 15	Group 16

At least 5 samples were tested for each group. The recorded elongation (mm), load at failure (kN), the exact specimen's dimensions (300mm × 100mm was our nominal

sizes) and observation notes (failure mode) for each of the tested samples were recorded for further analysis. While performing Test Series B, it has been observed that for samples at +20°C, samples were relatively soft and when they were pulled apart, they did not break and instead they elongated to the maximum length allowed by the test table (150mm). These samples did not break or debond. Since the loads applied to bring the samples to its maximum elongated length were so small (low stress), therefore the results were not usable for analysis, and hence the results of samples tested at +20°C were excluded from the analysis. Originally, the plan was to perform the analysis for samples tested at +20°C, 0°C, -10°C, and -20°C but due to above circumstances only results of samples tested at 0°C, -10°C, and -20°C will be presented. Table 3-5. presents the summary of Test Series B.

Table 3-5. Summary of Test Series B

Asphalt Mix	SP 19 PG64-34 for binder course & SP 12.5FC2 PG70-34 for top course
Test	Carleton University Asphalt Direct Tensile Strength (CUADTS) test at constant displacement rate & constant temperature
Displacement Rate (Table Pulling Rate)	0.06mm per second (a displacement-controlled test)
Asphalt Samples Size (When Received in the Lab)	600 mm (L) x 300 mm (W)x 100mm (T) (for double-layer samples) 600 mm x 300 mm x 50mm (for Single-layer Samples)
Sample Thickness	Both single-layer & double-layer samples
Asphalt Samples Size (When Tested)	300 mm x 100 mm x 100mm (for double-layer samples) 300 mm x 100 mm x 50mm (for single-layer samples)
Compaction Method	Conventional Compaction Method (CCM) in accordance with OPSS 310
Testing Temperature	+20°C, 0°C, -10°C, & -20°C
Temperature Cycling During each Test	No
Number of Samples Successfully Tested	171
Test Durations	0.5 Hour, applying adhesive and preparing samples on testing sheet 12 Hours, curing of glued sample to sampling sheet 24 Hours, conditioning in environmental chamber (minimum is 6 hours) 5-10 Minutes, testing on table

The samples tested under this test series showed 2 modes of failure as described below in details:

- Some samples broke into 2 parts under loading. A crack initiated at the bottom of the sample near the plates and expanded and moved upward toward the top of the sample as load increased and eventually sample broken into two parts. (see Figure 3-25)

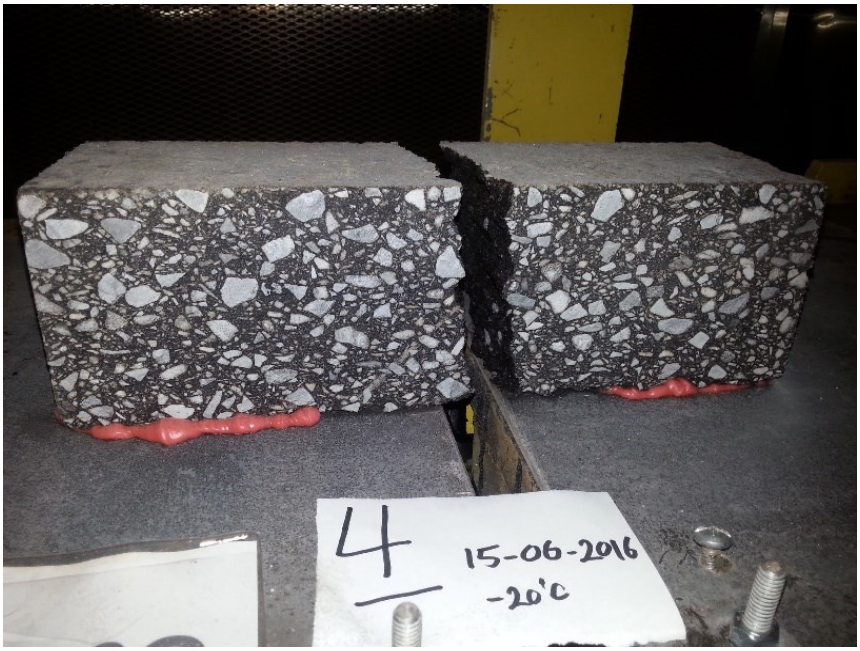

Figure 3-25. Example of double-layer sample tested for Test Series B (sample broken into 2 pieces)

Figure 3-26. Example of single-layer sample tested for Test Series B

Figure 3-27, Top view of a single-layer sample tested for Test Series B

- For the second failure mode, the initiated crack in the bottom of the sample did not reach the surface. The crack started at the bottom of the sample near the plates and expanded and moved upward toward the top of the sample, but then stopped. When the crack arrived at the horizontal joints between binder course and wearing course, the bottom layer of asphalt gets separated (debonded) from the top layer (see Figure 3-28).

Figure 3-28. Examples of samples tested for Test Series B (bottom layer broken but layers are separated)

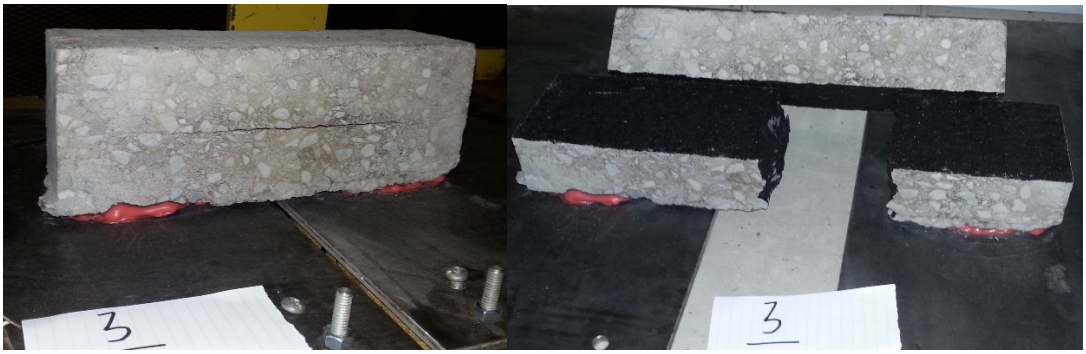

Figure 3-29. Sample tested at 0°C for Test Series B (bottom layer broken but layers are separated)

Figure 3-30 is a sample of elongation vs load graphs recorded for one of the specimens.

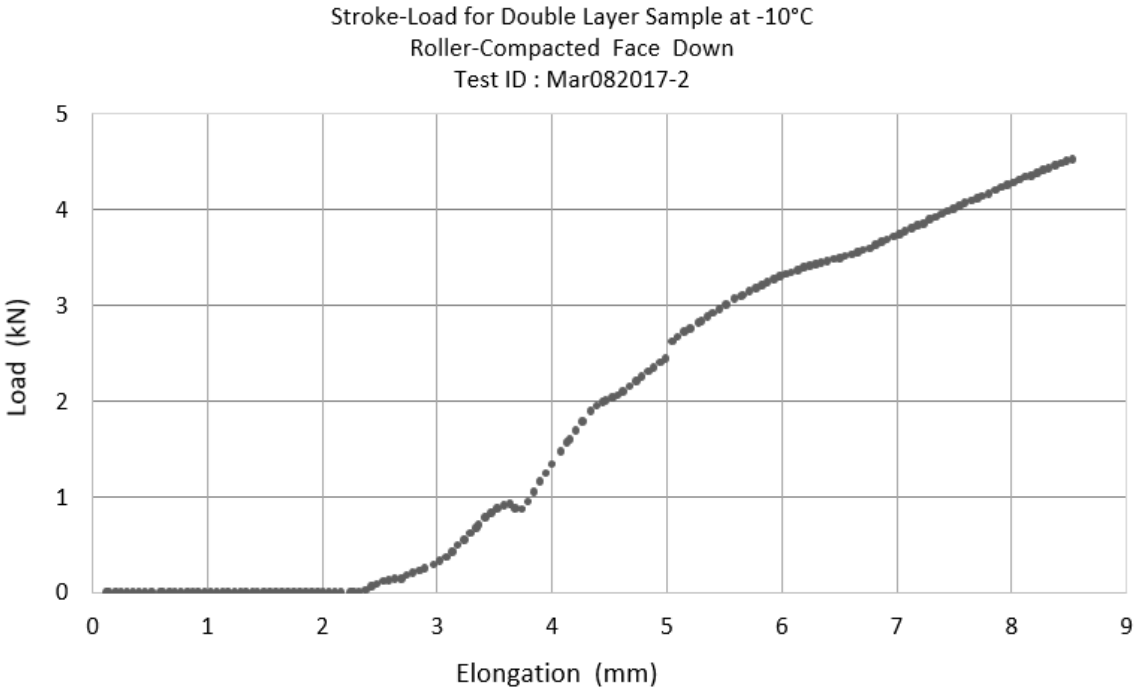

Figure 3-30. Sample Test Result Stroke (Elongation) vs. Load at -10°C

As mentioned in Sections 3.2.6 and 3.3.6 , the ACP samples were tested one by one. Each of the specimens was glued to a two-piece transfer plate (steel mounting plate), as shown in Figure 3-31. Then the steel mounting plates were placed on the fixed and movable plates of the table. These transfer plates were fixed by bolts to the fixed and movable plates underneath.

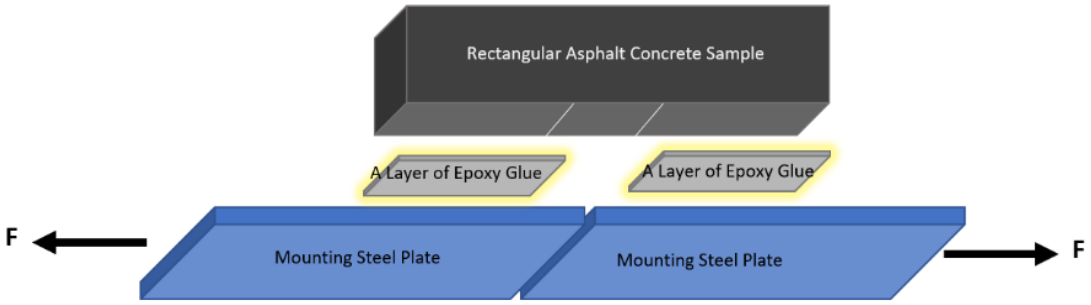

Figure 3-31. Diagram of the Mounting Steel Plates

When a sample was ready for testing and fixed to testing table, the pulling table was activated, and the sample was pulled apart at a constant strain rate of 0.06mm per second until it failed; a constant force was only applied in the horizontal direction (Figure 3-32 (a)). The loads applied to the fixed plates were transferred by steel mounting plates to the glued ACP sample (Figure 3-32(b)). In this case, by gluing the samples to the steel mounting plates, the external forces (F) are applied to the asphalt concrete sample as distributed loading (vs concentrated surface loading), as shown in Figure 3-32 (c). The steel mounting plates produce a force on the attached sample in the direction shown which stops movement of the sample in that direction. Figure 3-32 (c) illustrates the shear stress acting tangent on the ACP specimen. The shear force lies in the plane of the area, and is developed when the applied external loads tend to cause the two bodies (ACP specimen and steel mounting plates) to slide over one another.

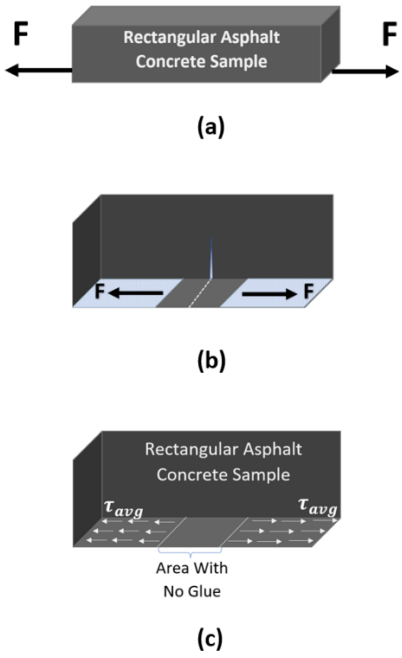

Figure 3-32. Schematic of Loads Applied to ACP Samples

The ACP sample shown in Figure 3-32 is held in equilibrium by the external forces shown. In order to determine the internal loadings acting on the middle section (where the crack is occurring) we pass an imaginary cut through the sample to determine the internal loadings acting on this specific region. In order to obtain the actual distribution of the applied loadings acting over that particular area of the sample, the following two assumptions regarding the properties of the ACP material should be made:

1- The material is continuous, with a uniform distribution and without any voids.

2- The material is cohesive, and all of its segments are connected without any breaks, cracks, or separations.

A free-body diagram of one of the parts is given in Figure 3-33, and the distribution of internal force acting on the visible area of the cut section is shown. These internal

forces are represented as the effects of the material on the left part of the ACP sample acting on the adjacent material on the right part.

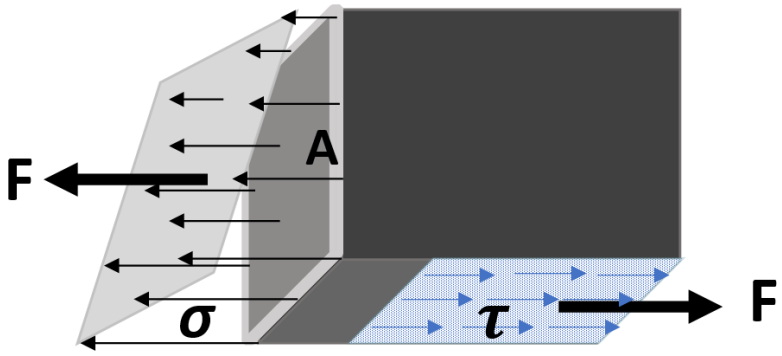

Figure 3-33. Free-body Diagram of ACP Sample

It is noted that after the crack is initiated, the normal and shear stresses are producing a couple moment on the member. Obviously, the equations of equilibrium are being satisfied, as the sample is not rotating and does not have accelerated motion. Consequently, the components of the forces and moments acting both normal and perpendicular to the sectioned area must be considered. The vertical loads from the sample's own weight and vertical reaction are not shown in this free-body diagram, with this diagram concerned only with the horizontal forces causing the sample to fail.

Assuming that the material of the ACP sample is both isotropic (with the same properties in all directions) and also homogeneous (with the same physical and mechanical properties throughout), and that the ACP sample will deform uniformly throughout the central region of its length when subjected to the axial load F, it is necessary for the cross-section be subjected to a constant normal stress distribution similar to what is shown in Figure 3-34 .

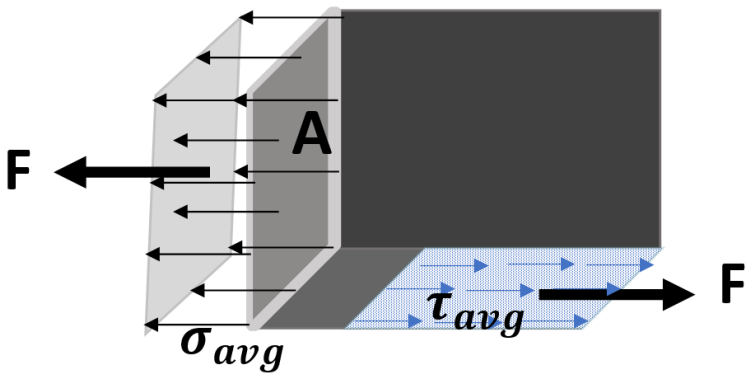

Figure 3-34. Free-body Diagram of ACP Sample

The test was continued until the sample failed. The measurable parameters during the CUADTS testing include the applied load (F), time, and test temperature. The fracture parameters that could be calculated from the CUADTS tests in this study include:

- The tensile strength (σ)
- The tensile strain at peak failure load (ε)
- The modulus of elasticity (E)
- HMA fracture energy or FE (G_f)

The tensile strength is determined according to the standard models of mechanics as the ratio of the peak failure load and the specimen x-sectional area, as follows:

$$\sigma_{avg} = \frac{F}{A} = \frac{F}{thickness \times width} \qquad \text{Equation 1}$$

$$\sigma_t = \frac{F_{max}}{A} = \frac{F_{max}}{thickness \times width} \qquad \text{Equation 2}$$

and the shear stress is calculated as follows:

$$\tau_{avg} = \frac{F}{A_{Glued\ Surface}} = \frac{F}{Length_{Glued\ Surface} \times Width}$$ Equation 3

where F_{max} is the axial peak load.

The tensile strain at peak load, or the ductility potential, is measured as:

$$\varepsilon_t = \frac{Displacement\ at\ peak\ load}{Displacement\ at\ zero\ load} = \frac{D_{Pmax} - D_0}{D_0}$$ Equation 4

where D_{Pmax} max and D_0 are the displacement at peak load and initial displacements, respectively. In order to study the stiffness of the material, the modulus of elasticity is often calculated. The ratio of the tensile strength and tensile strain is denoted as the modulus of elasticity. The modulus of elasticity E is also known as the tensile modulus, stiffness in tension, or Young's modulus. Equation 5 below represents the equation of the initial straight-lined portion of the stress–strain diagram up to the proportional limit of proportionality:

$$E_t = \frac{HMA's\ tensile\ strength}{HMA's\ tensile\ strain} = \frac{\sigma_t}{\varepsilon_t} \text{ or } \sigma = E\varepsilon$$ Equation 5

The modulus of elasticity E can be used only if the HMA to be assumed to have linear elastic behaviour.

The area under the stress-strain curve (Figure 3-35) reflects the work required to cause a fracture, and the fracture energy is defined as the work required to produce a crack of unit surface area, measured in J/m^2. This characteristic property of ACP is often referred to as "toughness" by ACP industry experts due to this ability of ACP to absorb energy up to a point of fracture. Therefore, a general expression for Fracture Energy can be written as:

$$G_f = \frac{Work}{Area\ of\ cracked\ section} = \frac{1}{A}\int f(x)dx \qquad \text{Equation 6}$$

Failure of the ACP structure may be controlled by the brittleness of the material, not by its strength. At low temperatures (e.g., 0°C, -10°C, or -20°C), asphalt acts as a brittle material (with little or no yielding before failure), whereas at above-zero temperatures it can be subjected to large strains before it fractures (i.e., acts as a ductile material). Usually, brittle materials do not have a well-defined tensile fracture stress, and instead the average fracture stress from a set of observed tests is generally reported. For ACP at low temperatures (e.g., 0°C, -10°C, or -20°C), applied loads will initiate microscopic cracks and then these cracks will spread rapidly across the specimen, causing a complete fracture.

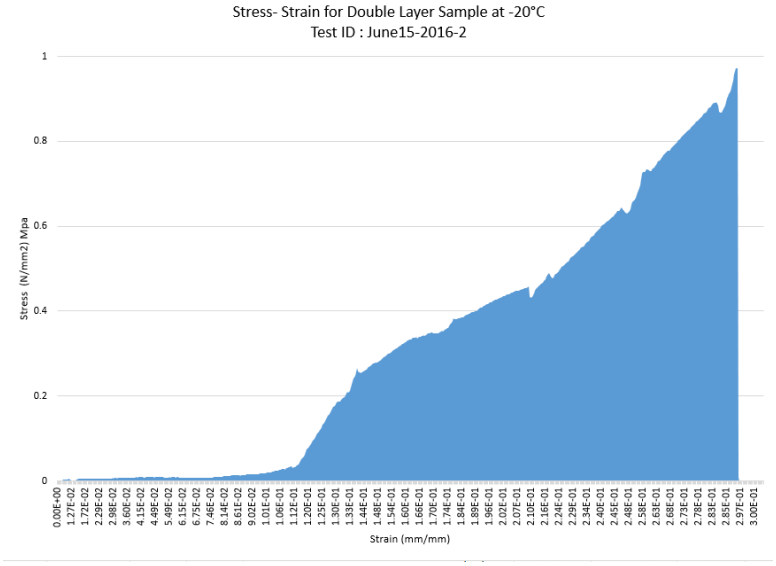

Figure 3-35. Toughness: Area under the stress-strain curve

Chapter 4. Results and Analysis

4.1 Results and Analysis - Test Series A (Temperature Cycling)

This test series resulted in many observations and findings, which are presented in four categories:

a) Paving day observations

b) Sampling day site observations

c) During the test observations

d) Final test results and analysis of Test Series A

4.1.1 Paving day observations

The paving was conducted, on November 15, 2017, by the contractor and observed by several senior engineers representing:

- The Ministry of Transportation of Ontario
- Project consultants and inspectors
- The Road Quality Control Division of the City of Ottawa
- Faculty members and graduate students from the Carleton Civil and Environmental Engineering Department

The asphalt mat for the area compacted by AMIR had a dense surface and different asphalt texture from the area compacted by the CCM (Figure 4-1). This was apparent, even when observed without optical aids.

In addition, several asphalt permeability tests (Figure 4-2) were conducted on the newly constructed road, and the results indicated that areas compacted with AMIR were

significantly less permeable than those compacted with traditional rollers; this reconfirmed the findings of Awadalla et al. (2016). The permeability and the relative density in the design mix procedure would provide a good indication of the actual as-built physical condition of newly constructed HMA road pavements. The permeability tests were beyond the scope of this thesis, and therefore those results were excluded.

Figure 4-1. Photo from paving day. In the photo the right-hand lane (northbound) was compacted with CCM and left-hand lane (southbound) with AMIR

Figure 4-2. Photo from Paving day. Asphalt permeability tests in process for both areas

4.1.2 Sampling day site observations

Samples were taken from two locations, as shown in Figure 3-2 (b).

- Area 1: Compaction with CCM (steel, pneumatic tire, and oscillating), double-layer asphalt on a granular base
- Area 2: Compaction with AMIR (Asphalt Multi-Integrated Roller), double-layer asphalt on a granular base

The following is a summary of the significant observations from the sampling day for the three areas.

  - For Area 1, Compacted using CCM, all ten samples were successfully cut to 300mm long, 100mm wide and 100mm thick. There was an adequate interlayer bond between the asphalt layers, and no de-bonding was observed during the sampling process, Figure 4-3.

Figure 4-3. Photo from Sampling Day - Area 1 and Area 2. The right-hand lane (northbound) is compacted with TCR and the left-hand lane (southbound) with AMIR

- Similarly, for Area 2, Compacted with AMIR, all of ten samples were successfully cut to 300mm long, 100mm wide and 100mm thick. There was an adequate interlayer bond between the asphalt layers, and no de-bonding was observed during the sampling process. In addition to the interlayer bond between the asphalt layers (top course of asphalt and binder course asphalt), there was a strong bond between the lower pavement layers (binder course) and the aggregate base layer below the asphalt.

4.1.3 Observations during the test

As explained in Chapter 3, the test set-up involved subjecting double-layer ACP samples to cyclic temperature changes while under constant tensile stress. At some point, the tensile stress will be higher than tensile strength of the bottom layer (binder course), which is the direct recipient of the tensile stresses, and eventually a crack starts at the

bottom layer. This crack extends through the whole thickness of the bottom layer until it reaches the joint between the binder course and surface course. At that point, the tensile stresses are passed to the top layer through the bond between the two layers. If the bond between the two layers is relatively weak, it will fail, while the top layer remains relatively intact. However, if the bond between the two layers is strong enough, further increases in stress will ultimately cause a failure by cracking the top layer when the tensile stress is greater than its tensile strength.

The tests in this phase showed that most of samples compacted with CCM experienced debonding issues during the testing. Figure 4-4 presents one of these samples which failed in the mode of complete separation or debonding of the two layers. On the other hand, there was no de-bonding or separation of the ACP layers in testing Group 2 samples (compacted with AMIR). The mode of failure for these samples was due to tensile stress where both layers of the samples broke at the same point (Figure 4-5). This shows that the AMIR- compacted samples had stronger interlayer bonding than the samples compacted by CCM. It may be argued that another possibility is that the tensile strength of the CCM top layer sample is greater than that of the AMIR sample; however, the results of Test Series B will show that this is not the case, and that the AMIR samples have higher tensile strength.

Asphalt layers are normally placed in multiple layers during construction, but they are considered as one thick layer at the time of the pavement design and evaluation. If de-bonding occurs between the asphalt layers, each layer is then essentially acting

independently, and as a result, the ACP cannot carry the anticipated stresses and will eventually fail.

An important observation is that the AMIR-compacted samples were able to maintain their bonding throughout Test Series A and after being subjected to multiple temperature cycles, in comparison with the CCM samples that were debonded. This better interlayer-bonding can be attributed to the special geometry of the AMIR roller and the longer compaction duration of each pass due to the longer contact time between the roller's belt and any specific point on the pavement. The bonding strength of interfaces between different contacting materials is proven to be influenced greatly by the pressure received during the compaction of layers (Tschegg et al. 1995). AMIR's multi-layered rubber belt mechanism and flat contact area are believed to increase the friction and mechanical interlocking between the pavement layers, and create a stronger interlayer bond. In order to achieve the fully bonded condition, a higher degree of compaction of the interfacing materials is required (Kruntcheva et al. 2006). One of the reasons that splitting of asphalt concrete layers happens is because the layers did not receive a sufficient degree of compaction.

Figure 4-4. Example of CCM sample failing due to debonding during cyclic temperature testing

Figure 4-5. Example of AMIR sample failing due to tensile stress during cyclic temperature testing

4.1.4 Observations 2 years after construction

The test-road paved for Test Series B (Didsbury Road in Ottawa) was revisited on May 13, 2019, approximately 2 years after paving to perform pavement condition

evaluations and compare the pavement compacted with AMIR and CCM. From a traffic point of view, Didsbury Rd. is a dead end road, and the test section only provides access to the patrol-yard of the Ministry of Transportation (MTO) where the highway maintenance team is stationed. Most of the traffic is heavy trucks.

It has been observed that while there were no cracks on the area compacted with AMIR (Figure 4-6), the section compacted with the traditional steel roller exhibited light cracks (1mm to 5mm wide single or multiple cracks) on more than 25% of its surface.

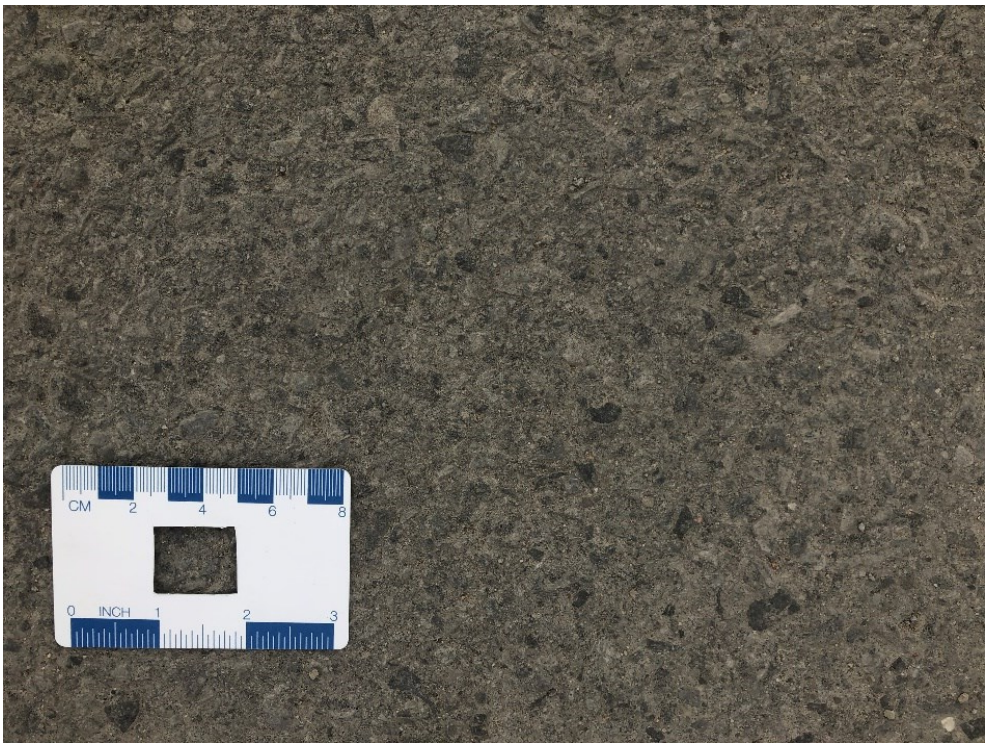

Figure 4-6. Example of the asphalt mat for the area compacted by the AMIR, 2 years after construction

Figure 4-7. Two Examples of the asphalt mat cracked, for the area compacted by the Steel roller, 2 years after construction

4.1.5 Test results and analysis – Test Series A

A total of 54 samples were tested in Test Series A, including the trial tests. After completion of the trial tests, 23 specimens were tested with the CUATC test method, and the analysis and conclusions are based on the results for these 23 samples. The change in length of a sample was measured with a Linear Variable Displacement Transducer (LVDT), and after the completion of each test, the elongation of the sample was plotted as a function of time. Figure 3-11 shows the tests done on samples compacted with the AMIR roller, and Figure 4-8 is an example of the test results for an asphalt sample compacted with the AMIR roller.

In Figure 4-8, the lines track changes in the length of a particular asphalt sample over a period of time. The graph indicates that the result of the temperature cycling test, which is time-dependent, is clearly a periodic waveform with a 24-hour period.

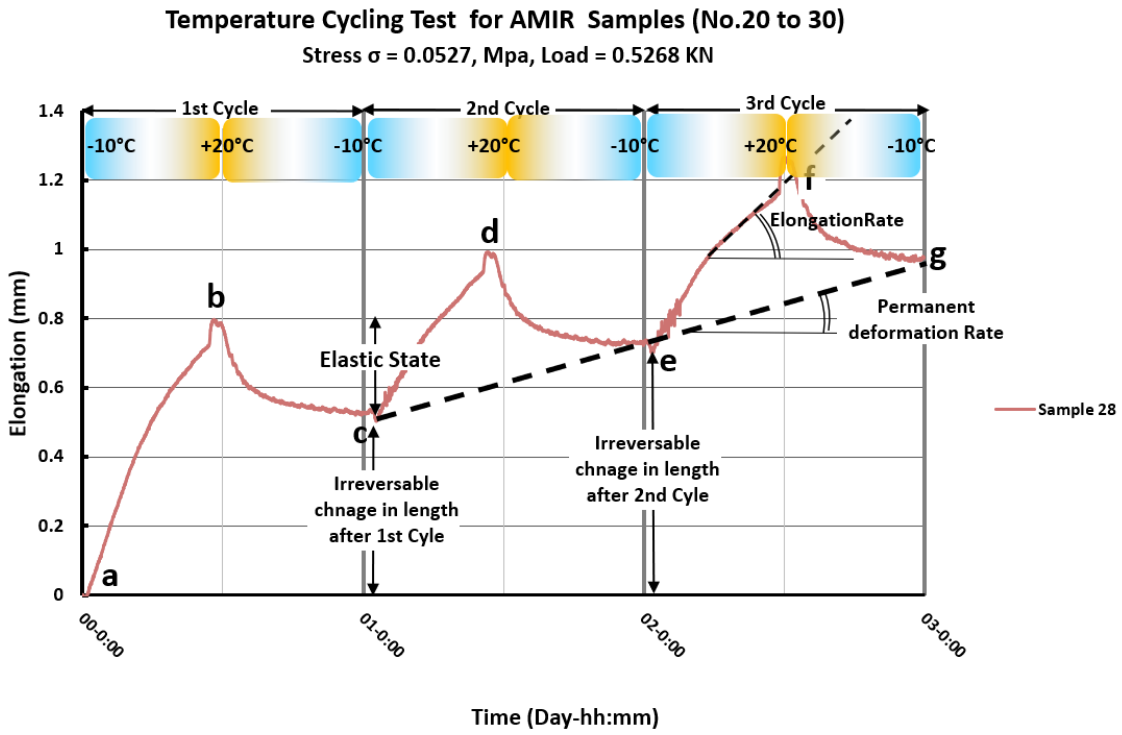

Figure 4-8. Test Series A - Example elongation vs time for three cycles of an AMIR sample

It is important to note that Test Series A is a simple performance test in the context of temperature loading rather than traffic loading. For a closer look at the test results, the process is divided into sets of three cycles of 24 hours each, and each cycle is divided into two phases (primary and secondary phase). Figure 4-8 illustrates the first three cycles of the sample shown previously in Figure 3-10, which was compacted with AMIR, and Figure 4-9 shows a similar graph for a sample compacted with CCM. In both graphs, the slope of the graph at any point represents the instantaneous rate of elongation, where the rate is positive for the primary phase of each cycle and negative for the secondary phase. The line connecting the end of all cycles would represent the rate of permanent elongation (or deformation) with time. As shown in Figure 4-8, the positive rate of permanent elongation indicates a build-up of strain with time. Eventually, after several cycles, asphalt

will have visible cracks that can be seen by the naked eye. The crack's width will increase during subsequent heating/cooling cycles until failure.

As mentioned before, the load was not removed throughout the test period. This fixed applied load is causing the time-dependent deformation (creep) in sample. Creep in asphalt pavements is usually affected by changing conditions of loading and temperature. During the test, the sample was undergoing temperature cycles which was causing strain (thermal strain). These strains were partly in elastic state and some in plastic state. This test is an evaluation of failure mode for asphalt pavements and describes the elongations that are mixture of creep and thermal contractions that follows asphalt concrete beyond the limit of elasticity. the experiment used proposed temperature cycling test on rectangular specimens, differing only on compaction method (exactly similar in mix types, air voids, sample size, temperature and all other aspects).

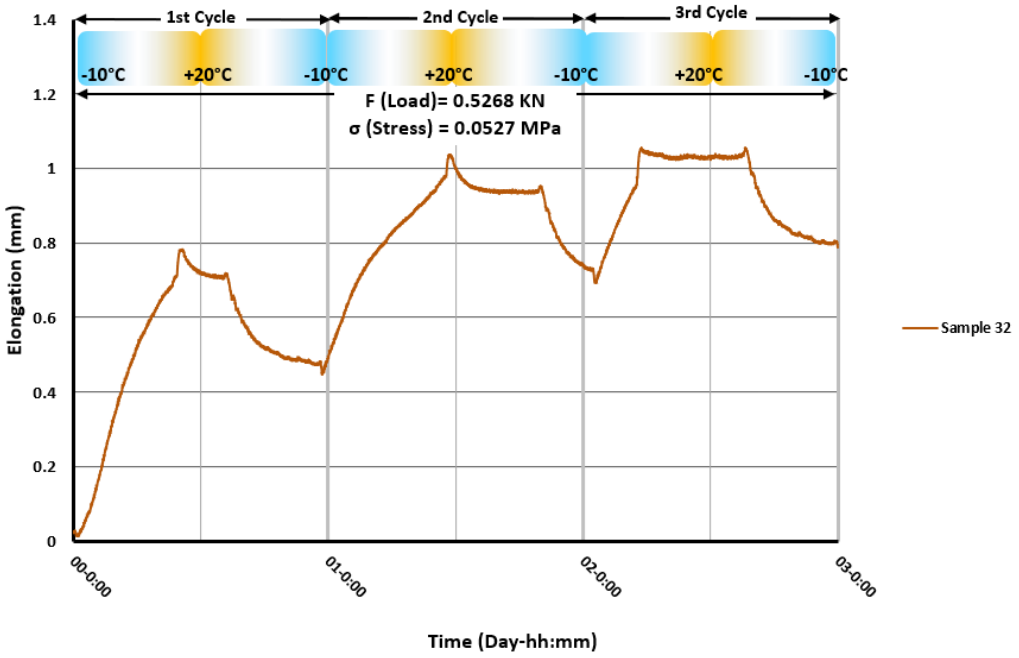

Figure 4-9. Test Series A - Example elongation vs time for three cycles of a CCM sample

- It is clear that the elongation vs time graph of AMIR compacted samples displays regular periodicity waveform, with similarities to sinusoidal waves. While 24 hours is the period of this curve, the amplitude of the curve is the maximum measured elongation of the sample in the cycle.
- It was observed that sample elongation increased rapidly after the test was started, when the sample was subjected to tensile stress only and the temperature gradually increases from -10°C to +20°C (i.e., Point A to Point B). This was the 'primary phase' of the first cycle, and occurred during the first 12 hours of the test. As expected, the increased temperature resulted in thermal expansion. As mentioned earlier, the elongation of the samples was due to the combined effect of creep (due to the applied load) and thermal expansion/contraction.
- Point (b) was the beginning of the 'second phase' of the first cycle, when elongation stops as the temperature was set to be decreased to go back to -10°C, applied load is still 0.5268 KN. The decrease in temperature causes contraction of the sample.
- Point (c) was the end of the first cycle, applied load is still 0.5268 KN, and the graph shows that the length change of the sample was not self-reversing after the temperature fell back to -10°C. The asphalt sample did not return to its original shape, the stress was enough to permanently change the sample's length and cause plastic deformation.

- With regard to the second and third cycles, the reaction of the samples to the temperature cycles was the same as in the first cycle. The sample length increased from Points C to D and points E to F, and decreased from Points D to E and Points F to G. At the end of each cycle, the permanent deformation was greater than it was for the previous cycle.
- Results showed that both primary and secondary phases affect the asphalt sample at every cycle until it breaks.
- The graph (Figure 4-10) also shows that at the end of the third cycle, a slight increase in the tensile load increases the elongation rate. The sample has larger permanent deformations after the third cycle.

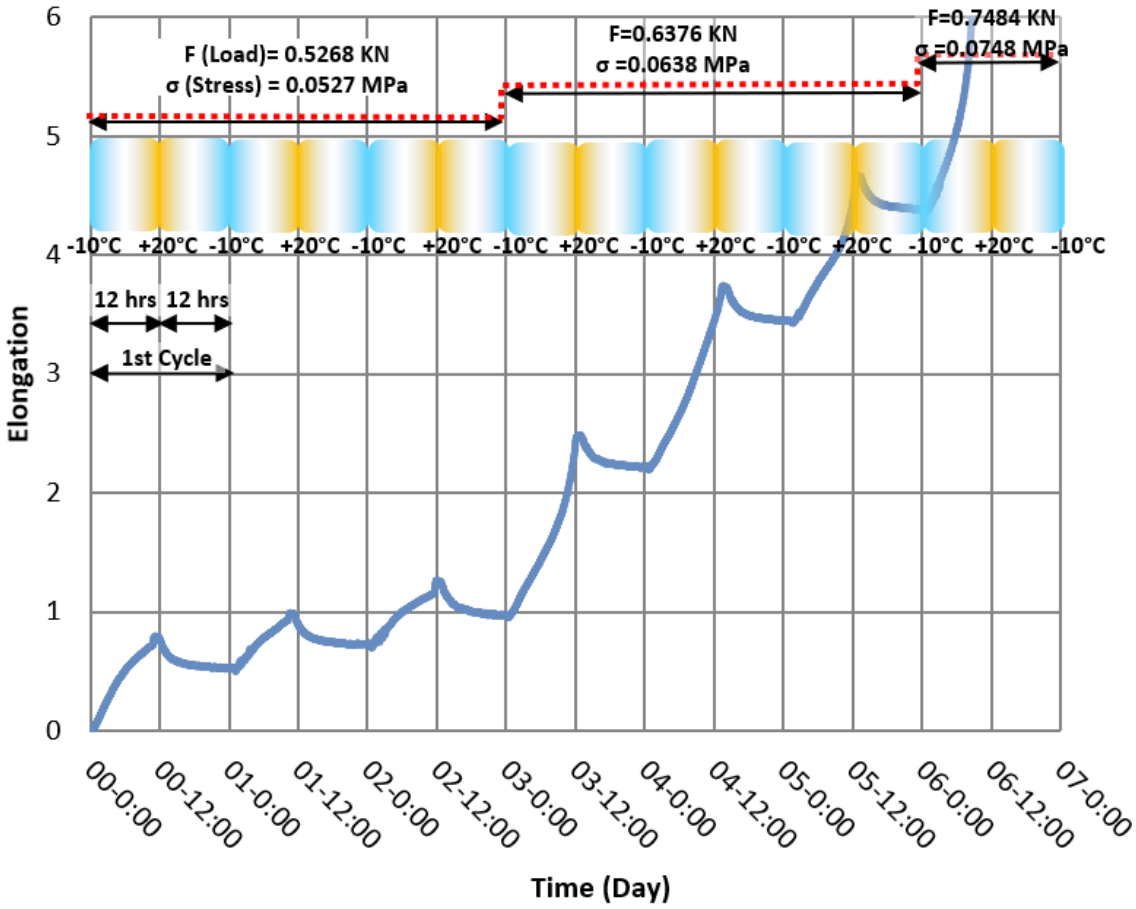

Figure 4-10. Elongation vs Time for 7 cycles of TCT for AMIR compacted sample

- After each cycle, the permanent deformation increased slightly (Figure 4-11). This phase could be named as 'crack initiation', and the crack grows rapidly after initiation. The slow increase is due to damage accumulation, and the rapid increase is caused by crack propagation.

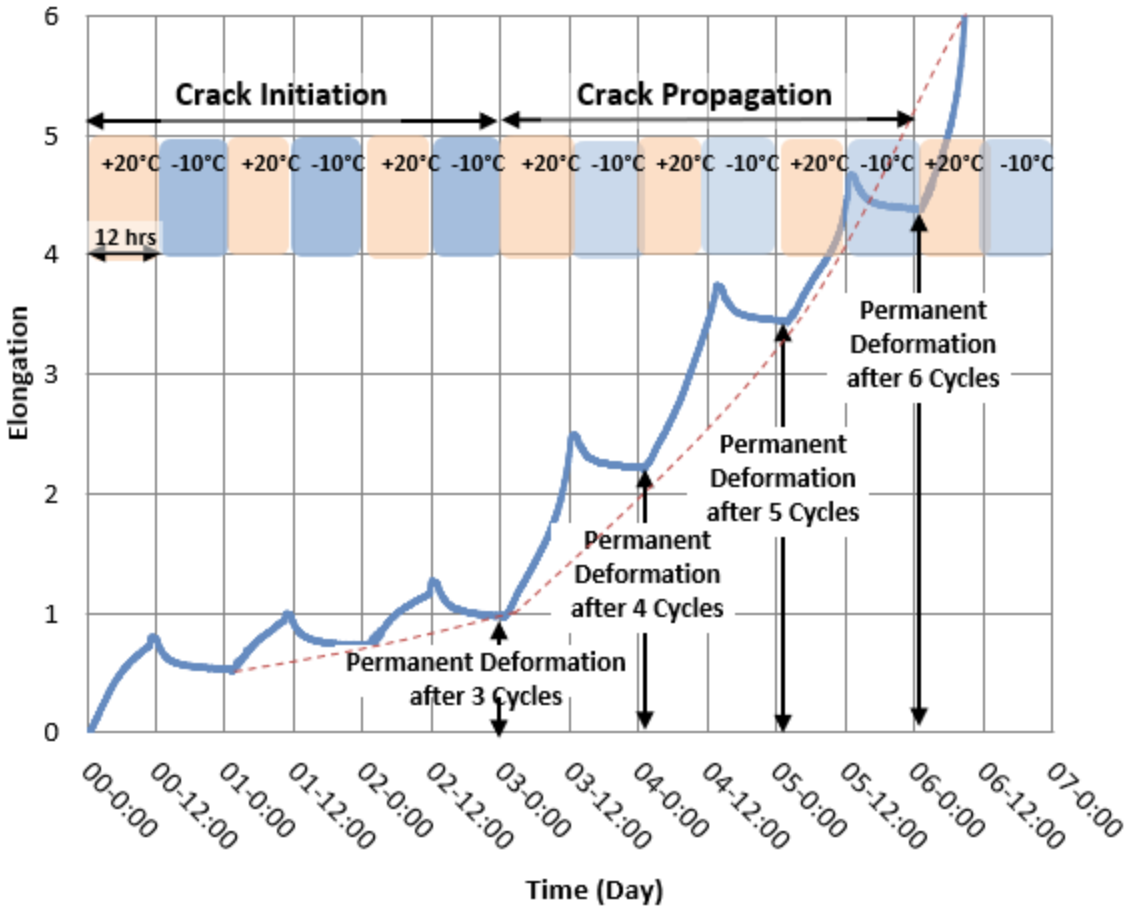

Figure 4-11. Crack Initiation & Crack Propagation

The above-plotted results for Test Series A demonstrate the time-dependent deformation of these asphalt samples under the specific applied loads (direct tensile strength test) and described simultaneous temperature cycling. The elongation trends of the asphalt samples are clear. Thermal expansion and contraction occur by rising temperatures and during cold cycle periods, respectively. As shown, there is a permanent strain after every cycle that results in surface cracks and reduced tensile strength of the pavement. Eventually, after several cycles, the asphalt will have visible cracks. In actual

road situations, after several cycles, ACP cracks and also loses its interlayer bond. The cracks' width will increase during subsequent heating/cooling cycles, which allows water to seep in and freeze during the next sub-zero temperature, thereby increasing expansion which in turn causes more cracking. At the same time, since the ACP loses its bond, the asphalt layers will not be able to work together against created stresses and the ACP will be more vulnerable. The above test results show that asphalt pavement loses a significant portion of its tensile strength while undergoing heating/cooling cycles, and sooner or later, by the appearance of wide cracks and potholes, the asphalt loses its integrity and there will be no tensile strength. is an example of the test results for an asphalt sample compacted with the AMIR roller. Figure 4-12 and Figure 4-13 presents more results of Test Series A for both CCM and AMIR compacted samples.

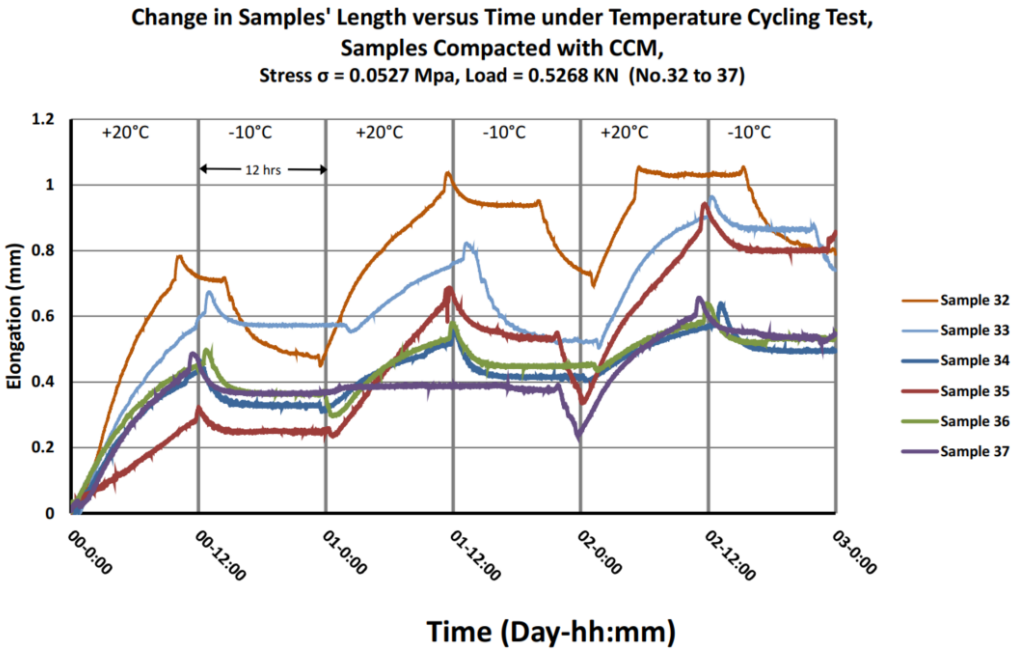

Figure 4-12.Test Series A - Elongation vs time for three cycles of 6 samples compacted with CCM

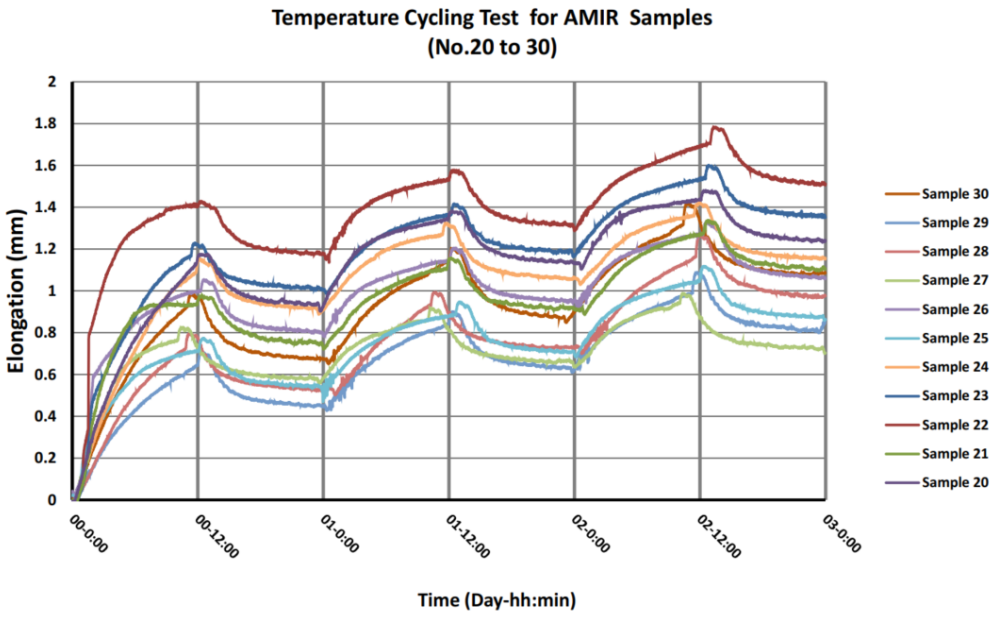

Figure 4-13. Test Series A - Elongation vs time for three cycles of 11 samples compacted with AMIR

4.1.6 Relationship Between Variables – Test Series A

In Test Series A, “change in length of the sample” or “elongation” is the dependent variable, and “compaction method” (AMIR or CCM), “time”, and “temperature” are the three independent variables that affect the dependent variable (elongation). The forward selection method was used for the linear regression analysis and it shoes that all of these independent variables contribute to the results of the elongation. The results of the ANOVA test showed that all three independent variables are significantly related to the dependent variable (change in length of the sample). See Appendix D for details of the above-mentioned regression analysis and completed ANOVA test and related discussions.

4.2 Results and Analysis - Test Series B

Figure 4-14 is an example of the box plot of the results of the samples tested for group 4, single-layer samples at -20°C.

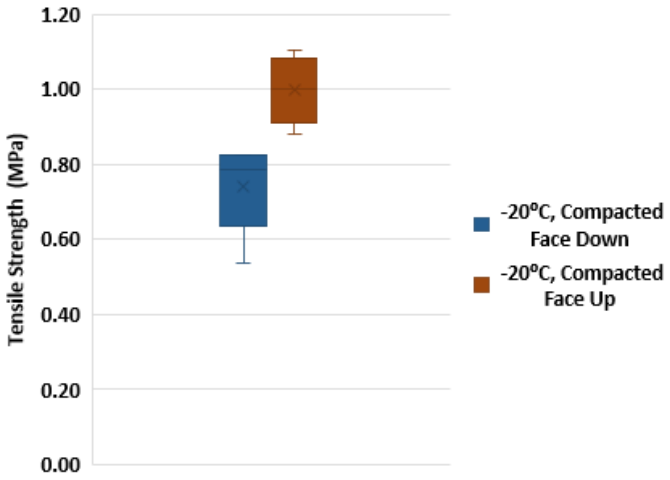

Figure 4-14. The box plot of the results of Test Series B for single-layer sample at -20°C

This figure shows that the calculated stress was lower for the samples tested with their roller-compacted faces down, in comparison with results of the samples tested while roller-compacted faces up. In other words, the samples required less loading to break when tested with their compacted surfaces facing down. Similar results were observed for the following five groups of samples, as summarized in Table 4-1:

- Double-layer samples tested at -20°C average tensile strength decreased by 7.97%
- Single-layer samples tested at -20°C average tensile strength decreased by 25.65%
- Double-layer samples tested at -10°C average tensile strength decreased by 6.47%
- Single-layer samples tested at -10°C average tensile strength decreased by 15.03%
- Single-layer samples tested at 0 °C average tensile strength decreased by 11.61%

As shown in Table 4-1, only the double-layer sample at 0°C did not follow this pattern, and the average tensile strength for roller-compacted face down was higher than the average tensile strength for roller-compacted face up. It should be noted that in this group (double-layer at 0°C) for samples tested with roller-compacted face up, out of 7 samples, only for 1 sample both layers cracked together. For 3 samples, only the bottom layers cracked, and the top layer did not crack and just disconnected from the tack coat line. For the remaining 3 samples, the glue failed but the sample was also cracked at the same time. For this group of samples, the double-layer sample at 0°C tested with roller-compacted face up, more than 19 tests were performed with the hope of obtaining at least 5 samples those both layers crack together before glue fails but unfortunately, for most of the samples, the glue has failed, and samples were disconnected from mounting plates before the sample cracks and therefore their results were excluded from the analysis. Considering the above details, the results of this group may not be considered in the final analysis.

Table 4-1. Percentage decrease in calculated tensile strength for each group of roller-compacted face down and roller-compacted face up samples

Temperature	**0 °C**	**-10 °C**	**-20 °C**
Double-layer samples	-5.94%	6.47%	7.97%
Single -layer samples	11.61%	15.03%	25.65%

As mentioned before, all the samples used for Test Series B were compacted with CCM. Theoretically, ACP of a specific thickness should fail at almost the same stress

regardless of whether the sample was set face-up or face-down (assuming the ACP is homogeneous and isotropic). However, the results indicated that the roller-compacted face-down samples failed at lower stresses than the face-up samples (except for double-layer at 0°C). Subsequent statistical analysis confirmed that these differences are statistically significant at a 5% level of significance at the -20°C testing temperature. This means that the same ACP has a weaker top layer than bottom, which can be attributed to the formation of microcracks during compaction. These construction-induced cracks can significantly reduce the tensile strength of asphalt layers and accelerate the development of cracks when the sample is subjected to tensile stresses, such as under cold winter temperatures. The samples tested with the roller-compacted faces up did not have the construction cracks at the interface between the loading plates and the sample, and as a result, higher stresses were required to break those samples. Figure 4-15 and Figure 4-16 are the box plots of the results for double-layer and single-layer samples tested for Test Series B at temperatures of 0°C, -10°C, and -20°C. Table 4-2 presents the descriptive statistics for these results.

In Figure 4-15, comparing the test results for the roller-compacted face-down double-layer samples at 0°C, -10°C, and -20°C, the results indicate that the samples failed at lower stresses when tested at 0°C than at -10°C. The same is observed for the single-layer samples when tested at the same two temperatures. However, comparing the results for the samples tested at -10°C and -20°C shows that that the samples failed under lower stresses when tested at -20°C than at -10°C. The drop in temperature is believed

to have increased the stiffness of ACP, resulting in excessive brittleness and reduced its resistance to the applied stresses.

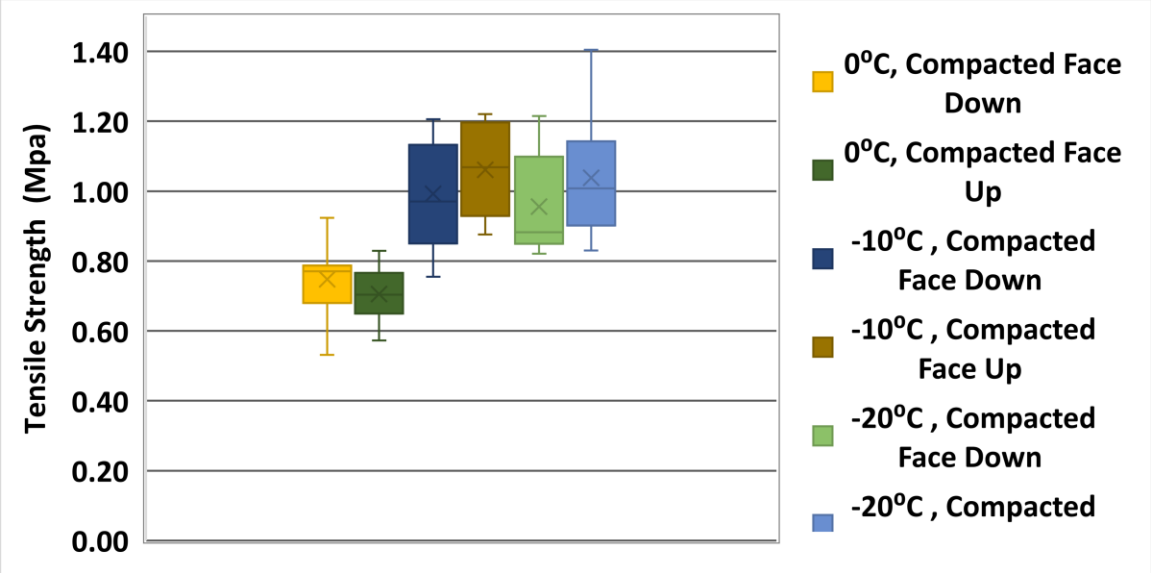

Figure 4-15. The box plot of the results for double-layer samples, Group 3 to 8

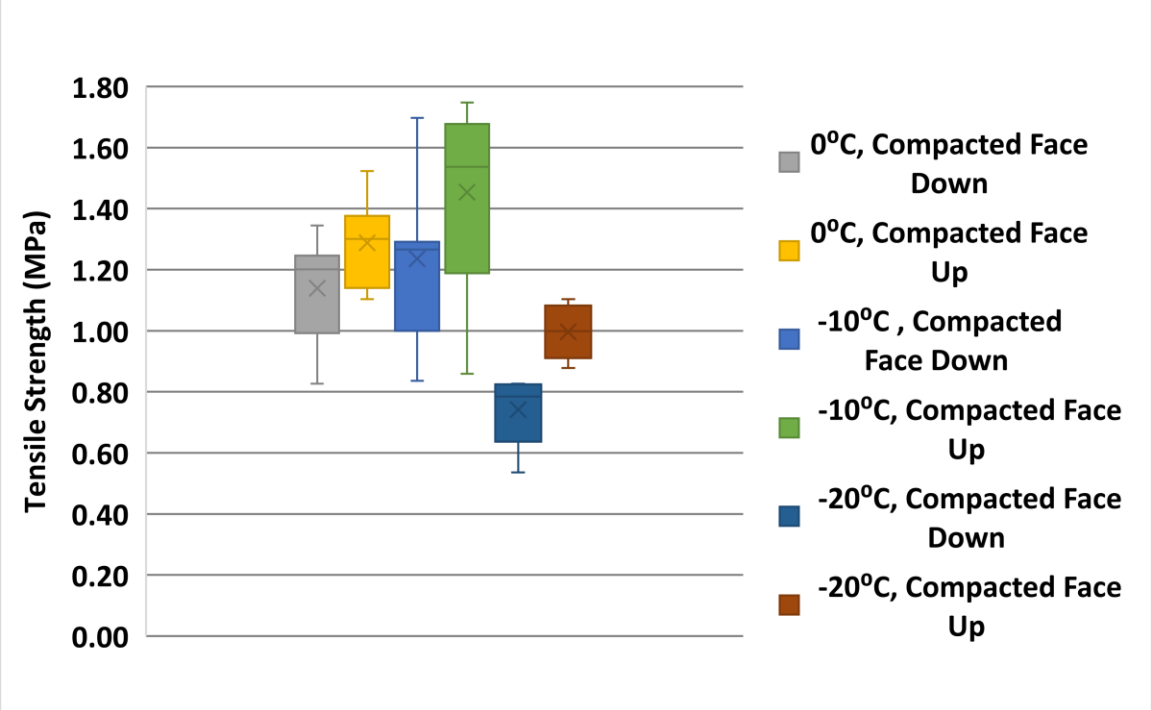

Figure 4-16. The box plot of the results for single-layer samples, Group 11 to 16

Table 4-2. The descriptive statistics, Test Series B Tensile Strength (N/mm2), Group 1 to 16

Single-Layer Samples	0°C, Compacted Face Down	0°C, Compacted Face Up	-10°C , Compacted Face Down	-10°C, Compacted Face Up	-20°C, Compacted Face Down	-20°C, Compacted Face Up
Mean	1.139	1.289	1.235	1.454	0.741	0.997
Median	1.201	1.301	1.266	1.537	0.785	0.999
Standard Deviation	0.180	0.139	0.269	0.344	0.120	0.090
Minimum	1.345	1.523	1.697	1.747	0.827	1.103
Maximum	0.827	1.104	0.836	0.860	0.536	0.878
Count	6	9	7	5	5	5

Double-Layer Samples	0°C, Compacted Face Down	0°C, Compacted Face Up	-10°C, Compacted Face Down	-10°C, Compacted Face Up	-20°C, Compacted Face Down	-20°C, Compacted Face Up
Mean	0.747	0.705	0.992	1.061	0.956	1.038
Median	0.771	0.704	0.970	1.068	0.882	1.008
Standard Deviation	0.102	0.082	0.161	0.137	0.156	0.198
Minimum	0.532	0.573	0.755	0.876	0.821	0.830
Maximum	0.924	0.829	1.206	1.220	1.215	1.404
Count	11	7	9	6	5	6

As mentioned in Chapter 3, in order to use Equation 3.1 and calculate σ_{avg}, it is assumed that the material is homogeneous and isotropic. Some may question HMA properties' to be qualified to be approximated as being both homogeneous and isotropic. Also, to consider the material a continuous material, it should have a uniform distribution of matter with no voids, while HMA does have voids between its aggregates (approximately 4%). Furthermore, as discussed in Chapter 3, the external forces (F) are being applied to the asphalt concrete sample via mounting plates as a distributed force, creating shear stress acting tangent to the ACP specimen. These forces produce a couple moment that was not included in the above stress calculation and comparisons. In order

to address these concerns, the recorded maximum applied load for each sample was used for the analysis instead of the tensile strength of the specimens. Table 4-3 presents the percentage decrease in maximum load (KN) for each group of roller-compacted face down and face up samples, and Table 4-4 has the descriptive statistics for Test Series B using Max Load (kN) instead of tensile strength for Groups 1 to 16. The results presented in Table 4-3 are very similar to the analysis presented in Table 4-1 when tensile strength was used for comparison (except that the group of single-layer samples at 0°C does not follow the noted pattern.

Table 4-3. Percentage decrease in maximum load (KN) for each group of roller-compacted face-down and face-up samples

Temperature	**0°C**	**-10°C**	**-20°C**
Double-layer samples	-8.35%	10.12%	8.14%
Single-layer samples	-2.52%	14.26%	19.87%

This table shows that the maximum loads required to break the samples (at -10°C and -20°C for both the single- and double-layer samples) were lower for the samples tested with their roller-compacted facedown, in comparison with the results of the samples tested while roller-compacted faceup. The samples required less loading to break when tested with their compacted surface facing down. Similar results were observed for the mentioned four groups of samples, as summarized in Table 4-3.

Table 4-4. Descriptive statistics, Test Series B, Max Load (kN), Groups 1 to 16

Single-Layer Samples	0°C, Compacted Face Down	0°C, Compacted Face Up	-10°C, Compacted Face Down	-10°C, Compacted Face Up	-20°C, Compacted Face Down	-20°C, Compacted Face Up
Mean	6.317	6.161	6.177	7.204	3.941	4.918
Median	6.609	5.934	6.330	7.303	3.924	5.220
Standard Deviation	0.825	0.650	1.347	1.788	0.889	0.732
Minimum	4.796	5.104	4.182	4.298	2.544	4.090
Maximum	6.974	7.234	8.484	9.130	4.959	5.765
Count	6	9	7	5	5	5

Double-Layer Samples	0°C, Compacted Face Down	0°C, Compacted Face Up	-10°C , Compacted Face Down	-10°C, Compacted Face Up	-20°C, Compacted Face Down	-20°C, Compacted Face Up
Mean	7.472	6.896	9.368	10.423	9.081	9.886
Median	7.709	7.037	9.703	10.648	8.524	9.503
Standard Deviation	1.020	1.066	1.525	0.861	1.481	1.844
Minimum	5.317	5.444	6.794	9.360	7.959	7.889
Maximum	9.238	8.267	11.048	11.591	11.544	13.340
Count	11	7	9	6	5	6

Figure 4-17 and Figure 4-18 are the box plot of the results for double-layer and single-layer and samples tested for Test Series B at temperatures of 0°C, -10°C, and -20°C using maximum applied loads (vs tensile strength)

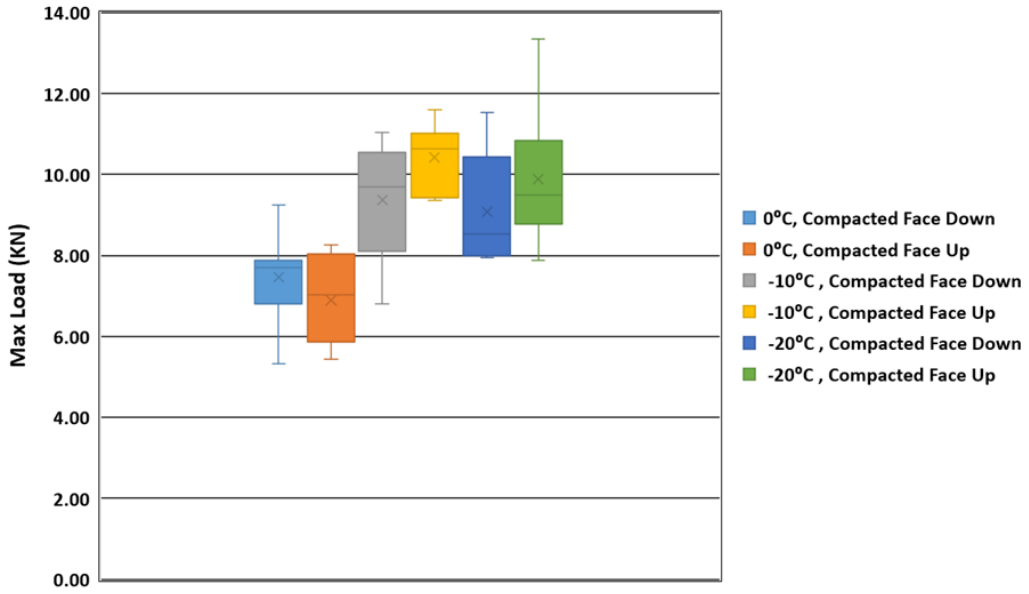

Figure 4-17. The box plot of the results for Max Load (KN) applied to double-layer samples, Group 3 to 8

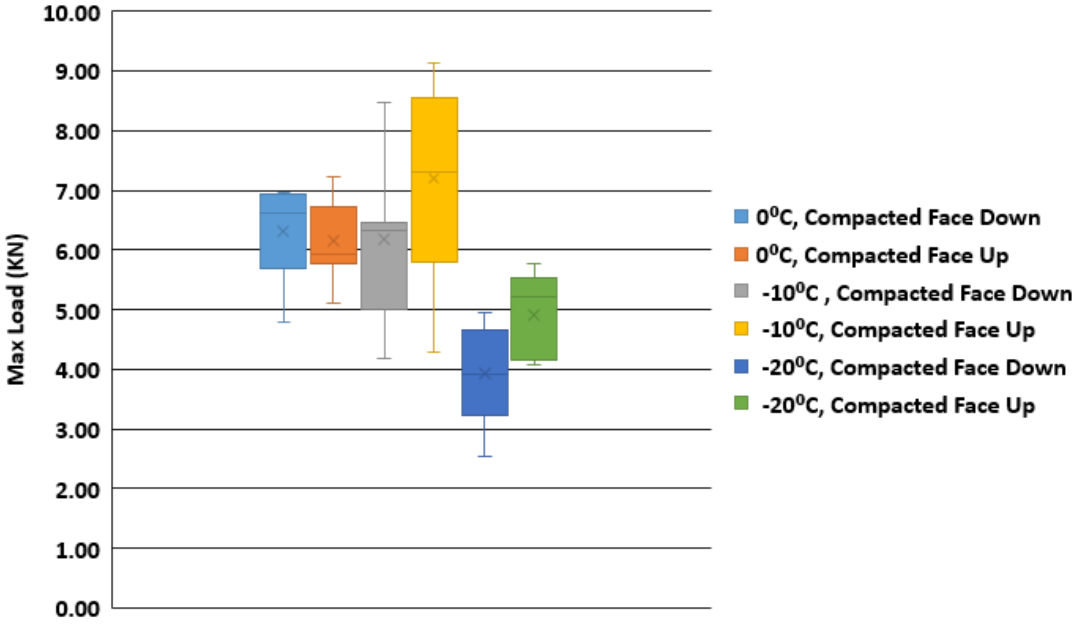

Figure 4-18. The box plot of the results for Max Load (KN) applied to single-layer samples, Group 3 to 8

It could be argued that increased stiffness in the top surface of the ACP, due to greater compaction, may be the reason for the lower load at failure for the face-down samples reported in Test Series B. However, the literature suggests that the stiffness of

a 90mm-thick ACP is almost the same from the top to bottom of the layer. The depth of influence of compaction is affected by several factors including but not limited to the roller's weight, size, number of passes, and type of bedding materials (such as aggregate base or rigid layer). Fathi et al.'s (2021) used site measurements and different simulation models to assess the depth of influence of compaction rollers. The results showed that the depth of influence in that study was much greater than the 90mm-thick double-layer samples used for this study, and therefore the stiffness of the material is expected to be almost the same from the top or bottom of the 90mm-thick layer of ACP. Furthermore, if the mentioned notion, compacted top of the layer is much stiffer than bottom of layer, was true for the same strain (displacement), the area with higher stiffness should be able to carry more load and result in higher load at failure.

4.2.1 Statistical Significance and Hypothesis Test – Test Series B

Independent t-tests were performed using the Analysis ToolPak in Microsoft Excel for the findings of both the single-layer and double-layer samples tested at temperatures of 0°C, -10°C, and – 20°C.

The tests started by assuming that the means of the below two groups were equal (null hypothesis is, the means of the two distributions are equal):

- the tensile strength for samples with the roller-compacted face down (with the construction-induced cracks facing the table)
- the tensile strength for samples with the roller-compacted face up

If the t-test rejects the null hypothesis, it indicates that the groups are highly probably different.

The significance level for this t-test was 5% (critical value is $\alpha = 0.05$), meaning that if we run the experiment 100 times, 5% of the time we will be able to reject the null hypothesis and 95% of the time we will not (in other words, the confidence interval (CI) always specifies a confidence level, usually 95%, which is a measure of the reliability of the procedure).

Table 4-5 presents examples of the P-value results of independent t-tests for the single-layer samples of Group 12 and Group 16, tested at -20^{o}C. Since the calculated P-value (0.005) is less than 0.05, therefore the differences between the average of the samples compacted face-up and the samples compacted face down is significant at -20^{o}C.

Table 4-6 presents the summary of the results of the independent t-tests performed on all 16 groups. As previously mentioned, these differences are statistically significant, at a 5% level of significance at the -20°C testing temperature.

Table 4-5. Results of the Independent T-Test for Single-layer Samples at -20^{o}C (Groups 12 & 16)

	-20^{o}C, Compacted Face Down	*-20^{o}C, Compacted Face Up*
Mean	0.741	0.996
Variance	0.014	0.008
Observations	5	5
P(T<=t) two-tail	0.005	
t Critical two-tail	2.306	

Table 4-6. Summary of the P-values, Results of the Independent T-Test

	Compacted Face	0 °C		-10 °C		-20 °C	
Double-layer samples	Up	Group 2	0.375	Group 3	0.407	Group 4	0.469
	Down	Group 6		Group 7		Group 8	
Single-layer samples	Up	Group 10	0.091	Group 11	0.244	Group 12	0.005
	Down	Group 14		Group 15		Group 16	

4.2.2 Analysis of Variance – Test Series B

The two-way analysis of variance (ANOVA) was performed on the results for Test Series B in order to examines the influence of two different categorical independent variables (i.e., presence of construction induced-cracks and temperature) on tensile strength (our dependent variable). The results of the two-way ANOVA in SPSS Statistics as performed on the double-layer and single-layer sample test results are presented in Table 4-7 and Table 4-8.

The results show that the effect of the “compaction face up/down” variable and the effect of “temperature” both significantly impact the tensile strength of the asphalt pavement based on the results obtained for the single-layer asphalt samples (

Table 4-8). As for the double-layer samples, it shows that only the influence of “temperature” significantly affects the dependent variable.

Table 4-7. Results of The Two-Way ANOVA Test for Double-layer Samples

Tests of Between-Subjects Effects[a]					
Dependent Variable: Stress					
Source	Type III Sum of Squares	df	Mean Square	F	Sig.
Corrected Model	.884[b]	5	.177	9.076	.000
Intercept	34.443	1	34.443	1767.382	.000
Temperature	.850	2	.425	21.810	.000
CompactedFace	.014	1	.014	.701	.408
Temperature * CompactedFace	.035	2	.018	.898	.416
Error	.741	38	.019		
Total	37.017	44			
Corrected Total	1.625	43			
a. DoubleSingleLayer = Double-Layer					
b. R^2= 0.544, (Adjusted R^2 = 0.484)					

Table 4-8. Results of The Two-Way ANOVA Test for Single-layer Samples

Tests of Between-Subjects Effects[a]					
Dependent Variable: Stress					
Source	Type III Sum of Squares	df	Mean Square	F	Sig.
Corrected Model	1.632[b]	5	.326	7.693	.000
Intercept	46.039	1	46.039	1085.092	.000
Temperature	1.285	2	.643	15.145	.000
CompactedFace	.381	1	.381	8.986	.005
Temperature * CompactedFace	.018	2	.009	.211	.811
Error	1.315	31	.042		
Total	53.009	37			
Corrected Total	2.947	36			
a. DoubleSingleLayer = Single-Layer					
b. R^2= 0.554, (Adjusted R^2= 0.482)					

4.2.3 Test Series B – Bond Between Layers

It was observed that of the 171 double-layer 600mm x 300mm slabs received from the sampling lot, 27 (26%) showed separation of the top course from the bottom course after being stored on laboratory shelves for approximately six months at +20 °C (Figure 4-19). These 27 samples were excluded from the testing program. Furthermore, it was observed that approximately one-third of all the double-layer slabs received from the sampling lot at the Carleton Laboratory showed debonding signs after being stored for 1 year at +20 °C. These findings are important, because they indicate that even without a load or exposure to low temperatures and tensile stress, the asphalt layers can still separate. The bonding condition between two layers of asphalt slabs was also examined during Test Series A at temperatures of +20°C, 0°C, -10°C, and -20°C. The results showed that 17 of the 171 slabs (10%) had bottom layer cracking and the top layer was disconnected from the bottom layer at the tack coat line (debonding). For the other slabs both layers cracked at the same time.

Figure 4-19. Asphalt slabs disconnect at the bond line prior to test.

Chapter 5. Conclusions

In summary, part of this research studied the bonding of different HMA layers in an ACP structure. With ACP usually constructed using two lifts or layers, the strength of the interlayer bonding and resistance to both cyclic temperatures and sustained cold temperature are very important for the pavement's long-term performance in cold regions. The experimental portions of the research consisted of two phases, in which the first phase (Test Series A) focused on resistance to cyclic temperature changes and the second phase (Test Series B) focused on resistance to thermal stresses at a sustained cold temperature. Both phases were performed using testing machines that were designed and built in-house. The cyclic temperature testing (Test Series A) showed that when ACP is exposed to temperature cycles (above and below freezing), it can experience a loss of interlayer bonding. The results showed that samples constructed using conventional compaction method (CCM) experience interlayer debonding while samples compacted using AMIR are able to maintain their interlayer bond. The loss of bonding, or layer debonding, would cause the two HMA layers to act independently and thus offer lower resistance to thermal forces.

The results of Test Series B, which focused on CCM samples, showed that the samples failed at different stresses depending on which surface was in contact with the test plates. The results showed that the samples surface-up had a higher strength compared to surface-down samples, indicating that the construction-induced cracks at the top surface help accelerate failure.

Considering the results of both Test Series, it could be concluded that if the pavement's bond survives cycles of low and high temperatures, the pavement will show superior tensile strength and better resistance to low-temperature cracking in cold winter temperatures. It shows that improving interlayer bonding by different means, including employing better compaction methods, will improve ACP's capability to withstand cyclic temperature changes.

This research and related laboratory tests explain how different types of equipment used for compacting the asphalt can affect the tensile strength and interlayer bond of asphalt pavement. Presented results show that hairline-cracks initiated during the construction process can reduce the tensile strength of newly paved asphalt layers. This suggests that current asphalt compaction equipment and processes play an important role and one of the major causes of crack initiation in asphalt layers. Due to the effects of traffic and cold temperatures, these cracks grow rapidly, and they will not be prevented unless construction methods change, and compactors are modified to avoid creating construction-induced cracks in paved asphalt layers. This view is in contrast to those who believe asphalt cracks are initiated due to thermal stresses.

5.1 Summary of Conclusions for Test Series A

Regarding Test Series A, the plotted results show the time-dependent deformation of rectangular asphalt samples from an actual road under specific applied loads. The study showed clear trends in the elongation of asphalt samples under a constant load with a direct tensile strength test, and simultaneously under thermal cycling and with sudden drops in temperature. The graphs show that asphalt thermal expansion

happens due to rising temperature, and that shrinkage occurs during cold-cycle periods. When the stress is removed, the material does not return to its previous dimensions, and there is permanent strain. Thus, asphalt pavement undergoes time-dependent changes in length. The developed stress exceeds the asphalt concrete's tensile strength to the extent that the asphalt mat can exhibit visible cracks after only a few cycles. The width of the cracks will change during subsequent heating/cooling cycles. Crack expansion allows water to seep in and freeze during the next sub-zero temperature, thereby increasing expansion, which causes more cracking. The test results show that asphalt pavement loses a significant portion of its tensile strength when undergoing heating/cooling cycles, particularly with the sudden temperature decreases in late fall and early winter. Asphalt cannot resist these thermal cycles and flash-freezing. Also, analysis of the results reveals that the effects of "resistance to temperature cycling" and "compaction method" are very important and should not be ignored when reviewing the performance of ACP.

5.1.1 AMIR Roller

- Asphalt concrete's tensile strength after final surface compacting by AMIR's flexible multi-layered rubber belt is improved. This is attributed to less roller-induced surface-cracking by AMIR. The superior impermeability of asphalt concrete's final surface is also related to the way the pavement's surface is formed by AMIR. Asphalt compacted with AMIR has a thick, condensed, and more uniform pattern when compared with asphalt surfaces compacted with conventional compactors. AMIR-compacted pavement has a very distinctive surface (see Figure 4-6).

- The fracture shape of the AMIR samples shows its superior interlayer bonding in comparison with CCM. Non of the AMIR-compacted samples debonded during the tests. A crack initiated at the bottom of the sample, expanded and moved upward toward the top of the sample as the load increased, and eventually the sample broke into two parts (Figure 3-11).
- The better interlayer bonding of the AMIR samples is also attributed to AMIR's special geometry (with flat roller surface) and longer contact time with the asphalt mat. These characteristics of AMIR improve the compaction quality and potentially increase the mechanical interlocking/friction between the asphalt layers. The pressure created by AMIR's multi-layered rubber belt creates superior interlayer bonding for constituent layers.

5.1.2 Conventional Compaction Method (CCM) Rollers

- Splitting of the samples into two layers while tested was observed in Test Series A, as the upper and lower layers of the samples de-bonded during the test. Also, the fracture shape was different from the AMIR samples. For the CCM samples, a crack initiated at the bottom of the sample near the plates, and expanded and moved upward toward the top of the sample, but it stopped when the crack arrived at the horizontal joint between the binder course and wearing course, and the bottom layer of asphalt separated (debonded) from the top layer. To explain this mode of failure, in the author's view, when the initiated crack moved upward and arrived at the horizontal joint between the asphalt layers, the

asphalt sample is resisting two stresses at the same time, in the horizontal and vertical directions. However, the interface failure in these cases was a result of overcoming the vertical stiffness to the interface bond. In these CCM samples, the applied method of compaction reduced the shear strength, and eventually the shear strength was reached and the interface cracked (de-bonding of layers). Inadequate shear stiffness and eventual inadequate interlayer bonding was created with CCM at the time of construction. Based on Kruntcheva et al.'s (2006) research, one of the reasons for the debonding issue observed in most of the samples could be the amount of the pressure received during the compaction of layers by CCM.

- The *elongation vs time graph* of the TCT for samples compacted with CCM (Figure 4-9) shows irregular elongation rates and patterns, especially in the secondary (cooling) phase of the cycles. This is because the homogeneity of samples compacted with CCM is negatively affected by its aggregate distribution due to the nature of the CCM method (push-pull). Asphalt is composed of discrete particles, so the homogeneity of asphalt mixtures can directly affect the overall properties of the pavement. Observed irregularity is a sign of this non-heterogeneous end-product of CCM.
- The tensile strength of the samples compacted with CCM was negatively affected by cracks. These construction-induced cracks are activated and grow as soon as the stress increases, and the tensile strength of the sample suffers.

Figure 4-9 shows the irregular elongation rate and pattern results because of the existence of many cracks with irregular and unpredictable behaviour.

5.2 Summary of Conclusions for Test Series B

In Test Series B of this research, the damage caused by microcracks that originate during the construction of ACP were assessed using CUADTS tests at temperatures of -10°C, 0°C, and -20°C.

Based upon the work presented here and summarized above, the following conclusions were drawn:

- There is a meaningful important and significant difference between samples tested with the roller-compacted faces up and those with the roller-compacted faces down. Slabs with the roller-compacted face up had higher stress resistance than similar samples with their compacted surfaces facing down. This suggests that construction cracks influence the tensile strength of asphalt pavement.
- This study demonstrates the negative impacts of compaction-induced microcracks on the structural behaviour of layers of new asphalt. The results indicate how these cracks can alter the structural responses of asphalt layers to applied stress and reduce the mechanical properties of newly laid asphalt pavement layers.
- It is proposed that reducing the number of cracks, particularly construction-induced cracks which propagate in colder temperatures, will strengthen asphalt layers and extend the service life of asphalt pavement.

5.3 Recommendations for Future Research

While the results of this investigation appear promising, there is a need to evaluate both of the test methods used in this study (CUADTS and CUATC) for repeatability and by testing mixes with different aggregate gradations and asphalt binders. Also, in order to use either of these methods (CUADTS and CUATC) in routine proof testing, there is a need to develop pass/fail criteria for the testing of hot mix asphalt (HMA). Furthermore, field validation trials and tests are needed to move the testing forward to the industry implementation stage.

Test Series A could be repeated with different temperature cycles, such as -10°C to + 10°C or -15°C to +10°C, and the results compared with the results of this study. This investigation has showed that a deeper understanding of failure mechanisms is necessary, as the results showed that some widely believed failure mechanisms might not be very reliable.

References

Abd El Halim, A., Pinder, F., Halim, A., Tayyeb, H., Chelliah, A.R. and Awadalla, M., 2016. Field and Laboratory Studies of AMIR II Compacted Asphalt Pavement. *Journal of multidisciplinary engineering science and technology*, pp.3159-0040.

Abd El-Halim, A. O. and Svec, O. J., 1990a. Field and Laboratory Evaluation of a New Compaction Technique. Proceedings, the Fourth International RILEM Symposium on Bituminous Mixes, Budapest, Hungary, October, pp. 37-54.

Abd El-Halim, A. O. and Svec, O. J., 1990b. Influence of Compaction Techniques on the Properties of Asphalt Pavements. Proceedings, the Canadian Technical Asphalt Association Annual Meeting, Winnipeg, Canada. November, pp.18-33.

Adlinge, S.S. and Gupta, A.K., 2013. Pavement Deterioration and its Causes. *International c of Innovative Research and Development,* Vol2(Issue 4), pp.437-450.

Andersson, T. and Rowcliffe, D.J., 1996. Indentation Thermal Shock Test for Ceramics. *Journal of the American Ceramic Society*, *79*(6), pp.1509-1514.

Arraigada, M., Piemontese, F., Hugener, M. and Partl, M. N., 2018. Field validation of High Content Recycled Asphalt Concrete Mixtures with Accelerated Pavement Testing. *Presented at the International Society for Asphalt Pavement (ISAP) conference 2018*. Fortaleza, Brazil, pp.1-7.

Aschenbrener, T. and Tran, N., 2020. Optimizing In-Place Density Through Improved Density Specifications. *Transportation Research Record*, *2674*(3), pp.211-218.

Aschenbrener, T., Leiva, F. and Tran, N.H., 2019. FHWA Demonstration Project for Enhanced Durability of Asphalt Pavements Through Increased In-Place Pavement Density, Phase 2 (No. FHWA-HIF-19-052). United States. Federal Highway Administration. Office of Asset Management, Pavements, and Construction.

Auditor General of Ontario, 2018. *Ministry Of Transportation—Road Infrastructure Construction Contracts Awarding and Oversight: Follow-Up Report*. 2018 Annual Report Vol. 2 of 2. [online] Toronto: Office of the Auditor General of Ontario. Available at: <https://www.auditor.on.ca/en/content/reporttopics/transportation.html> [Accessed 11 August 2020]

Awadalla, M., 2015. Field And Laboratory Investigation of Asphalt Pavement Permeability. Doctoral dissertation, Carleton University, Ottawa, Canada.

Awadalla, M., Abd El Halim, A.O., Hassan, Y., Bashir, I. and Pinder, F., 2017. Field and Laboratory Permeability of Asphalt Concrete Pavements. *Canadian Journal of Civil Engineering*, Vol. 44, No. 4, pp.233-243.

Bell, C.A., Hicks, R.G. and Wilson, J.E., 1984. Effect Of Percent Compaction on Asphalt Mixture Life. In Placement and Compaction of Asphalt Mixtures. *Publication of: ASTM Special Technical Publications*.

Birgisson, B., Roque, R. and Page, G.C., 2003. Evaluation of Water Damage Using Hot Mix Asphalt Fracture Mechanics (with discussion). *Journal of Association of Asphalt Paving Technologists Technical Sessions, 2003, Lexington, Kentucky, USA* (Vol. 72).

Blab, R., 2013. Performance-Based Asphalt Mix and Pavement Design. *Romanian Journal of Transport Infrastructure,* 2(1), pp.21-38.

Bolzan, P.E. and Huber, G.A., 1993. Direct Tension Test Experiments (No. SHRP-A-641). Strategic Highway Research Program, National Research Council, Washington, DC.

Brown, E.R., Kandhal, P.S. and Zhang, J., 2001. Performance Testing for Hot Mix Asphalt. National Center for Asphalt Technology Report, (01-05).

Chelliah, A.R., 2019. *Technical and Economic Development of Efficient Asphalt Multi-Integrated Compaction Technology* (Doctoral dissertation, Carleton University).

Chen, X. and Huang, B., 2008. Evaluation Of Moisture Damage in Hot Mix Asphalt Using Simple Performance and Superpave Indirect Tensile Tests. *Construction and Building Materials*, *22*(9), pp.1950-1962.

Chow, W.T. and Atluri, S.N., 1997. Composite Patch Repairs of Metal Structures: Adhesive Nonlinearity, Thermal Cycling, and Debonding. *AIAA journal*, *35*(9), pp.1528-1535.

California Test 104 Compactor, Method of Operation and Calibration of The Electronically Controlled Kneading, E.H.K., 2011. Department Of Transportation.

Das, R., Mohammad, L.N., Elseifi, M., Cao, W. and Cooper Jr, S.B., 2017. Effects of Tack Coat Application on Interface Bond Strength and Short-Term Pavement Performance. *Transportation Research Record*, *2633*(1), pp.1-8.

de OS, H. and Carlos, J., 1991. Associations of Distress and Diagnosis of Bitumen-Surfaced Road Pavements. Transportation Research Record, (1291).

Delak, K.M., Bova, P., Hartzell, A.L. and Woodilla, D.J., 1999, August. Analysis of Manufacturing-scale MEMS Reliability Testing. In *MEMS Reliability for Critical and Space Applications* (Vol. 3880, pp. 165-174). International Society for Optics and Photonics.

Dessouky, S., Masad, E. and Bayomy, F., 2004. Prediction of Hot Mix Asphalt Stability Using the Superpave Gyratory Compactor. *Journal of Materials in Civil Engineering,* 16(6), pp.578-587.

Easa, S.M., Shalaby, A. and Halim, A.A.E., 1996. Reliability-Based Model for Predicting Pavement Thermal Cracking. *Journal of transportation engineering*, 122(5), pp.374-380.

Environment and Climate Change Canada (2019). *Historical Climate Data - Climate - Environment and Climate Change Canada*. [online] Weather.gc.ca. Available at: https://climate.weather.gc.ca/.

Fathi, A., Tirado, C., Rocha, S., Mazari, M. and Nazarian, S., 2021. Assessing Depth of Influence of Intelligent Compaction Rollers By Integrating Laboratory Testing And Field Measurements. *Transportation Geotechnics*, *28*, p.100509.

Finn, F.N. and Epps, J.A., 1980. Compaction of Hot Mix Asphalt Concrete. Texas Transportation Institute, the Texas A & M University System.

Finn, F.N., 1967. Factors Involved in The Design of Asphaltic Pavement Surfaces. *NCHRP Report*, (39).

Freeman, T.J. and Ragsdale, J.E., 2003. Development of Certification Equipment for TxDOT Automated Pavement Distress Equipment (No. FHWA/TX-03/4204-1,). Texas Transportation Institute, Texas A & M University System.

Gale, M.S. and Darvell, B.W., 1999. Thermal Cycling Procedures for Laboratory Testing of Dental Restorations. *Journal of dentistry*, *27*(2), pp.89-99.

Gavin, J., Dunn, L. and Juhasz, M., 2003. The Lamont Test Road-Twelve Years of Performance Monitoring. In *Proceedings of the Forty-Eighth Annual Conference of the Canadian Technical Asphalt Association (CTAA): Halifax, Nova Scotia*.

Geller, M., 1984. Compaction Equipment for Asphalt Mixtures. In Placement and Compaction of Asphalt Mixtures. ASTM International.

Gibb, J.M., 1996. *Evaluation Of Resistance to Permanent Deformation in The Design of Bituminous Paving Mixtures* (Doctoral dissertation, University of Nottingham).

Girardi, G., Ramezani, M. and El Halim, A.A., 2017, July. Effect Of Construction Induced Cracks on Tensile Strength and Bonding Between Asphalt Concrete Layers of Pavement Under Different Temperatures. *In International Congress and*

Exhibition" Sustainable Civil Infrastructures: Innovative Infrastructure Geotechnology" (pp. 85-97). Springer, Cham.

Haas, R.C.G. and Phang, W.A., 1988. Relationships Between Mix Characteristics and Low-Temperature Pavement Cracking (with discussion). In *Association of Asphalt Paving Technologists Proc* (Vol. 57).

Hajj, E.Y., Hand, A.J., Chkaiban, R. and Aschenbrener, T.B., 2019. *Index-Based Tests for Performance Engineered Mixture Designs for Asphalt Pavements* (No. FHWA-HIF-19-103).

Harvey, J., Du Plessis, L., Long, F., Deacon, J., Guada, I., Hung, D. and Scheffy, C., 1997. CAL/APT Program: Test Results from Accelerated Pavement Test on Pavement Structure Containing Asphalt Treated Permeable Base (ATPB)–Section 500RF. *Davis and Berkeley, CA: University of California Pavement Research Center. (Report Numbers UCPRC-RR-1999-02 and RTA-65W4845-3)*.

Harvey, J., Eriksen, K., Sousa, J. and Monismith, C.L., 1994. Effects of Laboratory Specimen Preparation on Aggregate-Asphalt Structure, Air-Void Content Measurement, and Repetitive Simple Shear Test Results. *Transportation Research Record,* (1454).

Hesp, S.A., Soleimani, A., Subramani, S., Phillips, T., Smith, D., Marks, P. and Tam, K.K., 2009. Asphalt Pavement Cracking: Analysis of Extraordinary Life Cycle Variability in Eastern and Northeastern Ontario. *International Journal of Pavement Engineering*, 10(3), pp.209-227.

Hofko, B. and Blab, R., 2016. Performance-based Hot Mix Asphalt and Flexible Pavement Design-The European Perspective. In *Proc., Civil Engineering Conference in the Asian Region (CECAR7),* Waikiki, Oahu, Hawaii.

Hughes, C.S., 1989. Compaction of asphalt pavement. *NCHRP Report 152. Transportation Research Board,* National Research Council, Washington, DC.

Igboke, C.A., Elsayed, E. and Hassan, Y., 2020. Effects of Field Compaction Method on Water Permeability and Performance of Asphalt Concrete Pavements. In *Proceedings of the 9th International Conference on Maintenance and Rehabilitation of Pavements—Mairepav9* (pp. 795-804). Springer, Cham.

Im, S., 2012. *Characterization Of Viscoelastic and Fracture Properties of Asphaltic Materials in Multiple Length Scales*. Doctoral dissertation, The University of Nebraska-Lincoln.

Izzo, R.P. and Tahmoressi, M., 1999. Use of the Hamburg Wheel-Tracking Device for Evaluating Moisture Susceptibility of Hot-Mix Asphalt. *Transportation Research Record*, *1681*(1), pp.76-85.

Kandhal, P.S., 1992. *Moisture Susceptibility of HMA Mixes: Identification of Problem and Recommended Solutions* (No. NCAT 92-1,). Lanham, MD: National Asphalt Pavement Association.

Kandhal, P.S., Dongre, R. and Malone, M.S., 1996, February. Prediction of Low-Temperature Cracking Using Superpave Binder Specifications. In Paper presented at the Annual Meeting of the Association of Asphalt Paving.

Kirkner, D.J. and Shen, W., 1999. Numerical Simulation of Thermal Cracking of Asphalt Pavements. Transportation Research Board Preprint, Washington, DC.

Kruntcheva, M.R., Collop, A.C. and Thom, N.H., 2006. Properties of Asphalt Concrete Layer Interfaces. *Journal of Materials in Civil Engineering*, *18*(3), pp.467-471.

Lavin, P., 2003. Asphalt Pavements: A Practical Guide to Design, Production and Maintenance for Engineers and Architects. CRC Press.

Lees, G. and Salehi, M., 1969. Orientation of Particles with Special Reference to Bituminous Paving Materials. Highway Research Record, (273).

Linden, R.N., Mahoney, J.P. and Jackson, N.C., 1989. Effect of compaction on asphalt concrete performance. Transportation research record, (1217).

Marasteanu, M., Zofka, A., Turos, M., Li, X., Velasquez, R., Li, X., Buttlar, W., Paulino, G., Braham, A., Dave, E. and Ojo, J., 2007. Investigation of Low Temperature Cracking in Asphalt Pavements National Pooled Fund Study 776.

Miller, J.S. and Bellinger, W.Y., 2014. Distress Identification Manual for The Long-Term Pavement Performance Program (No. FHWA-HRT-13-092). United States. Federal Highway Administration. Office of Infrastructure Research and Development.

Ministry of Transportation— Road Infrastructure Construction Contract Awarding and Oversight. (2018). *2018 Annual Report*. Office of the Auditor General of Ontario, p.2.

Monismith, C.L. and Deacon, J.A., 1969. Fatigue of Asphalt Paving Mixtures. Transportation Engineering Journal of ASCE, 95(2), pp.317-346.

Muench, S. T., Moomaw, T., & Trainer, R. C. (2008). De-Bonding of Hot Mix Asphalt Pavements in Washington State: An Initial Investigation (No. WA-RD 712.1). Washington State Department of Transportation, Office of Research & Library Services.

Nemeth, P., 2001, May. Accelerated Life Time Test Methods for New Package Technologies. In *24th International Spring Seminar on Electronics Technology. Concurrent Engineering in Electronic Packaging. ISSE 2001. Conference Proceedings (Cat. No. 01EX492)* (pp. 215-219). IEEE.

Nemeth, P., 2001, May. Accelerated Life Time Test Methods for New Package Technologies. In *24th International Spring Seminar on Electronics Technology. Concurrent Engineering in Electronic Packaging. ISSE 2001. Conference Proceedings (Cat. No. 01EX492)* (pp. 215-219). IEEE.

Nevitt, H.G., 1957. Compaction Fundamentals. *Journal of the Association of Asphalt Paving Technologists*, 26, pp.201-206.

Nguyen, Q.T., Di Benedetto, H. and Sauzéat, C., 2012. Determination of Thermal Properties of Asphalt Mixtures as Another Output from Cyclic Tension-Compression Test. *Road Materials and Pavement Design*, 13(1), pp.85-103.

Omar Abd El Halim, A.E.H., Abd El Halim, A.O., Awadalla, M. and Adel Hassanin, M., 2015. Development of the Asphalt Multi-Integrated Roller Field and Experimental Studies. *Journal of Construction Engineering*, *2015*.

Park, H.J. and Kim, Y.R., 2015. Primary Causes of Cracking of Asphalt Pavement in North Carolina: field study. *International Journal of Pavement Engineering*, 16(8), pp.684-698.

Paterson, W.D.O., 1974. Consideration of Particle Orientation in The Compaction of Asphalt Concrete (ABRIDGMENT) (No. 517).

Pell, P.S., 1967, January. Fatigue of Asphalt Pavement Mixes. In Intl Conf Struct Design Asphalt Pvmts.

Pellinen, T.K. and Witczak, M.W., 2002. Use Of Stiffness of Hot-Mix Asphalt as A Simple Performance Test. *Transportation Research Record*, *1789*(1), pp.80-90.

Pellinen, T.K., 2001. *Investigation Of the Use of Dynamic Modulus as An Indicator of Hot-Mix Asphalt Performance*. Arizona State University.

Raab, C, Parti, M.N. 2009b. Long-Term Interlayer Shear Performance of Base and Subbase Layers in Asphalt Pavements. *6th International Conference on Maintenance and Rehabilitation of Pavements and Technological Control.* Mairepav6, Torino, Italy, Vol II, pp 646-653.

Raab, C., 2019, May. Improving Pavement's Properties Using the AMIR II Compactor. In *Bituminous Mixtures and Pavements VII: Proceedings of the 7th International Conference 'Bituminous Mixtures and Pavements'(7ICONFBMP), June 12-14, 2019, Thessaloniki, Greece* (p. 334). CRC Press.

Roberts, F.L., Kandhal, P.S., Brown, E.R., Lee, D.Y. and Kennedy, T.W., 1991. Hot Mix Asphalt Materials, Mixture Design and Construction.

Romanoschi, S.A., 1999. Characterization of Pavement Layer Interfaces.

Rushing, J.F. and Little, D.N., 2014. Static Creep and Repeated Load As Rutting Performance Tests for Airport HMA Mix Design. *Journal of materials in civil engineering*, *26*(9), p.04014055.

Said, D., Abd El Halim, A.O. and Pais, J.C., 2008. Study Of the Causes and Remedies of Premature Surface Cracking of Asphalt Pavements. *In EPAM3–3rd European Pavement and Asset Management Conference* (pp. 1-15).

Sánchez-Leal, F.J., 2007. Gradation Chart for Asphalt Mixes: Development. *Journal of materials in civil engineering*, *19*(2), pp.185-197.

SHAHIN, M., 1986. Effect of Layer Slippage on Performance of Asphalt-Concrete Pavements. *Transportation Research Pecord*, *1095*, pp.79-85.

Shalaby, A., Abd El Halim, A.O. and Easa, S., 1996, September. Influence Of Thermal Stresses on Construction-Induced Cracks. *In RILEM proceedings* (pp. 30-39). Chapman & Hall.

Soltani, A. and Anderson, D.A., 2005. New Test Protocol to Measure Fatigue Damage in Asphalt Mixtures. *Road materials and pavement design*, *6*(4), pp.485-514.

Szucs, Z., Nagy, G., Hodossy, S., Rencz, M. and Poppe, A., 2007, September. Vibration combined high Temperature Cycle Tests for capacitive MEMS accelerometers. In *2007 13th International Workshop on Thermal Investigation of ICs and Systems (THERMINIC)* (pp. 215-219). IEEE.

Tabatabaee, H.A., Velasquez, R. and Bahia, H.U., 2012. Predicting Low Temperature Physical Hardening in Asphalt Binders. *Construction and Building Materials*, 34, pp.162-169.

Test, Overlay. "Tex-248-F." Texas Department of Transportation, Austin (2009).

Timm, D.H., 2002. A Phenomenological Model to Predict Thermal Crack Spacing of Asphalt Pavements.

Tschegg, E.K., Kroyer, G., Tan, D.M., Stanzl-Tschegg, S.E. and Litzka, J., 1995. Investigation Of Bonding Between Asphalt Layers on Road Construction. *Journal of Transportation Engineering*, *121*(4), pp.309-316.

Turos, M.I., 2010. Determining The Flexural Strength of Asphalt Mixtures Using the Bending Beam Rheometer.

Tušar, M., Hribar, D. and Hofko, B., 2014, April. Impact Of Characteristics of Asphalt Concrete Wearing Courses on Crack Resistance at Low Temperatures. *In Transport Research Arena (TRA) 5th Conference: Transport Solutions from Research to Deployment.*

United States Department of Transportation, The Federal Highway Administration (FHWA) (2016). *2015 Status of the Nation's Highways, Bridges, and Transit: Conditions & Performance*. Report to Congress (C&P report). [online] p.xliv Highlights. Available at: https://www.fhwa.dot.gov/policy/2015cpr/index.cfm.

Vassen, R., Cao, X., Tietz, F., Basu, D. and Stöver, D., 2000. Zirconates As New Materials for Thermal Barrier Coatings. *Journal of the American Ceramic Society*, *83*(8), pp.2023-2028.

Vinson, T.S., Janoo, V.C. and Haas, R.C., 1989. Summary report, Low Temperature and Thermal Fatigue Cracking (No. SHRP-A/IR-90-001).

Walubita, L.F., et al., 2012. Comparison Of the Hamburg, Dynamic Modulus and Repeated Load Tests for Evaluation of HMA Permanent Deformation. *Presented in Transportation Research Board 91st Annual Meeting*, 22–26 January 2012 Washington, DC.

Walubita, L.F., Faruk, A.N., Koohi, Y., Luo, R., Scullion, T. and Lytton, R.L., 2012. The Overlay Tester (OT): comparison with other crack test methods and recommendations for surrogate crack tests (No. FHWA/TX-13/0-6607-2). Texas. Dept. of Transportation. Research and Technology Implementation Office.

Wang, W., Cheng, Y., Zhou, P., Tan, G., Wang, H. and Liu, H., 2019. Performance Evaluation of Styrene-Butadiene-Styrene-Modified Stone Mastic Asphalt with Basalt Fiber Using Different Compaction Methods. *Polymers*, 11(6), p.1006.

Willis, R.J. and Timm, D.H., 2006. Forensic Investigation of a Rich Bottom Pavement. NCAT Report 06-04. *National Center for Asphalt Technology, Auburn, Alabama*.

Wistuba, M.P., 2016. The German Segmented Steel Roller Compaction Method–State-Of-The-Art Report. *International journal of pavement engineering*, *17*(1), pp.81-86.

Witczak, M.W., Kaloush, K., Pellinen, T., El-Basyouny, M. and Von Quintus, H., 2002. NCHRP Report 465 *SIMPLE PERFORMANCE TEST FOR SUPERPAVE MIX DESIGN* (No. Project 9-19 FY'98).

Xu, J., Li, N. and Xu, T., 2022. Temperature Changes of Interlaminar Bonding Layer In Different Seasons and Effects on Mechanical Properties of Asphalt Pavement. *International Journal of Pavement Research and Technology, 15(3), pp.589-605.Vancouver*

Zaumanis, M., Poulikakos, L.D. and Partl, M.N., 2018. Performance-Based Design of Asphalt Mixtures and Review of Key Parameters. *Materials & Design*, *141*, pp.185-201.

Zhang, C., Wang, H., You, Z. and Ma, B., 2015. Sensitivity Analysis of Longitudinal Cracking on Asphalt Pavement Using MEPDG in Permafrost Region. *Journal of Traffic and Transportation Engineering (English Edition*), 2(1), pp.40-47.

Zhang, Z., Wang, K., Liu, H. and Deng, Z., 2016. Key Performance Properties of Asphalt Mixtures with Recycled Concrete Aggregate from Low Strength Concrete. *Construction and Building Materials*, *126*, pp.711-719.

Ziari, H., Aliha, M.R.M., Mojaradi, B. and Jebalbarezi Sarbijan, M., 2019. Investigating The Effects of Loading, Mechanical Properties and Layers Geometry on Fatigue

Life of Asphalt Pavements. *Fatigue & Fracture of Engineering Materials & Structures,* 42(7), pp.1563-1577.

Appendix A- Details of Addition Built for Testing Series B Apparatus

After completion of Test Series A and determination of the needs for Test Series B, modifications to the testing apparatus were made, as several tests failed when trying to perform Test Series B with the apparatus from Test Series A. Stanley Conley, Supervisor of the Civil and Environmental Engineering Laboratories, designed the steel structure required for the mentioned new addition. The required materials and parts were ordered and received in the lab (see Figure A-1). Jason Arnott performed most of the machine work, welding, assembly, and installations.

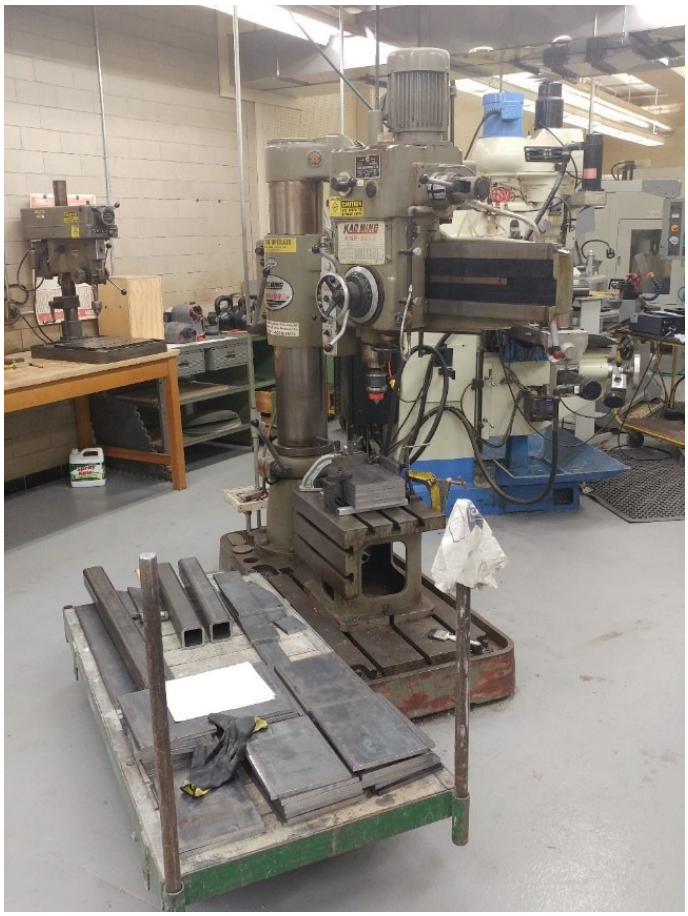

Figure A-1. Test Series B Apparatus Parts Before Assembly

- A small support frame fabricated of Hollow Structural Steel (HSS), bolted to existing holes in the frame rails;
- A weight system comprised of a lower span plate to which the force cables are attached, and that supports the required load plates;

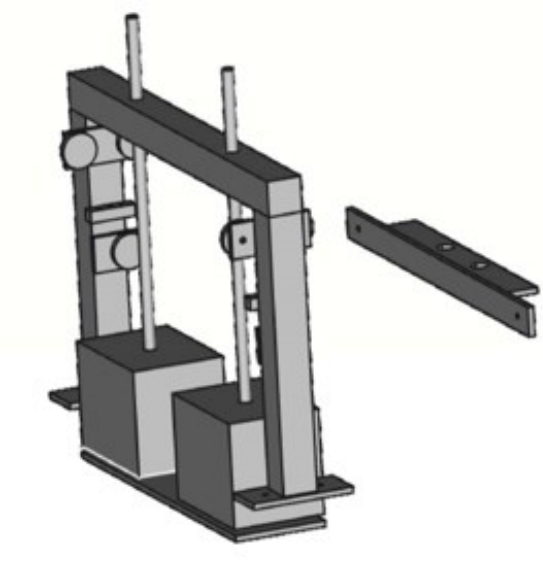

Figure A-2. 3D View of Designed Weight System

Figure A-3. View of the Load plates

- Load plates of approximately 5.65 kg that can provide the required dead load in potential increments of up to 20 load plates;
- A vertical threaded bar system to:
    - Constrain the motion of the load plates.
    - Move the load plates up to reset the table position at the beginning of a test.
    - Release the load onto the samples at the beginning of the test.
    - Limit the overall movement of the table after the sample fails.

Figure A-4. View of the Vertical Threaded Bar

- A detachable pull bar to allow the system to return to the initial state with minimal effort; and
- A Linear Variable Differential Transducers (LVDT) mechanism to monitor table motion.

Figure A-5. View of the Linear Variable Differential Transducers (LVDT) During Installation

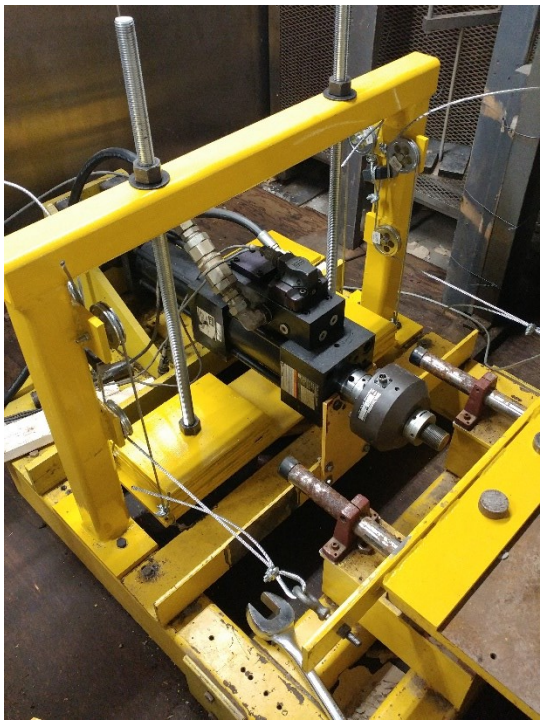

Figure A-6. Test Series B Apparatus After Assembly and Installation

Appendix B- Summary of Trial for Test Series B

Several trial tests were performed before current Test Series B was finalized. Here is a summary of a few of those trial tests performed prior to the development of Test Series B.

Trial Series 1: 11 single layer samples and 5 double layer samples were tested, all at -10°C. Table B-1 presents the details related to this trial series of tests, including sample sizes, adhesive used for connection of samples to plates as well as sample to sample, and also observation of researchers during the test.

Figure B-1. Example of Trial Series 1, Connection of sample to plate is by tack coat

Trial Series 2: For the next 15 tests Samples were placed beside each other and the direct tensile strength test was performed at several temperature (+22°C, -5°C, and -22 °C). 8 samples were pasted to each other by a tack coat and the remaining 7 samples were glued by epoxy.

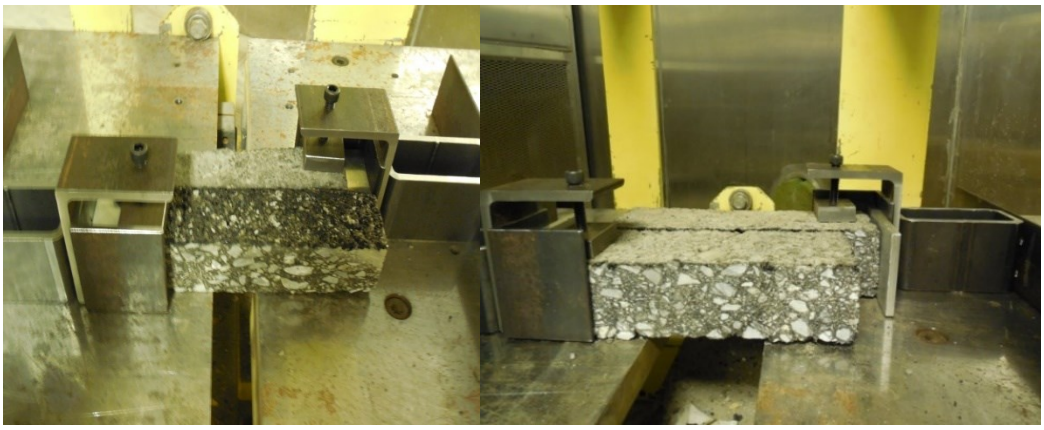

Figure B-2. Examples of Trial Series 2 (Testing slabs side by side)

Table B-1. Examples of Trial Tests Performed before Test Series B

No.	Bottom layer Size (cm) Thickness x Width x Length	Temp (°C)	Top layer Size (cm) T x W x L	Layers	Connection Sample to Plate:	Connection Sample to Sample:	Summary of Observations
1	5 x 15 x 30	-10°C	-	Single	Epoxy	-	Sample broken
2	5 x 15 x 30	-10°C	-	Single	Epoxy	-	Sample broken
3	5 x 15 x 30	-10°C	-	Single	Epoxy	-	Sample broken
4	5 x 15 x 60	-10°C	-	Single	Tack Coat	-	Sample broken
5	5 x 15 x 60	-10°C	-	Single	Tack Coat	-	Sample broken
6	5 x 15 x 30	-10°C	-	Single	Epoxy	-	Sample broken
7	5 x 15 x 30	-10°C	-	Single	Epoxy	-	Sample broken
8	5 x 15 x 30	-10°C	-	Single	Tack Coat	-	Slab did not break, just disconnected from the plate
9	5 x 15 x 30	-10°C	-	Single	Tack Coat	-	Slab did not break, just disconnected from the plate
10	5 x 15 x 30	-10°C	-	Single	Tack Coat	-	Slab did not break, just disconnected from the plate
11	5 x 15 x 30	-10°C	-	Single	Epoxy	-	Sample broken

12	5 x 15 x 22 each side	-10^{o}C	5 x 15 x 30	Double	Epoxy	Tack Coat	Top layer slab did not break, just disconnected from lower Layer slabs
13	5 x 15 x 22 each side	-10^{o}C	5 x 15 x 30	Double	Epoxy	Tack Coat	Top layer slab did not break, just disconnected from lower Layer slabs
14	5 x 15 x 30 each side	-10^{o}C	5 x 15 x 60	Double	Epoxy	Tack Coat	sample broken
15	6 x 15 x 30 each side	-10^{o}C	5 x 15 x 60	Double	Epoxy	Tack Coat	Top layer slab did not break, just disconnected from lower Layer slabs
16	7 x 15 x 30 each side	-10^{o}C	5 x 15 x 60	Double	Epoxy	Tack Coat	Top layer slab did not break, just disconnected from lower Layer slabs
17	5 x 6 x 16 each side	22^{o}C	Side by Side	Double	Tack Coat	-	Samples slide with no resistances
18	5 x 6 x 16 each side	22^{o}C	Side by Side	Double	Tack Coat	-	Samples slide with no resistances
19	5 x 6 x 16 each side	22^{o}C	Side by Side	Double	Tack Coat	-	Samples slide with no resistances
20	5 x 6 x 16 each side	-5^{o}C	Side by Side	Double	Tack Coat	-	Samples slide but much more resistance was observed than 22^{o}C test
21	5 x 6 x 16 each side	-5^{o}C	Side by Side	Double	Tack Coat	-	Samples slide but much more resistance was observed than 22^{o}C test
22	5 x 6 x 16 each side	-20^{o}C	Side by Side	Double	Tack Coat	-	Samples slide but more resistance was observed than -5^{o}C test
23	5 x 6 x 16 each side	-20^{o}C	Side by Side	Double	Tack Coat	-	Samples slide but more resistance was observed than -5^{o}C test
24	5 x 6 x 16 each side	-20^{o}C	Side by Side	Double	Tack Coat	-	Samples slide but more resistance was observed than -5^{o}C test

25	5 x 6 x 16 each side	22^{o}C	Side by Side	Double	Epoxy	-	sample broken
26	5 x 6 x 16 each side	22^{o}C	Side by Side	Double	Epoxy	-	sample broken
27	5 x 6 x 16 each side	22^{o}C	Side by Side	Double	Epoxy	-	sample broken
28	5 x 6 x 16 each side	-5^{o}C	Side by Side	Double	Epoxy	-	sample broken
29	5 x 6 x 16 each side	-5^{o}C	Side by Side	Double	Epoxy	-	sample broken
30	5 x 6 x 16 each side	-20^{o}C	Side by Side	Double	Epoxy	-	sample broken
31	5 x 6 x 16 each side	-20^{o}C	Side by Side	Double	Epoxy	-	sample broken
32	5 x 6 x 16 each side	-20^{o}C	Side by Side	Double	Epoxy	-	sample broken
33	5 x 6 x 16 each side	-20^{o}C	Side by Side	Double	Epoxy	-	sample broken

Appendix C- List of Asphalt Pavement Performance Test Methods

Below is the list of some of the ACO performance test methods currently in use by different agencies around the word:

A- Performance Tests for Permanent Deformation (Rutting)/ Stability

- Simulative tests (loaded wheel and wheel tracking tests):
    - Hamburg Wheel Tracking, HWT (AASHTO T324)
    - Asphalt Pavement Analyser, APA (AASHTO TP 63)
    - French Rutting Tester, FRT
    - Cooper Wheel Tracking Tests, CWTT (EN 12697-22)
- Static creep tests. (AASHTO - TP9)
- Repeated load axial tests:
    - Repeated load creep tests on viscoelastic materials:
        - Asphalt Mixture Performance Test (AMPT) (a repeated-load uniaxial test), by AASHTO T378, Standard Method of Test for Determining the Dynamic Modulus and Flow Number for Asphalt Mixtures Using the AMPT (Previously known as AASHTO TP 79). Repeated Shear at Constant Height (RSCH) Test (AASHTO T 320), This is very similar to the AMPT flow number test but uses the Superpave Shear Tester (SST)
    - European test EN 12697-25 (Blab, R., 2013):
        - Triaxial cyclic compression test (TCCT)

        - Uniaxial cyclic compression test (UCCT)
    - Proposed ASTM WK61395: Rutting Resistance of Asphalt Mixtures using Incremental Repeated Load Permanent Deformation Methodology

- Dynamic Modulus Tests.
    - AASHTO T342
    - AASHTO T378
- AASHTO TP132Empirical Tests- Marshal

B- Performance Test methods for measuring and characterizing HMA cracking and fatigue resistance (durability) potential:

- Overlay Tester
- Texas Overlay Tester (Tex-248-F) to determine number of cycles until failure.
- New Jersey Department of Transportation (NJDOT B-10), to determine critical fracture energy and crack resistance index.
- Monotonic Overlay Tester Test Method
- Cracking Tolerance Tests:
- By Monotonic Indirect-Tension (IDT)
- Repeated loading indirect-Tension (R-IDT) tests, also known as Indirect Tensile Cracking (formerly known as IDEAL-CT), (ASTMD8225-19 Standard Test Method for the determination of “Cracking Tolerance Index” of Asphalt Mixture using the Indirect Tensile Cracking Test at intermediate temperature (also a proposed WK60859 standard))

- Semi-Circular Bending (SCB) using Semicircular Bend Geometry (SCB) at Intermediate Temperature Monotonic Semi-Circular Bending (SCB) at Intermediate Temperatures (AASHTO TP105 & the ASTM D8044-16 Standard Test Method for Evaluation of Asphalt Mixture Cracking Resistance) for the Determination of “Critical strain energy release rate” , and repeated loading semi-circular bending (R-SCB) test AASHTO TP 124-20, Provisional Standard Method of Test for Determining the Fracture Potential of Asphalt Mixtures Using Semicircular Bend Geometry (SCB) at Intermediate Temperature
- Cyclic Fatigue Test, AASHTO TP 107 & AASHTO TP 133, Standard Method of Test for Determining the Damage Characteristic Curve and Failure Criterion Using the Asphalt Mixture Performance Tester (AMPT)
- Disk-shaped Compaction Tension Test (DSCTT), ASTM D7313, Standard Test Method for Determining Fracture Energy of Asphalt Mixtures Using the Disk-Shaped Compact Tension Geometry
- Flexural Bending Beam Fatigue, AASHTO T 321, Standard Method of Test for Determining the Fatigue Life of Compacted Asphalt Mixtures Subjected to Repeated Flexural Bending to determine the number of the cycles to failure. For this test, 380 mm long by 50 mm thick by 63 mm wide asphalt mixture beam specimens sawed from laboratory- or field-compacted asphalt mixtures and subjected to repeated flexural bending until failure

- Monotonic Direct-Tension (DT) and Repeated loading Direct-Tension (R-DT) tests
- Fatigue Failure by Four-Point Beam (4PB) Fatigue Device D8237-18 Standard Test Method for Determining Fatigue Failure of Asphalt-Aggregate Mixtures with the Four-Point Beam Fatigue Device (also a proposed WK63384 standard)
- Proposed ASTM WK61388 Resistance of Asphalt Mixtures to Fatigue Cracking using the Incremental Repeated Load Permanent Deformation (iRLPD) procedure

- European test EN 12697-26 (Blab, R., 2013):
  - Cyclic indirect tensile test (CIDT)
  - 4-Point-Bending test (4PB)

C- Performance Tests for low temperature performance:

- ASTM proposed WK60626 to determine the Thermal Cracking Properties of Asphalt Mixtures by measuring the Thermally Induced Stress and Strain.
- European test EN 12697-46 (Blab, R., 2013):
  - Temperature Stress Restrained Specimen Test (TSRST)
  - Uniaxial tension stress test (UTST)
  - Uniaxial Cyclic Tension Stress Test (UCTST)

D- Performance Tests for stiffness:

- Resilient Modulus of Bituminous Mixtures:

- D7369-11 Standard Test Method for Determining the Resilient Modulus of Bituminous Mixtures by Indirect Tension Test. (Also a proposed WK64107 standard)

- European test EN 12697-26 (Blab, R., 2013):
  - 2-Point Bending test with a trapezoidal specimen (2PBTR)
  - 2-Point Bending test with a prismatic specimen (2PBPR)
  - 3-Point Bending test (3PB)
  - 4-Point Bending test (4PB)
  - Cyclic Indirect Tensile Test (CIDT)
  - Direct Tension/compression Test (DCT)

E- Performance Tests for Asphalt Moisture Sensitivity:

- Indirect tensile tests:
  - AASHTO T283/ ASTM D4867, also known as modified Lottman and Root-Tunnicliff test, to measure the effect of moisture on asphalt concrete pavement (most road agencies use this test).
- Boil test, ASTM D3625: Focus on the effects of the water on bituminous-coated aggregates. This is a loose mix test to evaluate the bonding between the asphalt and aggregate (adhesion).
- ASTM D4867, Effect of Moisture on Asphalt Concrete Paving Mixtures:

  Used to evaluate moisture susceptibility and rutting and assess the effectiveness of antistripping additives. This is only done on lab-made samples, so the effect of compaction methods is not evaluated.

- AASHTO T324, Hamburg Wheel Tracking (HWT) test is also a performance test to address permanent deformation (rutting). Very few agencies use HWT for moisture sensitivity review, as AASHTO T324 is a better test than AASHTO T283 since it considers cyclic traffic as well as moisture. However, it does use lab-made samples with a linear kneading compactor, so the effect of field compaction equipment is also not considered.
- Immersion-compression Test, AASHTO T165 / ASTM D1075. One of the less common tests using the compressive strength of the specimens (Marshal Stability Testing).

Appendix D- Relationship Between Variables for Test Series A

As mentioned in Section 2.3, the focus of all the proposed and evaluated performance tests was to determine and quantify the main properties of HMA that can be used in a distress-prediction model to relate those properties for material (aggregate and binder) characterization. This section presents the analysis performed on the results of Test Series A in order to show the impact of the independent variables on the dependent variable, and not for stress prediction. In Test Series A, “change in length of the sample” or “elongation” is the dependent variable, and “compaction method” (AMIR or CCM), “time”, and “temperature” are the three independent variables that affect the dependent variable (elongation). Since the same HMA mix was used for all samples, asphalt mix type is not included as one of the variable factors in this study. Similarly, sample thickness is not considered, as all the samples were double-layer with the same thickness. The forward selection method was used for the linear regression analysis to investigate how compaction method, temperature, and time predict elongation. Forward stepwise selection usually begins with a model that contains no variables (called the Null Model), and then starts adding the most significant variables one after another until a pre-specified stopping point is reached or until all the variables under consideration are included in the model. In this forward selection, for each step, one variable that gives the single best improvement to the model is added. Table D-1 presents the list of independent variables and their order. The first model only used compaction method (AMIR or CCM), the second model used time and compaction, and for the third model, temperature was added to the time and compaction method and all three independent variables were

included in the analysis. Table D-2 summarises the R^2 (coefficient of determination) of the models and shows a value of 0.638 for the R^2 of the third model. This value, $R^2 = 0.638$, is considered to represent a good correlation and large effect, indicating that 63.8% of the variance in elongation (dependent variable) is predicted by the model and the combination of independent variables (compaction, time, and temperature). The ANOVA Table D-3 indicates that the third model has a $p < 0.001$, with all three variables significantly contributing to the prediction. The ANOVA Table D-3 indicates that the combination of predictors (independent variables) significantly predicts the dependent variable (elongation). The Coefficients (beta weights and significance values) for all the models are presented in Table D-4.

Table D-1. List of independent variables and their orders, Test Series A, Linear Regression

Model	Variables Entered	Variables Removed	Method
1	Comp2	.	Forward (Criterion: Probability-of-F-to-enter <= .050)
2	Time	.	Forward (Criterion: Probability-of-F-to-enter <= .050)
3	Temp	.	Forward (Criterion: Probability-of-F-to-enter <= .050)
a. Dependent Variable: Log_elg			

Table D-2. Models Summary, Test Series A, Linear Regression

Model	R	R Square	Adjusted R Square	Std. Error of the Estimate
1	.689[a]	.475	.475	.13604
2	.768[b]	.589	.589	.12033
3	.799[c]	.638	.638	.11295

a. Predictors: (Constant), Comp2

b. Predictors: (Constant), Comp2, Time

c. Predictors: (Constant), Comp2, Time, Temp

Table D-3. Results of the ANOVA test for proposed models (Linear Regression), Test Series A

ANOVA[a]

Model		Sum of Squares	df	Mean Square	F	Sig.
1	Regression	1127.143	1	1127.143	60904.960	.000[b]
	Residual	1246.456	67352	.019		
	Total	2373.599	67353			
2	Regression	1398.369	2	699.184	48286.824	.000[c]
	Residual	975.230	67351	.014		
	Total	2373.599	67353			
3	Regression	1514.346	3	504.782	39565.859	.000[d]
	Residual	859.253	67350	.013		
	Total	2373.599	67353			

a. Dependent Variable: Log_elg

b. Predictors (or independent variable): (Constant), Comp2

c. Predictors: (Constant), Comp2, Time

d. Predictors: (Constant), Comp2, Time, Temp

Table D-4. Coefficients for proposed three models (Linear Regression), Test Series A

Coefficients[a]					
Model		**Unstandardized Coefficients**		**t**	**Sig.**
		B	Std. Error		
1	(Constant)	-.286	.001	-323.679	.000
	Comp2	.271	.001	246.789	.000
2	(Constant)	-.415	.001	-338.199	.000
	Comp2	.271	.001	279.002	.000
	Time	5.548E-5	.000	136.862	.000
3	(Constant)	-.452	.001	-371.910	.000
	Comp2	.271	.001	297.237	.000
	Time	6.322E-5	.000	162.490	.000
	Temp	.003	.000	95.344	.000
a. Dependent Variable: Log_elg					

In the Coefficients table, the significance level (Sig.) is *p-value* < .001 (Sig. is shown as .000, but although SPSS truncates *p-values* of less than .001 to .000, the probability cannot be zero). The regression prediction is statistically significant because the *p-value* is less than 0.05. Thus, we can reject the null hypothesis of no association and state that the combination of predictors (or independent variables) significantly predicts the dependent variable (elongation). This analysis confirms that in addition to the compaction method, time can affect the elongation, and as ACP undergoes larger numbers of cycles, the elongation increases. Obviously, in each cycle (24 hours), elongation increases when temperature increases and decreases when temperature drops. An increase in time and

temperature can increase the elongation of ACP samples. The equations for the prediction of elongation from each model are presented in Table D-5.

Table D-5. Proposed three equations (Linear Regression), Test Series A

Model		Coefficients	Equation
1	(Constant)	-.286	$\log Elong = -0.286 + 0.271\ Comp$
	Comp2	.271	
2	(Constant)	-.415	$\log Elong = -0.415 + 0.271\ Comp + 0.00005548\ Time$
	Comp2	.271	
	Time	5.548E-5	
3	(Constant)	-.452	$\log Elong = -0.452 + 0.271\ Comp + 0.00006322\ Time + 0.003\ Temp$
	Comp2	.271	
	Time	6.322E-5	
	Temp	.003	

- Comp2=0, for CCM
- Comp2=1, for AMIR Roller
- Time (Minutes), 360 < Time < 4320
- Temp (Celsius), -10 °C < Temp <+20°C

From the ANOVA table we know that the third model is statistically significant, and by including all the independent variables, we can conclude that Equation D-1 reflects the best proposed model for Test Series A. As mentioned earlier, in this model, “change in length of the sample” or “elongation” is the dependent variable and “Compaction method” (AMIR or Traditional Steel-Drum rollers”, “Time”, and “Temperature” are

independent variables that showed significantly affect the dependent variable (elongation). As discussed in detail in Chapter 3, since these results used to generate the model are for the first 3 TCT cycles, the time will go to a maximum of 4,320 minutes. Furthermore, the first 6 hours (360 minutes) of the recordings are excluded to omit fluctuations of the early recordings. Figure D-1 presents the graph associated with the proposed linear regression model for Test Series A.

$$Elongation = 10^{-0.452+0.271\ Compaction+0.00006322\ Time+0.003\ Temperature}$$

Equation D-1.

Or

$$\log Elong = -0.452 + 0.271\ Compaction + 0.00006322\ Time + 0.003\ Temperature$$

Equation D-2.

- Compaction=0, for CCM
- Compaction=1, for AMIR Roller
- Time (Minutes), 360 < Time < 4320
- Temperature (Celsius), -10 °C < Temperature <+20 °C

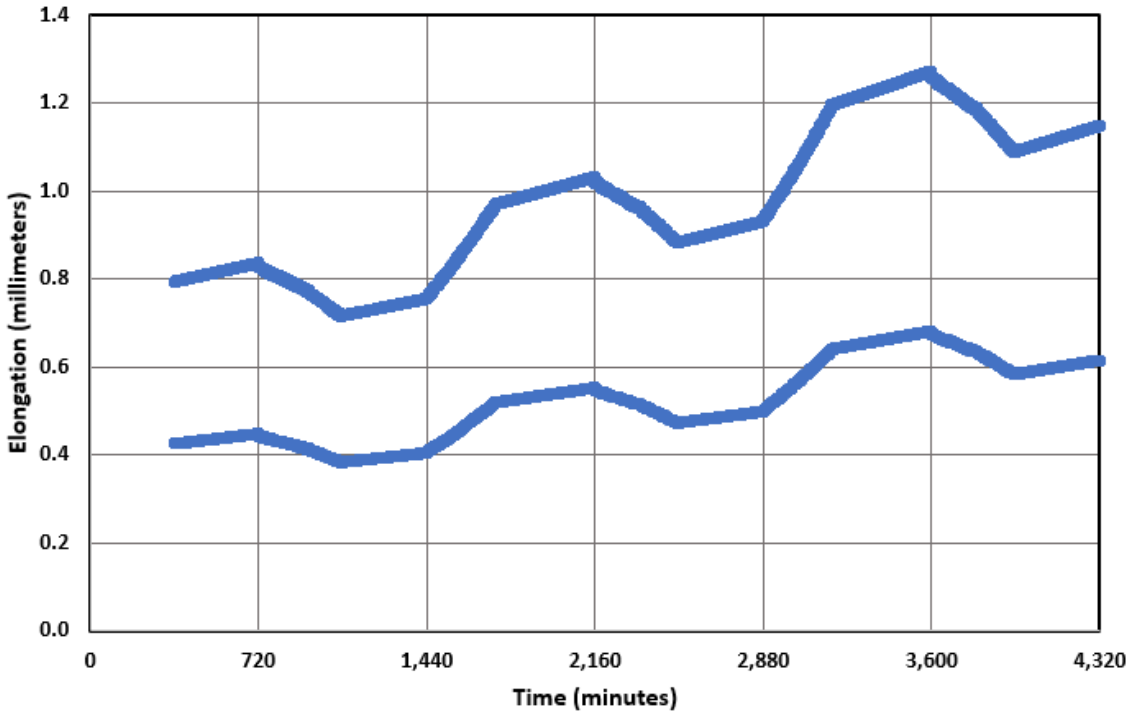

Figure D-1. Graph associated with proposed linear regression model for Test Series A